

[illegible]

Tamara Besselink

Propositions

1. When comparing chromatographic media or configurations, at least one will perform suboptimal. (this thesis)
2. A chromatographic monolith has advantages over a packed bed of porous particles only when very small or very large molecules are to be adsorbed. (this thesis)
3. More precise measurements do not always produce more precise results.
4. The word 'science' suggests a certainty that often does not exist.
5. You only truly understand something if you can explain it to others.
6. On-line social media often result in asocial behaviour in real-life.
7. Flexible working hours, especially when working from home, make it harder to balance work and private life.

Propositions belonging to the thesis:

'Protein isolation using affinity chromatography'

Tamara Besselink
Wageningen, 7 December 2012

Protein isolation using affinity chromatography

Tamara Besselink

Thesis committee

Promotor

Prof. dr. ir. R.M. Boom
Professor of Food Process Engineering
Wageningen University

Co-promotor

Dr. ir. A.E.M. Janssen
Assistant professor, Food Process Engineering Group
Wageningen University

Other members

Prof. dr. W.J.H. van Berkel, Wageningen University
Dr. ir. P.J.Th. Bussmann, TNO, Zeist
Prof. dr. ir. A.B. de Haan, Eindhoven University of Technology
Prof. dr. J.D. Mikkelsen, Technical University of Denmark

This research was conducted under the auspices of the graduate school VLAG (Advanced studies in Food Technology, Agrobiotechnology, Nutrition and Health Sciences).

Protein isolation using affinity chromatography

Tamara Besselink

Thesis

submitted in fulfilment of the requirements for the degree of doctor

at Wageningen University

by the authority of the Rector Magnificus

Prof. dr. M.J. Kropff,

in the presence of the

Thesis Committee appointed by the Academic Board

to be defended in public

on Friday 7 December 2012

at 1.30 p.m. in the Aula.

Tamara Besselink
Protein isolation using affinity chromatography
146 pages.

PhD thesis, Wageningen University, Wageningen, NL (2012)
With references, with summaries in Dutch and English

ISBN 978-94-6173-426-6

Contents

Chapter 1	Introduction	1
Chapter 2	Isolation of bovine serum albumin from whey using affinity chromatography	9
Chapter 3	The influence of pH and temperature on bovine serum albumin – VHH ligand binding	25
Chapter 4	Comparison of activated chromatography resins for protein immobilization	49
Chapter 5	Efficiency of protein-based ligand immobilization for affinity chromatography	67
Chapter 6	Are axial and radial flow chromatography different?	83
Chapter 7	General Discussion	109
	Summary	131
	Samenvatting	135
	Dankwoord	139
	Curriculum Vitae	141
	Publications	143
	Overview of completed training activities	145

Introduction

1.1 A short history of chromatography

According to IUPAC (International Union of Pure and Applied Chemistry) the official definition of chromatography is “a physical method of separation in which the components to be separated are distributed between two phases, one of which is stationary (stationary phase) while the other (the mobile phase) moves in a definite direction” [1]. Literally, the word chromatography means ‘colour writing’ and dates back to 1906. The Russian botanist Mikhail Tswett (his last name meaning ‘colour’ or ‘flowering’ in Russian) separated colourful plant pigments from each other using a column packed with an adsorbent [2]. Tswett investigated many different adsorbents (stationary phases) and solvents (mobile phases) to find an optimal separation method. It took over thirty years before the value of Tswett's work was recognized [3]. This was mainly due to the work of Nobel Prize winners A.J.P. Martin and R.L.M. Synge who described the chromatography process theoretically. From there gas chromatography and new types of liquid chromatography were developed. For a long time, chromatography was mainly used as an analytical tool using small sample sizes. Later on, the preparative use of chromatography was rediscovered (e.g., [4]), with its main applications in the pharmaceutical industry. The challenges in scale-up of chromatography processes, the batch-wise nature of the process, the amount of solvents (buffers) required, and the high costs of target-specific chromatography adsorbents are the main reasons why chromatography is not more widely used. For pharmaceuticals, purity is crucial and high separation costs can be acceptable in this field. A picture of a contemporary lab-scale preparative chromatography system is shown in Figure 1.1.



Figure 1.1. Example of a lab scale preparative chromatography setup with an Äkta Purifier (GE Healthcare, Uppsala, Sweden).

1.2 *Chromatography adsorbents and ligands*

Chromatography can be used to separate a mixture into its components. Two phases can be distinguished: the mobile phase, which can be a solvent but also the feed mixture itself, and the stationary phase, the adsorbent. The adsorbent or resin usually consists of spherical particles made of agarose, cellulose, polymethacrylate, silica and many other materials which are packed in a cylindrical column. The particles may be porous or non-porous. Membranes and monoliths can also be used as a stationary phase [5].

Several methods of separation exist in chromatography. In size-exclusion chromatography, also known as gel filtration chromatography, components are separated based on size. This method is mainly suitable for analytical purposes and final polishing, because the column cannot be loaded with the mixture to be separated for more than ~5% of the column volume.

Another possibility is to adsorb components to the stationary phase. This means that after adsorption, a change in buffer is required to desorb the components from the stationary phase. As an example, charged components can be separated using ion exchange, a method that is frequently applied in the pharmaceutical industry, and for example in the desalting of whey. To remove the adsorbed components, a salt gradient is used. On small scales, it is used in mechanical dish washers to remove multivalent ions from water.

The most specific method in chromatography is affinity chromatography. This type of chromatography relies on specific interaction between the target component and a

ligand immobilized onto the surface of the adsorbent. Many different ligands exist, for example synthetic dyes like Cibacron Blue, which can bind certain proteins; metal ions like nickel for the binding of His-tagged proteins; or Protein A for binding monoclonal antibodies; and antibodies themselves for binding their specific antigen (e.g., [6, 7]). Using antibodies for chromatography is called immunoaffinity chromatography [8]. This method is very costly and antibodies are not very stable, which restricts the use to smaller-scale analytical, pharmaceutical and medical applications.

Instead of using a complete antibody molecule, only the binding domain of the antibody can be used. Llamas produce antibodies lacking so-called light chains, so only the heavy chains remain (see Figure 1.2). From these chains, the binding region, called the variable heavy-chain region of the heavy-chain antibody, or VHH, can be isolated. These antibody fragments are much more stable than the full-size antibodies, but have similar binding strengths and specificities. Because of the approximately 10-fold lower molecular weight compared to normal, full-size antibodies, the VHH ligands are more efficient in terms of mass of target component adsorbed relative to the mass of ligands required for the separation. Moreover, the fragments can be produced on industrial scale by recombinant *Saccharomyces cerevisiae*. These properties make the VHH ligands promising for large-scale affinity chromatography [9-14].

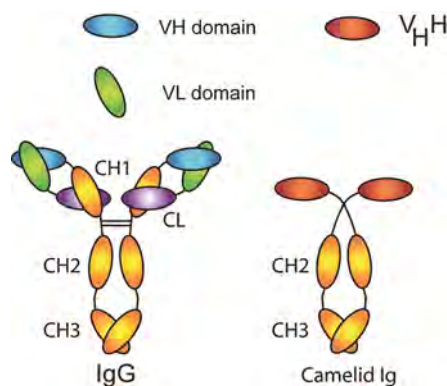


Figure 1.2. Schematic representation of a regular antibody (left) and a camelid antibody (right) with the individual domains: CH1-3 and CL are the constant regions and VH/VHH and VL the variable regions of the heavy (H), and light (L) chains of the antibody (reproduced with permission from BAC (Naarden, The Netherlands)).

Because of the strength of binding in affinity chromatography, an appropriate desorption strategy needs to be developed for product recovery and adsorbent regeneration. Desorption can be achieved by a change in solvent composition, such as salt concentration or acidity.

1.3 Configurations in chromatography

Packed bed chromatography with axial flow is the conventional configuration for chromatography. In most cases porous adsorbent particles are used which are poured into an axial column to form a more or less uniform bed (see Figure 1.3b). The interstitial liquid volume typically comprises about 40% of the total volume, since the particles are packed quite closely. In most cases, the feed stream is led through the column from top to bottom to avoid disturbance of the bed packing. Because of this liquid flow, a pressure drop is developed over the column. Besides the difficulty of handling large pressure drops, softer particles may be compressed and deformed, thus deteriorating the separation. To avoid large pressure drops on an industrial scale, the columns should be short and wide instead of tall and narrow. In addition, fluids that contain particulate matter or components prone to cause fouling (such as proteins), may induce clogging of the interstitial pores between the stationary phase particles, thus leading to reduction of the flow, or an increase of the pressure drop required for maintaining the same flow rate.

A variation of the axial flow column for packed bed chromatography is the radial flow column (see Figure 1.3c). In this column the particles are poured in between two concentric cylinders. Flow is usually directed from the outside inwards, but can also be directed from the inside outwards. The bed length is in this case horizontal and can be quite short, resulting in a low pressure drop. The column can be scaled up vertically by using longer concentric cylinders as opposed to the axial flow column, which needs to be scaled up horizontally.

Because the fluid flow in the packed bed is almost plug flow, the dispersion in the direction of the flow is small, and the number of theoretical equilibrium stages is large. The separation of target components from the feed is therefore efficient. However, because of the narrow channels between the particles, packed beds cannot be used directly with a feed that contains a significant amount of particulate material, or other material that may stick to the particles, like fat globules.

Adsorbent particles can also be used in a stirred tank for batch or finite bath adsorption (see Figure 1.3a). Batch adsorption is often used to determine the equilibrium behaviour and adsorption kinetics. This configuration is only economically feasible if the adsorption of the target component to the ligand is very strong. The particles have to be recovered from the vessel (e.g., by microfiltration) and washed before the component can be desorbed. Desorption in batch configuration is

not favourable, because the target component will be hardly concentrated or may even be diluted.

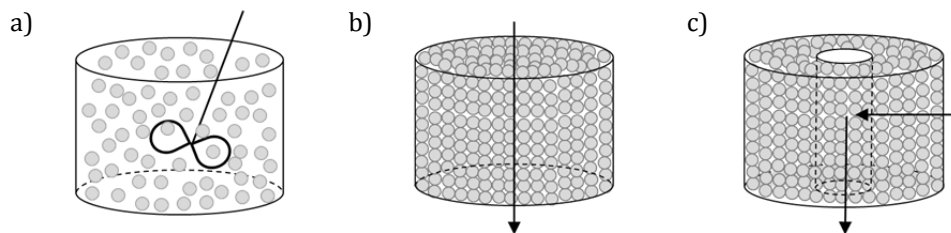


Figure 1.3. Schematic representations of batch adsorption (a), axial packed bed adsorption or axial flow chromatography (b), and radial packed bed adsorption or radial flow chromatography (c).

Besides the packed bed configurations, particles can also be suspended in a fluidized or expanded bed allowing particulate matter to pass through the column. In most cases, desorption of the target component is performed in a packed bed configuration, due to the high resolution and smaller volumes of desorption buffer required to release the target component. Also magnetic particles may be used which are captured with a magnetic field.

It is also possible to use a stack of membranes or a monolith instead of adsorbent particles. A monolith is a solid material, which is highly porous, and in which pores are highly interconnected. Porous membranes and monoliths are similar to packed beds, except for the lack of intraparticle diffusion as in porous particles. Because of large through-pores, the pressure drop is generally lower than for packed beds. A drawback of membranes and monoliths is that the adsorption capacity is usually lower than for a packed bed of porous particles.

1.4 Research aim

Preparative affinity chromatography is a very selective method of separation. However, it is not a continuous process, it is labour intensive and requires significant amounts of solvents. On top of that, the affinity ligands are often costly. As a consequence, affinity chromatography is mainly used in the pharmaceutical industry. The aim of the research described in this thesis was to investigate the potential of affinity chromatography for isolating low-concentrated (minor) proteins in the food industry. The streams in the food industry are usually much larger and less pure than in the pharmaceutical industry and many target components are present in low concentrations. Besides, food products offer an economical challenge as compared to

pharmaceuticals, since the prices of the products are usually much lower than for pharmaceuticals. In this research we identified the opportunities and challenges for successful application of VHH ligand affinity chromatography on a large scale in the food industry. In addition, we set up a window of operation regarding different aspects of affinity chromatography, such as the choice of resin, process yields and process design.

1.5 Thesis outline

Bovine serum albumin (BSA) was chosen as a model minor protein in dairy streams. A BSA-binding VHH ligand was used. Bovine whey was chosen as a model feed stream for the food industry. The purification of BSA from bovine whey is described in **Chapter 2**. The adsorption isotherm of BSA binding to the affinity resin was measured, and a complete purification process with adsorption, washing and desorption steps was set up and demonstrated on lab-scale for pure BSA solutions with high and low BSA concentration and for bovine whey.

To design an affinity chromatography process, characterization of the ligand is essential. In **Chapter 3**, the binding reaction between the VHH ligand and BSA is investigated using isothermal titration calorimetry. With this method it is possible to accurately determine the thermodynamics of binding over a range of pH and temperature values. This information can be used to find the optimal conditions for adsorption and desorption.

A ligand has to be immobilized onto a stationary phase before it can be used in affinity chromatography, and the immobilization itself can strongly influence the performance of the system. Many adsorbents with different backbone materials and immobilization chemistries are commercially available. In **Chapter 4**, we compare several different resins for packed bed chromatography and propose a method to determine which adsorbent is best based on process requirements.

Compared to for example adsorbents for ion exchange chromatography, the adsorption capacity of affinity chromatography adsorbents is relatively low. The feasibility of a cost-efficient chromatography process relies on efficient use of the adsorbent. In **Chapter 5** we describe the challenges to be overcome in immobilization of ligands such as the VHH used in this research.

Most research on affinity chromatography is based on the use of axial flow columns. However, a radial flow column may be an option for scale-up. In **Chapter 6** the similarities and differences between the two configurations are described using experiments and mathematical modelling.

Chapter 7 concludes this research with a general discussion on the opportunities and challenges for affinity chromatography in the food industry. A few other popular configurations for affinity chromatography, such as membrane chromatography, are described and the research discussed in the preceding chapters is put into a broader perspective.

References

1. IUPAC. 2012. *Gold Book*. [cited: 2012, April 26]. Available from: <http://goldbook.iupac.org/>.
2. Sakodyskii, K. 1972. *The life and scientific works of Michael Tswett*. Journal of Chromatography A, 73(2): p. 303-360.
3. Livengood, J. 2009. *Why was M. S. Tswett's chromatographic adsorption analysis rejected?* Studies In History and Philosophy of Science Part A, 40(1): p. 57-69.
4. Engelhardt, H. 2004. *One century of liquid chromatography: from Tswett's columns to modern high speed and high performance separations*. Journal of Chromatography B, 800(1-2): p. 3-6.
5. Gustavsson, P.-E. and P.-O. Larsson. 2006. *Support materials for affinity chromatography*, in *Handbook of Affinity Chromatography*, D.S. Hage, Editor. Taylor & Francis: Boca Raton p. 15-34.
6. Hage, D.S. 2006. *Handbook of affinity chromatography*. 2nd ed. Chromatographic science series. Vol. 92. Taylor & Francis: Boca Raton. 944p.
7. Urh, M., et al. 2009. *Affinity chromatography: general methods*, in *Methods in Enzymology*. Academic Press. p. 417-438.
8. Hage, D.S. and T.M. Phillips. 2006. *Immunoaffinity chromatography*, in *Handbook of Affinity Chromatography*, D.S. Hage, Editor. Taylor & Francis: Boca Raton. p. 127-172.
9. Hamers-Casterman, C., et al. 1993. *Naturally occurring antibodies devoid of light chains*. Nature, 363: p. 446-448.
10. Frenken, L.G.J., et al. 2000. *Isolation of antigen specific Llama VHH antibody fragments and their high level secretion by Saccharomyces cerevisiae*. Journal of Biotechnology, 78(1): p. 11-21.
11. Muyldermans, S. 2001. *Single domain camel antibodies: current status*. Reviews in Molecular Biotechnology, 74(4): p. 277-302.
12. Dumoulin, M., et al. 2002. *Single-domain antibody fragments with high conformational stability*. Protein Science, 11(3): p. 500-515.
13. Verheesen, P., et al. 2003. *Beneficial properties of single-domain antibody fragments for application in immunoaffinity purification and immuno-perfusion*

- chromatography*. Biochimica et Biophysica Acta (BBA) - General Subjects, 1624(1-3): p. 21-28.
14. Harmsen, M. and H. De Haard. 2007. *Properties, production, and applications of camelid single-domain antibody fragments*. Applied Microbiology and Biotechnology, 77(1): p. 13-22.

Isolation of bovine serum albumin from whey using affinity chromatography

Abstract

The adsorption of bovine serum albumin (BSA) to a chromatography resin with immobilized llama antibody fragments as affinity ligands was investigated using batch adsorption and packed bed chromatography. The maximum adsorption capacity of the affinity resin was 21.6 mg/ml with a Langmuir equilibrium constant of 20.4 ml/mg ($1.37 \times 10^6 \text{ M}^{-1}$). Using packed bed chromatography, BSA was adsorbed from pure solutions with 1 mg/ml BSA and 0.1 mg/ml BSA. Full recovery of BSA was achieved by desorption at pH 3. BSA could be concentrated to 6.9 and 7.7 mg/ml for the 1 mg/ml and 0.1 mg/ml experiment respectively, when pooling the desorption fractions with a concentration higher than 1 mg/ml. These pools comprised over 95% of the total desorption peak for both concentrations. BSA was also isolated from filtered bovine cheese whey containing less than 0.1 mg/ml BSA. Together with BSA, β -lactoglobulin and α -lactalbumin concentrations were analysed. The purified BSA was in this case concentrated to 7.4 mg/ml BSA for the desorption fractions with a concentration higher than 1 mg/ml. This pool comprised over 90% of the total BSA desorbed. The presence of other components in the feedstock did not alter the adsorption capacity of the affinity resin. Trace amounts of β -lactoglobulin and an unidentified component were found in the desorption peak; no α -lactalbumin was found. The results show that high recovery combined with high purity can be obtained using affinity chromatography; the affinity process presented in this chapter can be easily translated to the isolation of other minor proteins in the food industry.

This chapter will be submitted as: Besselink, Tamara; Janssen, Anja E.M.; and Boom, Remko M. Isolation of bovine serum albumin from whey using affinity chromatography.

2.1 Introduction

Whey is a by-product in the dairy industry that has become an increasingly interesting source of proteins with high nutritional or pharmaceutical value. Whey is a dilute solution, containing less than 7% (w/w) dry matter. Only 1% (w/w) protein is present in whey; other components are lactose, fat, minerals and vitamins. The two proteins β -lactoglobulin (β -LG) and α -lactalbumin (α -LA) are the most abundant proteins [1]. Besides these two proteins, other minor proteins are present such as bovine serum albumin (BSA), immunoglobulins and enzymes.

The main challenge in the isolation and purification of specific whey proteins is the low concentration of these proteins and the complexity of whey. Several methods for whey protein purification and fractionation are described in literature. An overview of these methods is for example given by Zydney [2], and El-Sayed and Chase [1]. The most important methods are ion exchange chromatography and membrane filtration; however, these processes are usually not suitable for isolation of individual minor proteins because of their limited selectivity.

Affinity chromatography is a more promising method for the isolation of specific components. In affinity chromatography a ligand attached to a stationary phase (e.g., a bead made of silica or agarose) interacts strongly with the component of interest. To recover the component, it is desorbed using a desorption buffer, usually with a low pH or high salt concentration. Many examples of affinity chromatography exist with various types of ligands and stationary phases. We found several reports on affinity chromatography for protein purification from whey (for example, [3-6]). Heparin affinity chromatography can for example be used to isolate protein fractions or lactoferrin. With immobilized antibodies a specific component can be isolated, but at high costs that limits the use to analytical purposes.

In this research we focus on the use of antibody-derived ligands for selective protein isolation. These ligands are made from the binding domain fragment from antibodies from *Camelidae* species. These antibodies lack so-called light chains [7]. The small binding domain fragment called the VHH (variable heavy-chain region of the heavy-chain antibody) can be isolated from these antibodies. These VHH ligands, with a molecular weight of 12-15 kDa, have high thermal and physical stability, which are important qualities for ligands in bioprocessing. The VHH can be expressed in microorganisms, such as *Saccharomyces cerevisiae* [8, 9], for industrial-scale processes. Like the conventional monoclonal antibodies, the VHH can be raised

against one specific antigen. Therefore, the VHH ligands can be an efficient and cost-effective alternative for conventional immunoaffinity chromatography. Recently, a commercialized resin with immobilized VHH ligands has been investigated by Zandian and Jungbauer [10].

In this study the use of VHH for purification of bovine serum albumin (BSA) from cheese whey is investigated. The VHH ligand was developed for multi-species albumins by BAC (Naarden, The Netherlands) and was provided immobilized onto NHS Sepharose 4 Fast Flow resin (GE Healthcare, Uppsala, Sweden). The adsorption capacity and equilibrium constant were determined with equilibrium measurements using pure BSA solution. The recovery, final concentration and purity of BSA purified from filtered cheese whey were measured to determine whether the chromatography process is suitable for minor protein purification. Furthermore, we investigated the productivity of the purification process.

2.2 Materials and methods

2.2.1 Materials

Bovine serum albumin (BSA) type A3059 ($\geq 98\%$ pure) was purchased at Sigma-Aldrich (Zwijndrecht, The Netherlands). NHS-Sepharose 4 Fast Flow with immobilized multi-species albumin ligand was supplied by BAC BV (Naarden, The Netherlands). Bovine cheese whey was supplied by FrieslandCampina (Amersfoort, The Netherlands). All other reagents used were of analytical grade and purchased at Merck (Darmstadt, Germany). Pure water was obtained from a Milli-Q system (Millipore, Billerica, USA).

2.2.2 Buffer preparation

A phosphate buffer was prepared by mixing 10 mM solutions of Na_2HPO_4 and KH_2PO_4 containing 50 mM NaCl until pH 6.5 was reached. The pH and ionic strength of the phosphate buffer were similar to the values for whey. This phosphate buffer was used as the adsorption buffer for the experiments with pure BSA solutions and as the wash buffer for all experiments. The desorption buffer was prepared by acidifying a 0.1 M glycine solution with 1 M HCl until a pH of 3 was reached. Prior to the chromatography experiments the buffers were filtered over a 0.22 μm nylon filter under vacuum.

2.2.3 Batch uptake experiments

A resin slurry was prepared by repetitive washing and draining the affinity resin over a 0.45 µm filter. Most of the liquid was removed by applying a vacuum over the filter. The remaining resin is called the drained resin. The resin was washed 3 times with Milli-Q water and 3 times with 10 mM phosphate buffer with 50 mM NaCl, pH 6.5. Then buffer was added to the desired dilution (25-50% resin). One millilitre of drained resin corresponds to approximately 1.1 ml of packed resin. The resin slurry was then transferred to tubes and BSA solutions of 0 to 5 mg/g were added. The tubes were then gently rotated for 24 hours at room temperature. Afterwards, the resin was allowed to settle and the protein content of the supernatant was measured using a UV spectrophotometer at 280 nm.

A non-linear fit between the equilibrium BSA concentration and the amount of adsorbed BSA was performed using the Langmuir equation:

$$q = \frac{q_m K_a C}{1 + K_a C} \quad (2.1)$$

In Equation 2.1, q represents the amount of BSA bound to the resin, q_m the maximum adsorption capacity of the resin, c the concentration of unbound BSA in the surrounding fluid, and K_a the equilibrium constant defined as the adsorption rate constant divided by the desorption rate constant.

The amount of BSA adsorbed to the resin seemed to increase further than the predicted isotherm describes, which may suggest multilayer adsorption. Therefore, also a BET adsorption isotherm was used to fit the batch uptake data:

$$q = \frac{q_m K_a C}{\left(1 + K_a C - \frac{C}{C_s}\right) \left(1 - \frac{C}{C_s}\right)} \quad (2.2)$$

In Equation 2.2, q represents the amount of BSA bound to the resin, q_m the maximum monolayer adsorption capacity of the resin, c the concentration of unbound BSA, K_a the equilibrium constant and c_s the saturation concentration of BSA.

2.2.4 Packed bed adsorption experiments

Packed bed experiments were performed using a Tricorn 5/50 column attached to an Äkta purifier 100 system from GE Healthcare (Uppsala, Sweden). The height of the resin bed was 4.75 cm. Proper packing of the column was evaluated by determining

the asymmetry of the retention peak of 1-2 v/v% acetone in ultrapure water at a superficial liquid velocity of 30 cm/h. According to the manufacturer's specifications the asymmetry should be above 0.8 and below 1.5. When the asymmetry was outside of this range, the column was disassembled and re-packed. Between experiments, the column was stored at 4°C in 20% ethanol in Milli-Q water.

BSA solutions of 1 mg/ml and 0.1 mg/ml were used as a feed solution as well as a sample of bovine cheese whey. The BSA solutions were filtered under vacuum over a 0.45 µm PVDF filter (Steritop, Millipore, Billerica, USA). The cheese whey had been frozen at -18°C prior to use. Before use, the whey was thawed and centrifuged for 3 minutes at 5000 rpm and filtered under vacuum over a 0.45 µm PVDF filter (Steritop, Millipore, Billerica, USA) with a glass pre-filter. The pre-filter had to be replaced several times during filtration.

For the experiments with a BSA concentration of 0.1 mg/ml and for the whey experiments, the BSA solution or whey was cooled in a water bath to a temperature of approximately 9°C. The column was cooled by wrapping a tube connected to the water bath around the column and insulating the assembly with aluminium foil. The temperature inside a similar column filled with water was approximately 10°C. This cooling prevented potential microbial growth which could otherwise have occurred at the relatively long loading time of up to 800 minutes.

Before each experiment, the column was rinsed with at least 3 column volumes (CV) of Milli-Q water and subsequently with phosphate buffer until a stable conductivity signal was reached. The feed solution was pumped over the column via the system pump. To avoid protein loss, the in-line filter was removed from the Äkta system. The flow rate was 0.5 ml/min throughout the experiment.

Protein permeating through the column was detected using the Äkta's in-line UV detector at 280 nm. After adsorption, the column was rinsed with several column volumes of phosphate buffer (4 CV for 1 mg/ml BSA, 6 CV for 0.1 mg/ml BSA and 10 CV for whey).

The UV absorbance data from the Äkta were converted to BSA concentrations using a calibration curve for the pure BSA solutions. This curve was obtained by measuring the stable absorbance signal of BSA samples at concentrations ranging from 0 to 20 mg/ml without attaching a column. However, using this curve the maximum outlet concentration in the adsorption phase of the experiment with 1 mg/ml BSA was found to be overestimated by approximately 0.05 mg/ml. For the experiment with 0.1

mg/ml BSA this value was overestimated by approximately 0.02 mg/ml. We corrected the calibration curve accordingly to be able to calculate the BSA recovery.

For the cheese whey experiments fractions were taken and frozen at -18°C until they were analysed using HPLC. The average eluate volume of each sample was used to plot the concentration profile.

2.2.5 HPLC analysis

The levels of BSA and the major whey proteins α -lactalbumin and β -lactoglobulin were determined using RP-HPLC. A Surveyor HPLC system by Thermo Scientific (Waltham, USA) was used with a Polymer Labs PLRP-S column (300 Å, 8 μm , 150 \times 4.6 mm). The method used was slightly adapted from the method supplied by the manufacturer. Solvent A was a solution of 0.1% trifluoroacetic acid in ultrapure water, solvent B was a solution of 0.1% trifluoroacetic acid in acetonitrile. Elution took place using the following gradients of A: 65-62%, 0-8 minutes; 62-68%, 8-16 minutes; 58-54%, 16-22 minutes; 54-0%, 22-22.5 minutes; 0-0%, 22.5-23.5 minutes; 65-65%, 23.5-29.5 minutes. A UV detector at 220 nm was used for protein quantification.

2.3 Results and discussion

2.3.1 Batch uptake experiments

With equilibrium batch uptake experiments the characteristics of the adsorption of BSA to the immobilized ligand can be determined. We incubated the resin with BSA for approximately 24 hours, which was long enough for diffusion and adsorption of BSA as was found in prior (unpublished) experiments. The characteristics that can be determined are the maximum adsorption capacity of the resin, q_m , and the equilibrium constant, K_a . The equilibrium constant is equal to the adsorption rate constant divided by the desorption rate constant. A high K_a value therefore indicates strong binding.

The maximum adsorption capacity q_m was 23.8 mg BSA/g of drained resin, which corresponds to 21.6 mg BSA/ml of packed resin (see Equation 2.1 and Figure 2.1). This value is similar to the adsorption capacity of Cibacron Blue Sepharose from the same manufacturer (GE Healthcare, Uppsala, Sweden), a resin with an immobilized synthetic dye.

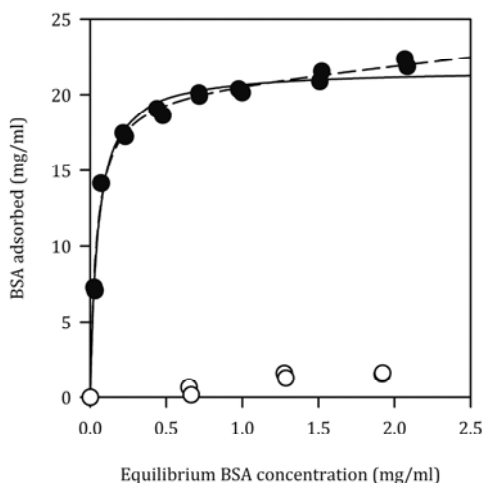


Figure 2.1. BSA adsorbed to the affinity resin as a function of equilibrium BSA concentration with 10 mM phosphate buffer, 50 mM NaCl pH 6.5 (●) and 0.1 M glycine buffer pH 3 (○) at room temperature after 24 hours of adsorption. The solid line represents the Langmuir fit with $q_m = 21.6$ mg/ml and $K_a = 20.4$ ml/mg; the dashed line represents the BET fit with $q_m = 22.5$ mg/ml, $K_a = 23.7$ ml/mg, $c_s = 24.4$ mg/ml.

The isotherm depicted in Figure 2.1 indicates an equilibrium constant (K_a , see Equation 2.1) value of 20.4 ml/mg or approximately 1.37×10^6 M⁻¹ (the molecular weight of BSA is approximately 67 kDa). The adsorption kinetics of the VHH ligand were also characterized by the manufacturer BAC (Naarden, The Netherlands) using Surface Plasmon Resonance (SPR). According to their measurements the ligand has a K_a value of 3.84×10^7 M⁻¹ or approximately 573 ml/mg, which indicates a higher binding strength than measured with our uptake experiments. There are several possibilities to explain the difference between the two values. First, the adsorption buffers and immobilization method used for SPR were different from those used for the batch experiments. Second, in the pores of a chromatography resin, steric hindrance may occur, by blocking of pores by adsorbed protein, and by ligands being immobilised too close to each other to allow a protein molecule to be bound on each ligand. The ligand density is very low in SPR so steric hindrance is in that case unlikely. Third, the immobilization method and material are different and these aspects influence the binding kinetics.

Zandian and Jungbauer also found a lower value for the binding strength in batch uptake experiments compared to SPR [10]. They ascribed this mainly to the slow diffusion in the resin, which is not present in the SPR measurement. However, they have measured the adsorption in time, while in our study we only measured

equilibrium data after allowing a considerable time for diffusion. Therefore, diffusion limitation is probably not the cause of the differences we found here.

The adsorption data have also been fitted to the BET model, because the curve seems to show some form of multilayer sorption. In the case of BSA the assumption that only monolayer adsorption takes place may not be valid since BSA is known to form dimers [11]. It is therefore possible that BSA does not only adsorb to the ligand, but also binds to other BSA molecules in the resin particle, which results in multilayer adsorption. The BET model takes the possibility of protein association or aggregation into account. The values found for the BET fit are maximum adsorption capacity $q_m = 22.5$ mg/ml packed resin, $K_a = 23.7$ ml/mg, and $c_s = 24.4$ mg/ml packed resin (see Equation 2.2 and Figure 2.1). The deviation between the two adsorption models, Langmuir and BET, becomes most apparent at BSA concentrations above 1.5 mg/ml. For minor component separation, the Langmuir isotherm would therefore suffice.

The adsorption of BSA to the affinity resin was also measured with the desorption buffer (Figure 2.1). The amount of BSA adsorbed was very low in this buffer, so the desorption buffer is effective.

2.3.2 *Packed bed experiments with pure BSA solution*

The adsorption of BSA to the immobilized ligand was also studied using packed bed chromatography. In Figure 2.2 the outlet BSA concentration as a function of the outlet volume is shown. At the start of the experiment a BSA solution is applied and BSA is adsorbed to the column. Somewhat later BSA starts to break through and finally the outlet concentration is equal to the inlet concentration. The little 'hump' at the start of the curve may be due to mass transfer limitation: some of the BSA molecules entering the column may not have had enough time to diffuse into the beads and adsorb. After full breakthrough, the inlet solution is switched to the washing buffer and so the non-adsorbed BSA is flushed from the column until the outlet concentration reaches zero. The inlet solution is changed to desorption buffer and the adsorbed BSA is released in a tall and narrow peak.

The total area underneath the chromatogram should represent the total amount of BSA applied to the column if all BSA is desorbed from the column. The area underneath the adsorption and washing stage is due to column overloading and represents BSA that was not adsorbed by the column. The area underneath the desorption peak was adsorbed and later released.

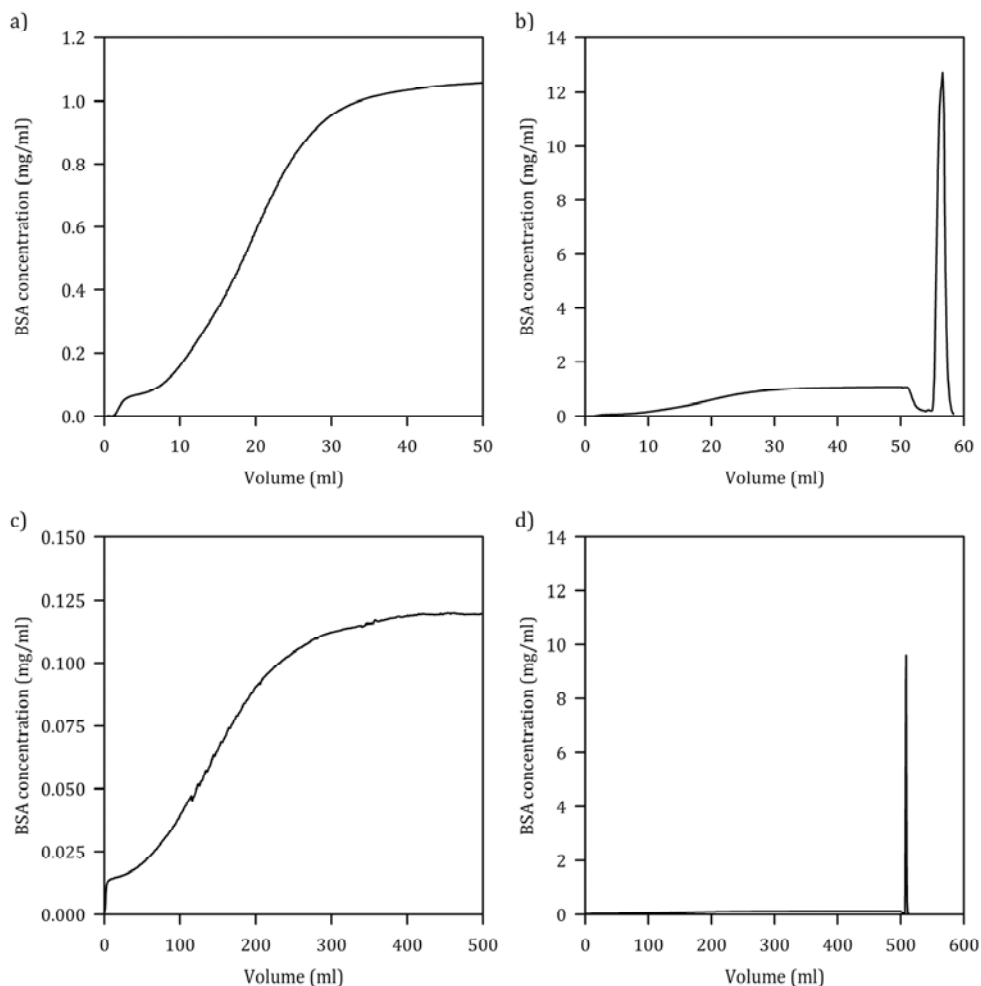


Figure 2.2. BSA outlet concentration as a function of outlet volume. The BSA concentrations of the feed solution were 1 mg/ml (a and b, room temperature) and 0.1 mg/ml (c and d, ~10°C). Adsorption and washing with 10 mM phosphate buffer, 50 mM NaCl, pH 6.5, desorption with 0.1 M glycine pH 3 at a flow rate of 0.5 ml/min.

For the experiment with approximately 1 mg/ml BSA we applied approximately 57 mg in total, and the area underneath the chromatogram represents approximately 53 mg. For the 0.1 mg/ml experiment we applied 59 mg of BSA and calculated a recovery of 60 mg. In both cases we may assume total recovery because the difference between BSA applied and calculated is less than 10%.

From Figure 2.2 we may conclude that the BSA sample in the desorption peak is more concentrated than the initial sample. For the high concentration experiment a total of 18.2 mg of BSA is desorbed from the column. Since the column volume is 0.93 ml, the adsorption capacity equals 19.5 mg/ml packed resin. This is in accordance with the equilibrium adsorption capacity found in the adsorption isotherm in Figure 2.1. If we would pool the entire desorption peak, the concentration would be approximately 3.7 mg/ml. If we would only pool the fractions with a concentration higher than the feed concentration of 1 mg/ml, the concentration would be approximately 6.9 mg/ml. This part of the desorption peak comprises 96.7% of the total peak.

For the low concentration experiment 17.2 mg of BSA is desorbed, which equals 18.5 mg/ml packed resin, which is slightly higher than expected from the isotherm. Also here the BSA is more concentrated in the desorption peak: approximately 2.69 mg/ml for the entire peak and 7.7 mg/ml for the part of the peak higher than 1 mg/ml (95.6% of the entire peak). This indicates a concentration factor of up to 77. For minor component separation, it is crucial that the component can be retrieved in a much more concentrated form.

2.3.3 *BSA adsorption from filtered whey*

BSA was also purified from 400 ml bovine cheese whey that had been frozen prior to use. We filtered the whey prior to the purification because of the particulate matter and HPLC analysis of the samples. Filtration after the packed bed adsorption could lower the amount of proteins present in the sample and would thus introduce a source of experimental error in the HPLC analysis. The concentrations of the major whey proteins β -LG and α -LA were measured as well as the BSA concentration. The initial concentrations in the filtered whey sample were 2.3 mg/ml for β -LG, 0.5 mg/ml for α -LA and 0.1 mg/ml for BSA. Normally, the concentrations of these proteins are higher in whey. Some of the protein probably precipitated due to freezing and was removed in the following filtration.

In Figure 2.3a the chromatograms for BSA, β -LG and α -LA are shown. In the adsorption phase up to 400 ml outlet volume breakthrough of all three proteins is observed. Then the concentrations drop to zero due to washing. At approximately 410 ml desorption starts and it is clearly visible that BSA elutes from the column in a sharp peak.

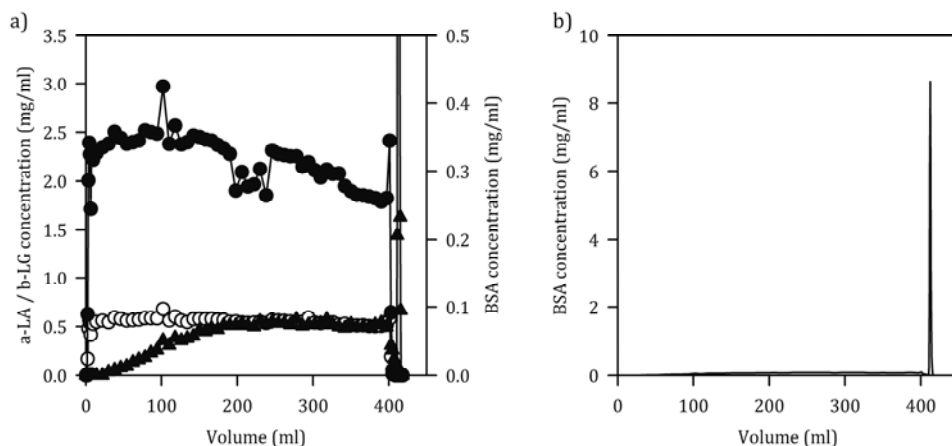


Figure 2.3. α -LA (\circ), and β -LG (\bullet ; both left Y-axis) and BSA concentration (\blacktriangle , right Y-axis) as a function of outlet volume (a); BSA concentration as a function of outlet volume (b). Adsorption with filtered whey, washing with 10 mM phosphate buffer, 50 mM NaCl pH 6.5 and desorption with 0.1 M glycine pH 3 at a flow rate of 0.5 ml/min at approximately 10°C.

2.3.3.1 Adsorption and washing

In the adsorption phase (see Figure 2.3a) we can clearly see that BSA is adsorbed to the column, and this is proven in the desorption peak in the final stage of the chromatography process. Both α -LA and β -LG break through sooner than BSA. There are some fluctuations in the β -LG concentration, the reason for this fluctuation is unknown.

At the washing stage, the protein concentrations drop significantly. At the end of the 10 CV washing stage, the protein concentrations were 0.008 mg/ml for β -LG and 0.014 mg/ml for BSA, α -LA was not present. The higher concentration for BSA in the washing stage is an indication that BSA is more strongly retained by the column than the other proteins. The washing stage could have been prolonged to remove all proteins from the column. However, 10 CV volumes of washing buffer is already more than for the experiments with pure BSA solutions (4 and 6 CV for 1 mg/ml and 0.1 mg/ml BSA). Washing is clearly slower for the whey experiment than for pure BSA, indicating that all proteins are somehow more strongly retained by the column. It is possible that unbound proteins inhibit the diffusion of proteins from within the particle, but the exact reason for the longer washing stage is unknown. It is however important to note the large wash volume, because in industrial-scale applications, washing and equilibration may thus require larger amounts of buffer than expected. This does not only reduce the productivity of the column, but it also requires large

buffer storage tanks and results in significant waste streams. In this experiment we applied approximately 400 CV of whey and 10 CV of washing does not seem much. However, at 200 ml (approximately 200 CV), the outlet BSA concentration has reached the inlet concentration and the adsorption stage could have been terminated. It is even more common to terminate adsorption and switch to washing at 10% breakthrough of the target component, which in this case would be at 40 CV. In that case, the volume required for washing would equal 25% of the sample volume. The washing stage is therefore very important. We will further elaborate on this issue in Section 2.3.4.

2.3.3.2 *Desorption, purity and recovery*

The desorption peak shows a maximum BSA concentration of approximately 8.6 mg/ml (see Figure 2.3b). The amount of BSA in the desorption peak equals 14.7 mg, which would correspond to 15.8 mg/ml packed resin. According to the Langmuir isotherm shown in Figure 2.1, we would expect a capacity of approximately 14.5 mg/ml. The deviation is most likely due to experimental error, for example because of the different protein quantification methods (direct UV measurement versus HPLC). We may therefore conclude that the presence of other components in whey does not significantly alter the adsorption capacity of the resin.

The BSA concentration in the total desorption peak was 2.5 mg/ml, and 7.4 mg/ml for the part of the peak higher than 1 mg/ml (91.9% of the total peak). This result is similar to the 6.9 mg/ml and 7.7 mg/ml obtained in the pure BSA experiments.

A little peak of β -LG was present in the desorption peak of BSA. The total amount was less than 0.02 mg with the highest concentration measured being 0.007 mg/ml. Unfortunately this minor amount of β -LG was eluted together with BSA. The β -LG must have been retained to the column, but the adsorption is expected to be non-specific. A possible reason could be that β -LG diffused into a particle and then got 'trapped' when BSA molecules were adsorbed. The β -LG could not diffuse out of the particle until some BSA molecules were desorbed, which only happened in the final stages of the process. This could also explain the larger wash volume required for whey compared to pure BSA solutions. In former experiments (not presented in this chapter) also minor quantities of β -LG were present in the desorption peak. The reason that α -LA was not observed is probably because of the almost five-fold lower concentration of α -LA compared to β -LG.

Other than a trace of β -LG, an unidentified component was seen in the HPLC chromatograms of the desorption fractions. The retention time for BSA for the HPLC method used was approximately 15 minutes and the unknown component eluted at around 18 minutes. The component was not seen on the HPLC chromatograms of whey, probably because of its low concentration. In terms of HPLC peak area, the unknown component comprised less than 5% of the BSA peak area. We tested whether the peak originated from the buffer, but this was not the case. Because we do not know what the component is, we cannot calculate the exact purity of BSA. It is, however, likely that the purity well exceeds 90% based on the proteins we measured.

By dividing the amount of each protein in the column eluate by the amount of the protein present in the whey sample applied we could calculate the recovery of each protein. For β -LG the recovery was 97%, for α -LA and BSA both 104%, which represents full recovery taking into account experimental error.

2.3.4 *Optimization of column productivity*

In this chapter we measured full breakthrough curves, which is not common for industrial-scale processes. As mentioned in Section 2.3.3.1, the adsorption stage in these processes is often terminated at 10% breakthrough, which is a probably a good choice for high-value products that have been produced specifically. Examples are antibodies, drugs, and fermentation products. However, in the case of minor component separation from large streams, the 10% breakthrough value may not be the most ideal in terms of productivity.

In Figure 2.4 the productivity and the yield of the adsorption processes for 0.1 mg/ml and 1 mg/ml BSA solutions, as discussed in Section 2.3.2, are shown as a function of BSA breakthrough. We define the productivity here as the amount of BSA that can be purified with the given column divided by the process time. The figures were generated with the same data; no model was applied. The little 'hump' from the breakthrough curves (see Figure 2.2) is somewhat magnified in the productivity curve. In Section 2.3.3.1 we state that the washing stage takes at least 10 CV for BSA purification from whey. Desorption takes another 10 CV and then the column needs to be regenerated for the next batch, which takes at least 4 CV. Apart from the adsorption phase, a total of 24 CV of buffers is required for the process, which is part of the process time. The adsorption time naturally varies with the degree of BSA breakthrough and is directly calculated from the chromatograms shown in Figure 2.2. We assume no influence of the degree of breakthrough on the length of the washing,

desorption and regeneration steps. The yield is calculated from the chromatograms as the amount of BSA adsorbed divided by the amount of BSA applied, since we assume full recovery of the BSA adsorbed. The flow rate equals 0.5 ml/min throughout the process.

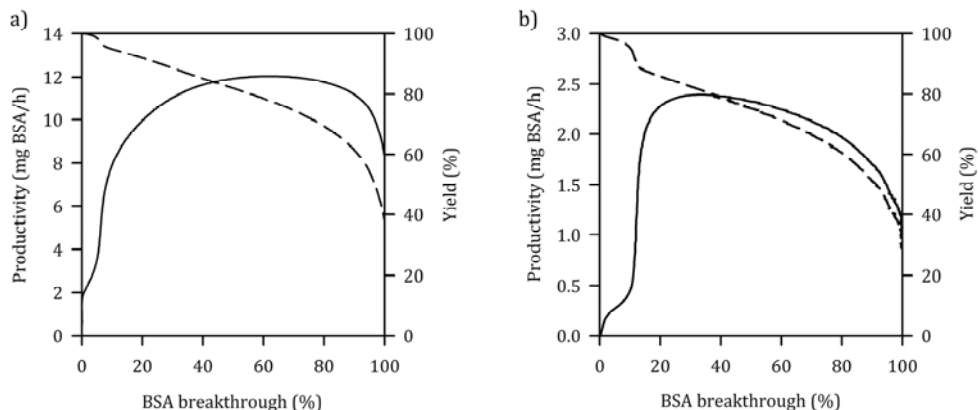


Figure 2.4. Productivity (solid lines, left axis) and yield (dashed lines, right axis) as a function of BSA breakthrough for 1 mg/ml BSA solution (a), and 0.1 mg/ml BSA solution (b). Data were calculated using the chromatograms of Figure 2.2.

From Figure 2.4 it is clear that the productivity of the process is about five times higher with the higher BSA concentration, even though the equilibrium adsorption capacities are not that far apart (18.5 mg/ml resin for 0.1 mg/ml BSA and 19.5 mg/ml resin for 1 mg/ml BSA). The reason for the higher productivity for higher feed concentration is that less feed solution is required to saturate the column, resulting in a lower adsorption time than for a low feed concentration. When the 'traditional' 10% breakthrough point would be used, the productivities would have been 7.9 mg/h for the high concentration and 0.5 mg/h for the low concentration, with 95% yield for both cases. The optimal productivity would be 62% breakthrough resulting in 12 mg/h for the high concentration with 78% yield, and 33% breakthrough resulting in 2.4 mg/h with 81% yield for the low concentration. The productivities are very low, because of the small-scale column used. However, the productivity and yield calculations show that it is worthwhile to determine the breakthrough point at which the adsorption process should be terminated to obtain maximum productivity.

2.4 Conclusions

In this chapter we have shown that the affinity resin with immobilized VHH ligands provides a highly selective tool for purification of BSA, leading to concentration factors of more than an order of magnitude. Full recovery of BSA can be obtained with an acidic desorption buffer. When a real feedstock such as bovine cheese whey is used, BSA can also be retrieved in a much more concentrated and purified form.

The degree of protein breakthrough at which the adsorption process is terminated has a significant influence on the productivity of the process. Instead of applying the commonly used 10% breakthrough, an optimum can be found by calculating the productivity of the process as a function of protein breakthrough, which can result in more efficient use of the chromatography column. This is of particular interest for purification processes where the feed is not specifically produced for the target protein, for example for otherwise invaluable waste streams.

Since the VHH ligands can be produced for many different target components, the purification of other components from whey or other feedstock in the food industry can be envisaged. Because of the high selectivity, this method is particularly useful for minor component isolation.

Acknowledgements

This project was supported by FrieslandCampina (Amersfoort, The Netherlands), DSM Biotechnology Center (Delft, The Netherlands), BAC BV (Naarden, The Netherlands) and SenterNovem (project IS054084).

References

1. El-Sayed, M. and H. Chase. 2011. *Trends in whey protein fractionation*. Biotechnology Letters, 33(8): p. 1501-1511.
2. Zydney, A.L. 1998. *Protein separations using membrane filtration: new opportunities for whey fractionation*. International Dairy Journal, 8(3): p. 243-250.
3. Puerta, Á., et al. 2002. *Adsorption kinetics of β -lactoglobulin on a polyclonal immunochromatographic support*. Journal of Chromatography A, 953(1-2): p. 17-30.
4. Tu, Y.Y., et al. 2002. *Characterization of lactoferrin (LF) from colostral whey using anti-LF antibody immunoaffinity chromatography*. Journal of Food Science, 67(3): p. 996-1001.

5. Chen, L., et al. 2007. *Isolation of lactoferrin from acid whey by magnetic affinity separation*. Separation and Purification Technology, 56(2): p. 168-174.
6. Ben Ounis, W., et al. 2008. *Separation of minor protein components from whey protein isolates by heparin affinity chromatography*. International Dairy Journal, 18(10-11): p. 1043-1050.
7. Hamers-Casterman, C., et al. 1993. *Naturally occurring antibodies devoid of light chains*. Nature, 363: p. 446-448.
8. Verheesen, P., et al. 2003. *Beneficial properties of single-domain antibody fragments for application in immunoaffinity purification and immuno-perfusion chromatography*. Biochimica et Biophysica Acta (BBA) - General Subjects, 1624(1-3): p. 21-28.
9. Harmsen, M. and H. De Haard. 2007. *Properties, production, and applications of camelid single-domain antibody fragments*. Applied Microbiology and Biotechnology, 77(1): p. 13-22.
10. Zandian, M. and A. Jungbauer. 2009. *Engineering properties of a camelid antibody affinity sorbent for Immunoglobulin G purification*. Journal of Chromatography A, 1216(29): p. 5548-5556.
11. Peters Jr, T. 1995. 7 - *Practical aspects: albumin in the laboratory*, in *All About Albumin*. Academic Press: San Diego. p. 285-318.

The influence of pH and temperature on bovine serum albumin – VHH ligand binding

Abstract

The thermodynamics of the binding reaction between bovine serum albumin and a multi-species albumin VHH (llama antibody fragment) were measured using isothermal titration calorimetry (ITC). The pH was varied between pH 5 and pH 8.5, and the temperature between 20 °C and 50 °C. The equilibrium constant (K_a) showed a maximum at pH 6.5 at 40 °C: $4.86 \times 10^7 \text{ M}^{-1}$. The lowest value for K_a was measured at pH 8.5 at 50 °C: $1.83 \times 10^6 \text{ M}^{-1}$, which is not enough for efficient desorption. The Gibbs free energy of binding (ΔG) was on average -10 kcal/mol, ranging between -9.1 kcal/mol (pH 8.5, 20 °C) and -11.0 kcal/mol (pH 5, 50 °C and pH 6.5, 40 °C). Entropy-enthalpy compensation seems to occur, where the enthalpy ΔH becomes more negative with increasing temperature, and the entropy (as $-T\Delta S$) becomes more positive. At higher pH values, the values for ΔH are also more negative, and consequently $-T\Delta S$ more positive. The compensation between entropy and enthalpy seems logical, since the binding of the two proteins results in a more negative value for ΔH , but at the expense of conformational freedom, hence the positive value for $-T\Delta S$.

3.1 Introduction

The current demand for pure specialty compounds requires highly specific purification steps, such as affinity chromatography. A promising ligand for this type of chromatography is a fragment from a llama antibody, called the VHH (variable heavy-chain region of the heavy-chain antibody) [1-6]. This small-sized protein of approximately 12 to 15 kDa is heat and acid stable and can bind antigens with similar binding strength as the often used monoclonal antibodies. Furthermore, it is possible to produce these VHH ligands on a large scale in a *Saccharomyces cerevisiae* strain [2, 5] after immunisation and isolation. The combination of these properties makes the VHH ligand a promising ligand for industrial-scale affinity chromatography.

In this study we investigated the binding between bovine serum albumin (BSA) and a multi-species albumin VHH. According to the VHH ligand's manufacturer (BAC BV, Naarden, The Netherlands), the adsorption equilibrium constant, K_a , between the ligand and BSA is $3.84 \times 10^7 \text{ M}^{-1}$ at neutral pH. This value was measured using surface plasmon resonance, which requires ligand immobilisation to a gold surface. This value may be different from the situation in which the ligand is free in solution or immobilised to a different surface, such as an activated resin, and is likely to depend on pH. Zandian and co-workers determined the equilibrium constants for a commercially available resin with immobilized VHH for IgG purification. The equilibrium constants were $2.38 \times 10^8 \text{ M}^{-1}$ and $2.5 \times 10^7 \text{ M}^{-1}$ using surface plasmon resonance and batch uptake experiments respectively [7]: almost a factor 10 difference. For both the albumin ligand as the IgG ligand the binding between the VHH and the target protein is clearly strong. This is beneficial for protein adsorption, but usually requires harsh desorption conditions: in both cases a buffer of pH 3. Even though the ligand may be stable at these conditions, the target protein may well denature at such harsh conditions.

Even though it is possible to select VHH ligands that allow a relatively high pH for desorption (around pH 4), this still requires large volumes of buffer and therefore large quantities of chemicals. To neutralise the pH for further processing, a base is required, eventually leading to saline solutions which need to be desalted. If it would be possible to use a different method for desorption which does not require chemicals, a significant cost reduction could be achieved.

In 2001, Pérez and co-workers [8] found that the VHH ligand they investigated unfolded reversibly in two stages. The first stage was local unfolding up to 313 K and

global unfolding above 333 K. If the unfolding would result in antigen release, it could be possible to use a relatively mild temperature increase for desorption. In that case, the quantity of chemicals could be reduced and further processing could be simplified, but this obviously depends on the heat stability of the protein that is adsorbed to the VHH ligand. Dolk *et al.* [9] found that a VHH that binds to a synthetic dye shows induced refolding by the dye at elevated temperatures, which may limit the possibilities of using increased temperature for desorption. However, a slight shift in both temperature and pH may still be effective.

To our knowledge, the binding between a VHH ligand and its target protein has not yet been studied as a function of pH and temperature. We studied the adsorption reaction between a multi-species albumin VHH ligand and BSA in detail using isothermal titration calorimetry (ITC). With ITC it is possible to determine the Gibbs free energy ΔG , enthalpy ΔH , entropy ΔS and equilibrium adsorption constant K_a of the adsorption reaction.

3.2 Materials and methods

3.2.1 Materials

BSA (type A3059, $\geq 98\%$ pure lyophilized powder, MW ~ 67 kDa) was purchased at Sigma-Aldrich (Zwijndrecht, the Netherlands) and used as such. The multi-species albumin VHH (MW 12.559 kDa) was provided by BAC BV (Naarden, The Netherlands) in solution with 50 mM sodium phosphate, 0.5 M sodium chloride at pH 7.4. Other reagents were of at least analytical grade. All solutions were prepared with pure water obtained using a Milli-Q system (Millipore, Billerica, USA).

3.2.2 Buffer and sample preparation

Phosphate buffered saline (PBS) was used containing 10 mM phosphate with 137 mM NaCl and 2.7 mM KCl at a pH range between 4 and 8.5. For pH 5 through 8.5, 10 mM of saline Na_2HPO_4 solution was mixed with 10 mM saline KH_2PO_4 solution to achieve the desired pH. For pH 4, a saline solution of 10 mM phosphoric acid and 10 mM Na_2HPO_4 were mixed to reach the desired pH values.

3.2.3 ITC measurements and analysis

The VHH solution was dialysed against the appropriate phosphate buffer using Slide-A-Lyzer Dialysis cassettes with a molecular weight cut-off value of 3.5 kDa (Thermo Fisher Scientific Inc., Waltham, USA). It was not possible to dialyse the VHH solution to pH 4; even dilution prior to dialysis could not prevent the protein solution becoming turbid. The concentrations of the VHH solutions at pH 5, 6 and 8.5 were determined using HPLC with the original VHH solution as a reference (Tosoh TSKgel G2000SWxl 7.8 mm × 30 cm (Tosoh Bioscience, Tokyo, Japan), eluent 30% acetonitrile in Milli-Q water (Millipore, Billerica, USA) with 0.1% trifluoroacetic acid, flow rate 1.5 ml/min at room temperature, detection at 214 nm). For pH 6.5 and pH 7.4, the VHH concentration was determined using UV spectrometry at 280 nm. BSA was dissolved in the same buffer as used for VHH dialysis.

The heat changes due to BSA-VHH adsorption at pH 5, 6 and 8.5 were measured using an ITC₂₀₀ from MicroCal (GE Healthcare, Uppsala, Sweden). The reference cell was filled with degassed Milli-Q water. The sample cell was filled with 200 µl degassed VHH solution and the syringe was filled with 40 µl BSA solution. For pH 6.5 and pH 7.4 a VP-ITC was used from MicroCal (Northampton, USA) with 1.4 ml cell volume and 274 µl syringe volume. The measurement principles are the same for both ITC devices. Time intervals were adjusted to suit each measurement. The VHH and BSA concentration, injection volume and number of injections for each measurement can be found in Table 3.1. For each pH, the ITC measurements were performed at 20 °C (25 °C for pH 6.5 and pH 7.4), 40 °C and 50 °C at least in duplicate.

The heat of dilution of BSA was measured by repeating the measurements with buffer in the sample cell instead of VHH solution. The dilution heats were then subtracted from the BSA-VHH heats. For some measurements, direct subtraction of the dilution heats resulted in a final plateau for the integrated heat plot deviating from zero, which could not result in a proper fit. Therefore, the mean value of the final plateau was subtracted from the curve. Shifting the integrated heat plot along the y-axis does not influence the values of the equilibrium constant K_d , the enthalpy ΔH or the stoichiometry. Because the values of the entropy and Gibbs free energy are derived from these three values, these also do not change. However, this is only valid if this shift in heat does not depend on the molar ratio. Furthermore, using the mean value of the last few points requires that a plateau is reached, to ensure saturation of the ligand in the sample cell. For all the measurements at pH 7.4 a shift was required

which varied between -6.5 and -13 kcal/mol. For other measurements the correction was smaller or zero.

The corrected data were fitted to the one-site binding model in the ITC module of Origin 7 (OriginLab, Northampton, MA, USA) provided by MicroCal (GE Healthcare, Uppsala, Sweden) to obtain values for the reaction enthalpy (ΔH), entropy (ΔS), Gibbs free energy (ΔG) and equilibrium constant (K_d).

Table 3.1. Experimental conditions for the ITC measurements. The measurements for pH 5, 6 and 8.5 were performed with an ITC₂₀₀ (MicroCal, GE Healthcare, Uppsala, Sweden); for pH 6.5 and pH 7.4 a VP-ITC was used (MicroCal, Northampton, USA).

pH	Temp. (°C)	[VHH] (mM)	[BSA] (mM)	Injection volume (μ l)	Number of injections
5	20, 40	0.0125	0.129	1.2	20 ¹
5	50	0.0125	0.129	2	18
6	20, 40	0.0125	0.129	1.2	20
6	50	0.0125	0.129	2	18
6.5	25, 40, 50	0.0084	0.100	7	25
7.4	25	0.0216	0.259	7	25
7.4	40	0.0108	0.259	7	25
7.4	50	0.0109	0.259	7	25
8.5	20, 40, 50	0.0399	0.278	2.4	16

¹ One out of three measurements was done with 16 injections for 20°C and 17 for 40°C.

3.3 Results and discussion

ITC measurements provide insight into the thermodynamics of the adsorption reaction by directly measuring the heat released or adsorbed during this reaction. Small amounts of BSA are titrated into ligand solution and each titration results in a small temperature increase (for exothermic reactions) or decrease (for endothermic reactions) in the sample cell containing the ligand solution. The ITC equipment has to either add or remove heat from the sample cell to maintain the same temperature as the reference cell. These heats are recorded for each injection and, after correcting for the baseline, result in a raw heat plot as in the top section of Figure 3.1. The first negative peaks in this plot indicate that the first part of the reaction is exothermic, later on it becomes endothermic. Integration of each peak results in an integrated heat

plot, see Figure 3.1, bottom section. For more extensive information on ITC, we refer to, for example, [10-13].

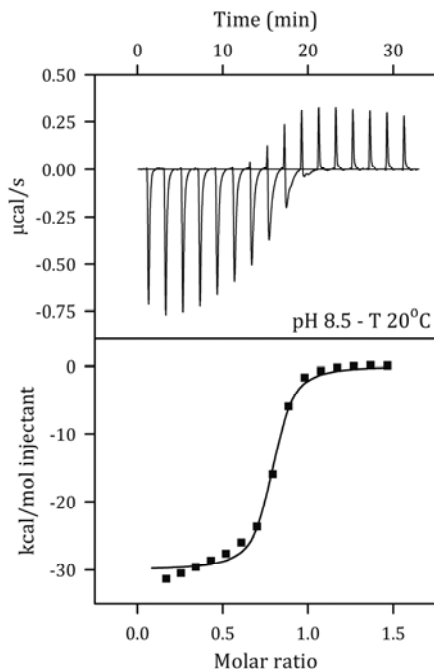


Figure 3.1. Example of an ITC measurement (pH 8.5 at 20°C, see Table 3.1). Top section: raw heat plot with heat adsorbed or released as a function of time, each peak represents an injection with BSA solution into the sample cell containing the VHH. Bottom section: integrated heat of every peak as a function of the molar ratio between BSA and VHH.

Other than the heat of the adsorption reaction, there are other processes that influence the heat signal. These are heat of dilution (of both ligand and BSA), possibly the heat of stirring and the heat of re-conformation (agglomeration, folding/unfolding). The heat of ligand dilution is in this case not taken into account, because the sample cell is much larger than the amount of BSA solution injected. Therefore, the heat of ligand dilution is often regarded as negligible. All the data were, however, corrected for the dilution heat of BSA. There may have been other components, such as lyophilisation salts, present in the BSA sample, which also caused some minor dilution effects. These effects are accounted for in the dilution heat measurements because the same BSA sample was used.

To obtain values for the reaction stoichiometry, equilibrium constant, enthalpy, entropy and Gibbs free energy, the integrated heat plot is fitted to the built-in One Set of Sites Model in the ITC module of Origin 7 (see Section 3.2.3). This means that we

have assumed that there is only one site at which the binding between BSA and the VHH ligand occurs. The raw heat plots and integrated heat plots of all measurements are included in the Appendix.

3.3.1 *Equilibrium constant*

In Figure 3.2 the values of the equilibrium constant K_a for each temperature (20 °C or 25 °C, 40 °C and 50 °C) are shown as a function of pH. In general, the equilibrium constant decreases with increasing pH. On average, the equilibrium constant is highest at 40 °C, which seems logical since both BSA and the VHH are of animal origin where they need to perform best around body temperature. However, at around the pH of blood, pH 7.4, the bond is not the strongest, but lower than at pH 5, 6 and 6.5. Within this temperature and pH range, the maximum binding strength is at pH 6.5 with a K_a -value of $4.86 \times 10^7 \text{ M}^{-1}$ (on average) at 40 °C. At pH 5 and 50 °C there also seems to be a maximum, but the errors are quite large, which may be the result of, for example, protein denaturation.

A possible explanation for the high equilibrium constants at pH 5 is the opposite net charge of the proteins at this pH value. The isoelectric points are 5.65 for the VHH ligand (BAC, Naarden, The Netherlands) and 4.7 for BSA [14]. Between those two pH values the net charges of the proteins are opposite and this could strengthen the bond. Below pH 4.7 and above pH 5.65 the proteins would repel each other in terms of net charge, which would explain a decrease in the value for the equilibrium constant from pH 6.5 onwards (see Figure 3.2). Still lower pH values would probably also result in less favourable adsorption, but unfortunately we could not obtain a VHH ligand solution of appropriate concentration to perform ITC measurements below pH 5 (see Section 3.2.3). The turbid solution we obtained when preparing the VHH solution at pH 4 could be a result of a change in conformation of the VHH protein. This may also explain the lack of binding at lower pH values (see Chapter 2).

The lowest equilibrium constant is obtained at pH 8.5 at 50 °C: $1.83 \times 10^6 \text{ M}^{-1}$. This value is still too high for desorption. A buffer with high pH would also not present clear advantages over using an acidic buffer which results in more efficient desorption (see Chapter 2).

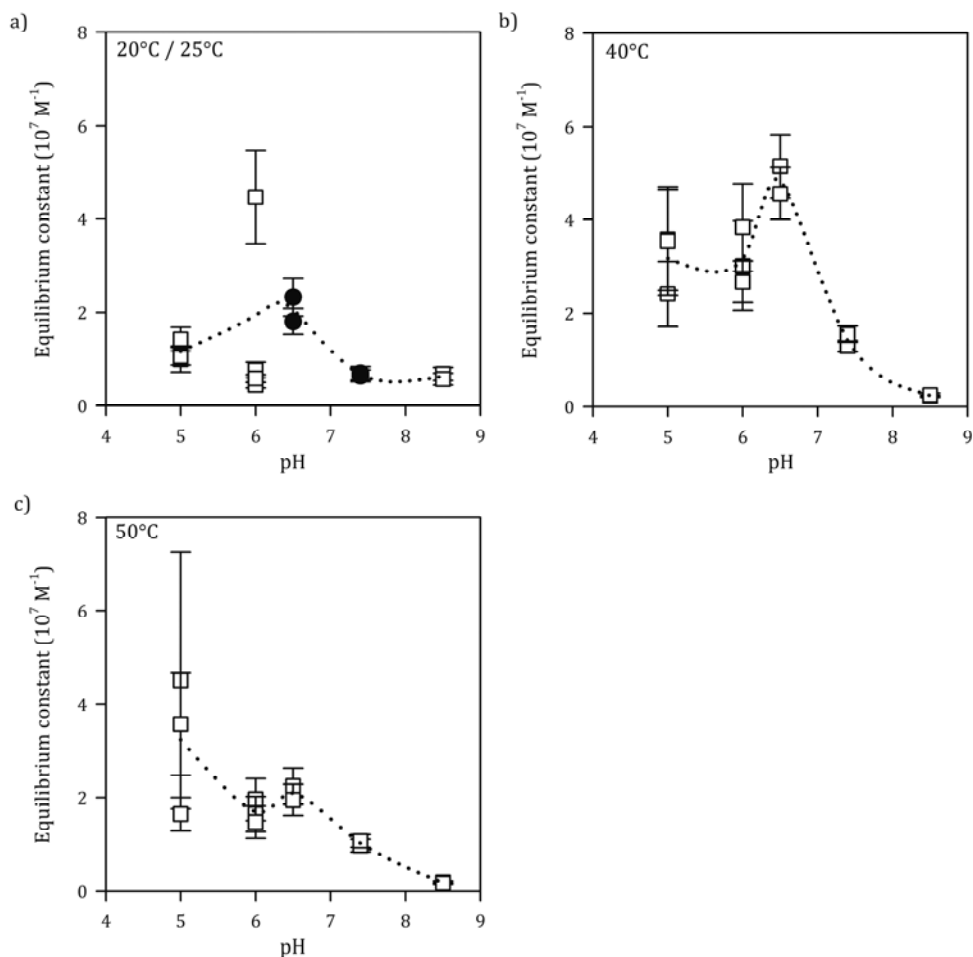


Figure 3.2. Equilibrium constant K_a as a function of pH for 20°C (pH 5, 6, and 8.5, open symbols) and 25°C (pH 6.5 and 7.4, black symbols) (a), 40°C (b), and 50°C (c). Error bars are the errors as calculated with the One Set of Sites Model in Origin 7, the dotted line represents the average values for K_a .

The error in the equilibrium constant is largest at the highest values, which is due to the nature of the measurement. The K_a value is obtained from the slope of the S-shaped curve as shown in Figure 3.1, bottom section. When the K_a value is high, there are only few points available to determine the slope, which results in a larger error compared to a lower K_a value. Generally, good estimates can be made when the product of the ligand concentration and the K_a value, the c -value, is between 10 and preferably 100, but definitely lower than 1000. When the c -value is too low, the slope is too shallow; when it is too high, the slope is too steep to accurately determine the value for the equilibrium constant. For our measurements the c -values were between approximately 50 and 600, with the majority around 150. This indicates that the

ligand concentrations could have been reduced in some cases to obtain better estimates for K_d . However, the heats measured were very low, the largest being approximately $-1.5 \mu\text{cal/s}$. This implies that the concentrations could not have been significantly lowered, since this would reduce the signal even further.

The equilibrium constant determined by the manufacturer was $3.84 \times 10^7 \text{ M}^{-1}$ at neutral pH, which is higher than the values we observed at pH 7.4 at 25°C , namely $6.72 \times 10^6 \text{ M}^{-1}$ on average. However, both values lie within the same order of magnitude. The difference may be caused by the measurement method, but also the sample preparation, BSA sample used, and many other factors. In Chapter 2 we used immobilised VHH to obtain an adsorption isotherm at pH 6.5 at ambient temperature, with a buffer with slightly lower ionic strength. The equilibrium constant obtained was approximately $1.4 \times 10^6 \text{ M}^{-1}$, which is clearly lower than the value measured with ITC: $2.07 \times 10^7 \text{ M}^{-1}$. This may be due to the immobilisation of the VHH ligand which could limit the conformational changes necessary for binding BSA.

3.3.2 Stoichiometry

For the adsorption reaction, we assumed that one BSA molecule binds to one VHH molecule. Theoretically, the ITC measurements should therefore indicate a stoichiometry close to 1. The stoichiometry can be determined from the inflection point of the S-curve in the lower section of Figure 3.1. At the inflection point, the amount of BSA titrated into the sample cell is equal to the amount of binding sites available; in our case equal to the amount of VHH ligand since we assume 1 binding site per ligand molecule. At that point less binding occurs resulting in smaller values of ΔH until complete saturation. In the case of infinitely strong binding, there would not be an inflection point, but just a step change in ΔH , because all binding sites would be occupied instantly.

As indicated in Figure 3.3, the stoichiometry was not equal to 1, but varied between 0.4 and 0.9. The stoichiometry seems to increase with increasing pH and, except for pH 6.5 and 7.4, with increasing temperature. A deviation in the stoichiometry could be due to different effective concentration of either of the two proteins involved. We expect that the error in concentration is the highest for the ligand solution, because of the dialysis and dilution. We did measure the protein content after dialysis, but part of the ligand may have become inactive. This may also hold for possibly denatured or otherwise dysfunctional BSA.

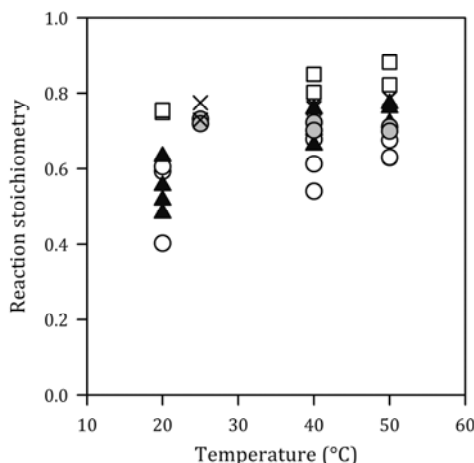


Figure 3.3. Reaction stoichiometry as a function of temperature for pH 5 (○), pH 6 (▲), pH 6.5 (×), pH 7.4 (●) and pH 8.5 (□). Error bars were too small to be plotted.

A difference in initial active concentrations could explain that the stoichiometry is not equal to 1, but it does not explain the temperature and pH dependence of this value. Other processes, such as protein denaturation and agglomeration may play a role, but the exact mechanism is unclear. The fitted stoichiometry value does not influence the heat of binding nor the equilibrium constant.

3.3.3 Reaction enthalpy, entropy and Gibbs free energy.

The most distinctive feature of ITC measurements is the direct measurement of the reaction enthalpy, ΔH . Using a model, the equilibrium constant K_a can be determined and through that the Gibbs free energy ΔG (via $\Delta G = -RT\ln(K_a)$) and entropy ΔS of the reaction (via $\Delta G = \Delta H - T\Delta S$). In Figure 3.4 the enthalpy (ΔH), entropy ($-T\Delta S$) and Gibbs free energy (ΔG) are plotted for each pH as a function of temperature.

To begin with, the adsorption reaction is, as expected, favourable, which can be concluded from the negative value for ΔG : between -9.1 kcal/mol for pH 8.5 at 20 °C, and -11.0 kcal/mol for pH 5 at 50 °C and pH 6.5 at 40 °C. The value drops slightly as temperature is increased, except for pH 8.5 where the ΔG remains constant over the temperature range. The values for ΔG are slightly higher at pH 7.4 and 8.5 than at the acidic pH values, which is also visible from the K_a values in Figure 3.2.

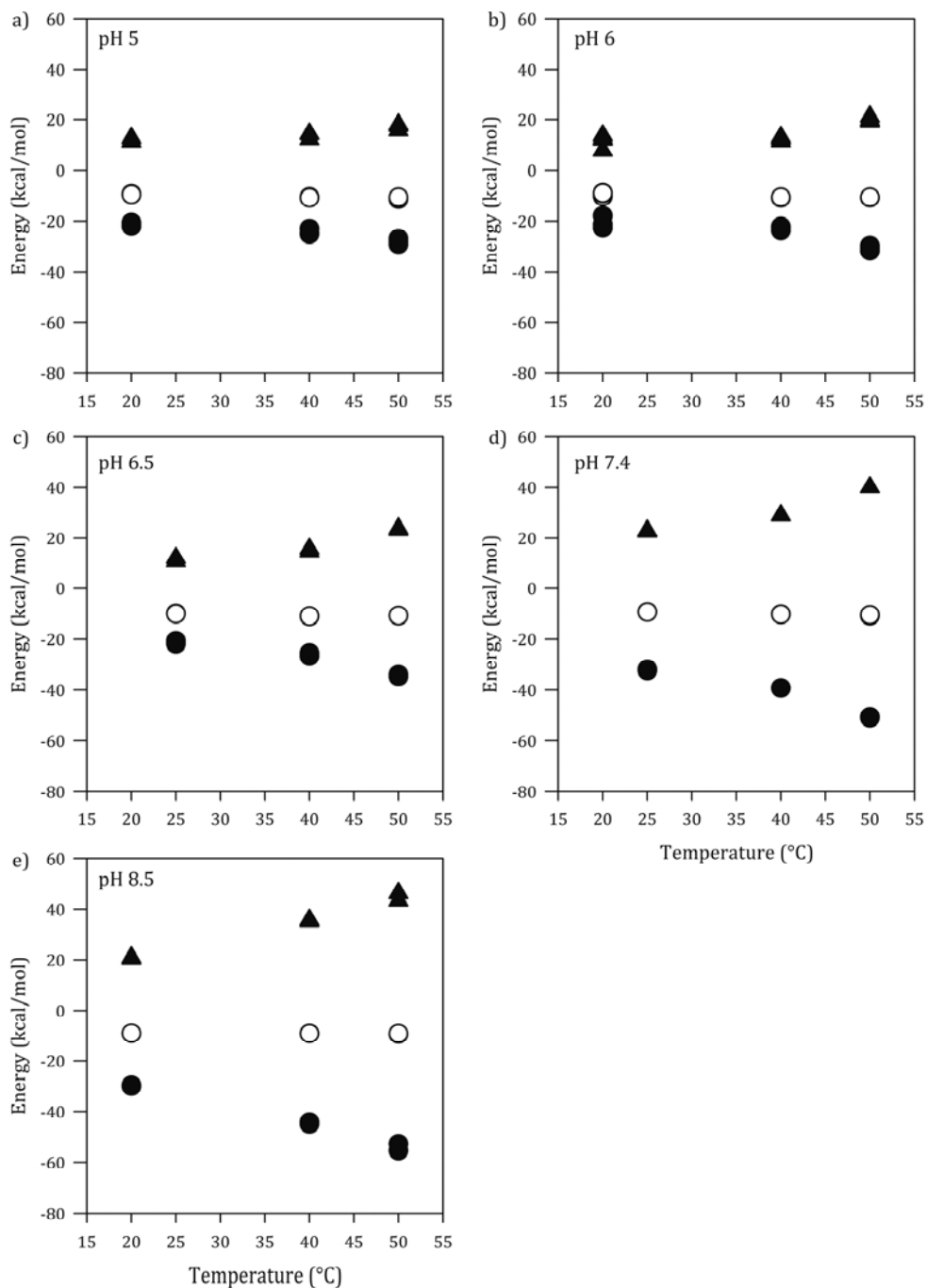


Figure 3.4. Reaction enthalpy (ΔH , ●), entropy ($-T\Delta S$, ▲) and Gibbs free energy (ΔG , ○) as a function of temperature measured using ITC for a) pH 5; b) pH 6; c) pH 6.5; d) pH 7.4; and e) pH 8.5. Standard deviations for the enthalpy ranged between 0.2 and 1.1 kcal/mol (not shown).

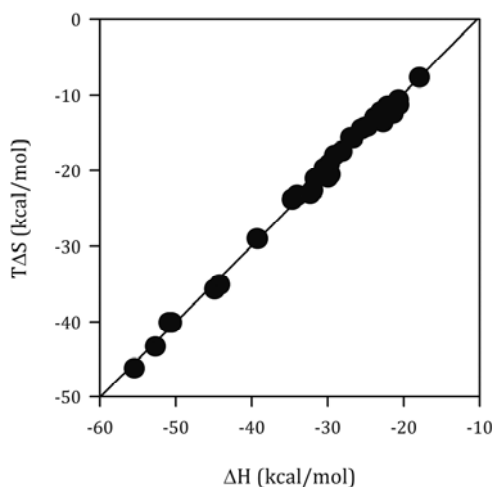


Figure 3.5. Entropy ($T\Delta S$) as a function of ΔH for all ITC measurements.

The binding between the VHH ligand and BSA is favourable from an enthalpy point of view, but unfavourable in terms of entropy. It seems logical that $-T\Delta S$ increases at higher temperature: due to the greater thermal energy the proteins gain more freedom of motion. Binding will result in less conformational freedom when the bonds between the two proteins replace the bonds with water molecules. In short this means that there is good bonding between the two molecules resulting in a negative enthalpy, but there is an increase in order because a complex is formed, resulting in a positive value for $-T\Delta S$. This phenomenon is referred to as enthalpy-entropy compensation [15], and is more clearly illustrated in Figure 3.5 where $T\Delta S$ is plotted against ΔH . The relation between entropy and enthalpy is practically unity, with a slope of 1.008.

There is some debate whether the enthalpy-entropy compensation is real or an effect of the constraints of the measurement (e.g., [16, 17]). This discussion arose from the deduction of enthalpy and entropy values from the van 't Hoff equation, where the natural logarithm of the equilibrium constant is plotted against the reciprocal temperature. The enthalpy can then be derived from the slope and the entropy from the intercept of the plot. However, an error in the slope also introduces an error in the intercept. On top of that, the errors tend to be rather large, which seemed to explain some cases of the enthalpy-entropy compensation found in literature.

With ITC, the value for the enthalpy and the equilibrium constant, and thus the Gibbs free energy, are derived more independently. However, the equilibrium constant could not be very accurately determined in some cases (see Figure 3.2). To prove that

the compensation effects found in this study are statistically significant more extensive statistical analysis is required, which is beyond the scope of this study.

In any case, it seems that the entropy-enthalpy compensation is not entirely equal at each temperature. Between 20 °C and 40 °C there is a slight decrease in ΔG (except for pH 8.5 where ΔG is constant), which results in a tighter bond. At this temperature range, the enthalpic contribution to binding increases more than the entropic contribution. The difference in ΔG between 40 °C and 50 °C could not be determined with sufficient accuracy.

The enthalpy and entropy do not only vary with temperature, they also vary with pH. Above pH 6, the enthalpy is more negative and the entropy more positive. This may be due to conformational changes of either the BSA or the VHH ligand molecule or the charge of the molecules. The exact mechanism is, however, unclear.

3.4 Conclusions

In this chapter we used ITC measurements to investigate the influence of pH and temperature on the adsorption of BSA to a multi-species albumin VHH ligand. The aim was to possibly find another method for desorption than a drastic pH decrease. We did not find a conclusive answer, but a slight pH increase with an increase in temperature has a negative effect on the adsorption. However, this is not enough for efficient desorption.

The ITC measurements revealed that the bond between BSA and VHH ligand is driven by enthalpy and negatively influenced by entropy. Enthalpy-entropy compensation seems to occur, but further statistical analysis is required to determine whether this effect is a result of the measurement constraints or an actual mechanism.

Acknowledgements

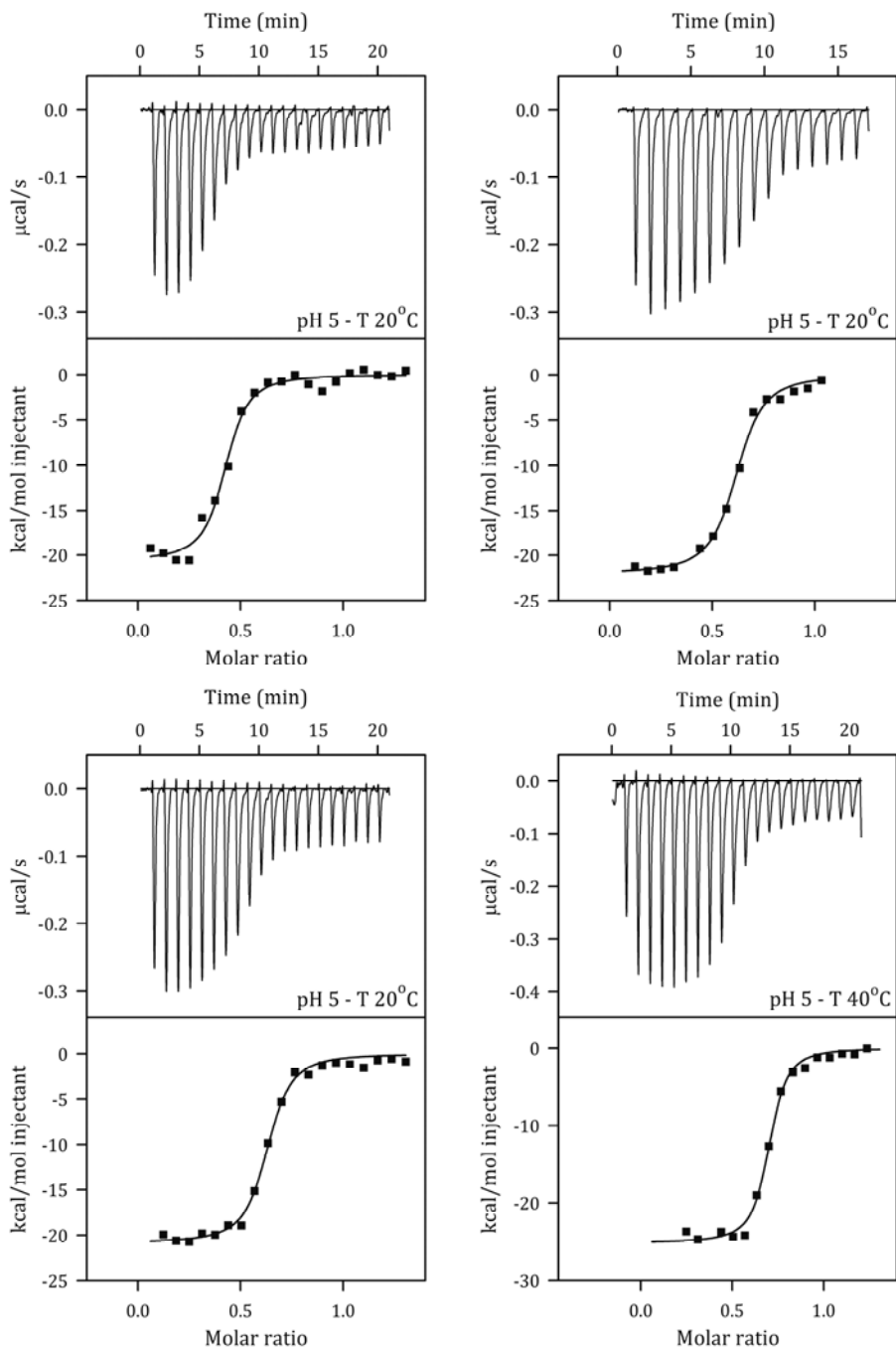
The authors wish to thank Jie Bai for performing the ITC measurements at pH 6.5 and 7.4. This project was supported by FrieslandCampina (Amersfoort, The Netherlands), DSM Biotechnology Center (Delft, The Netherlands), BAC BV (Naarden, The Netherlands) and SenterNovem (project IS054084).

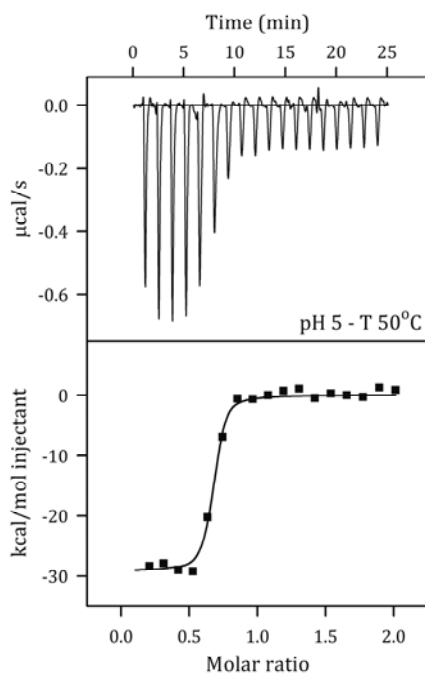
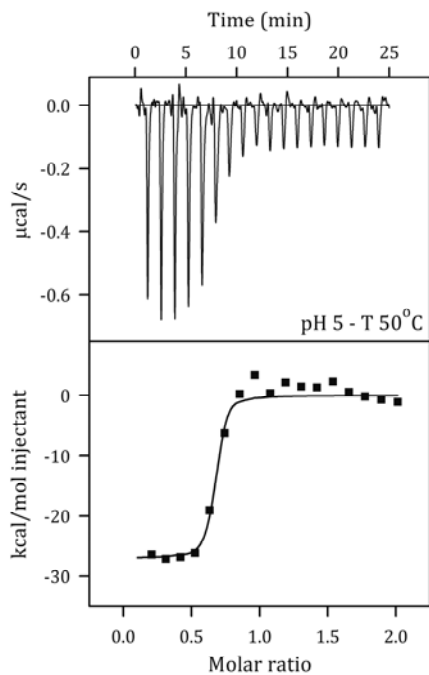
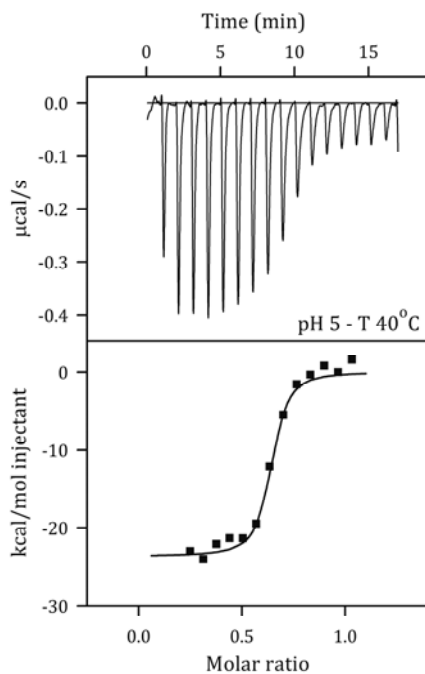
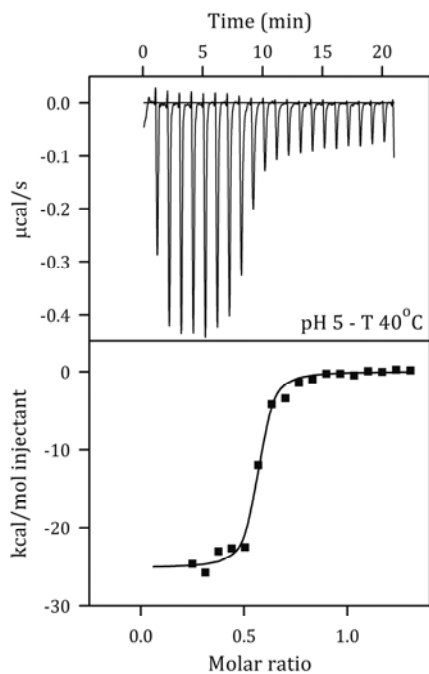
References

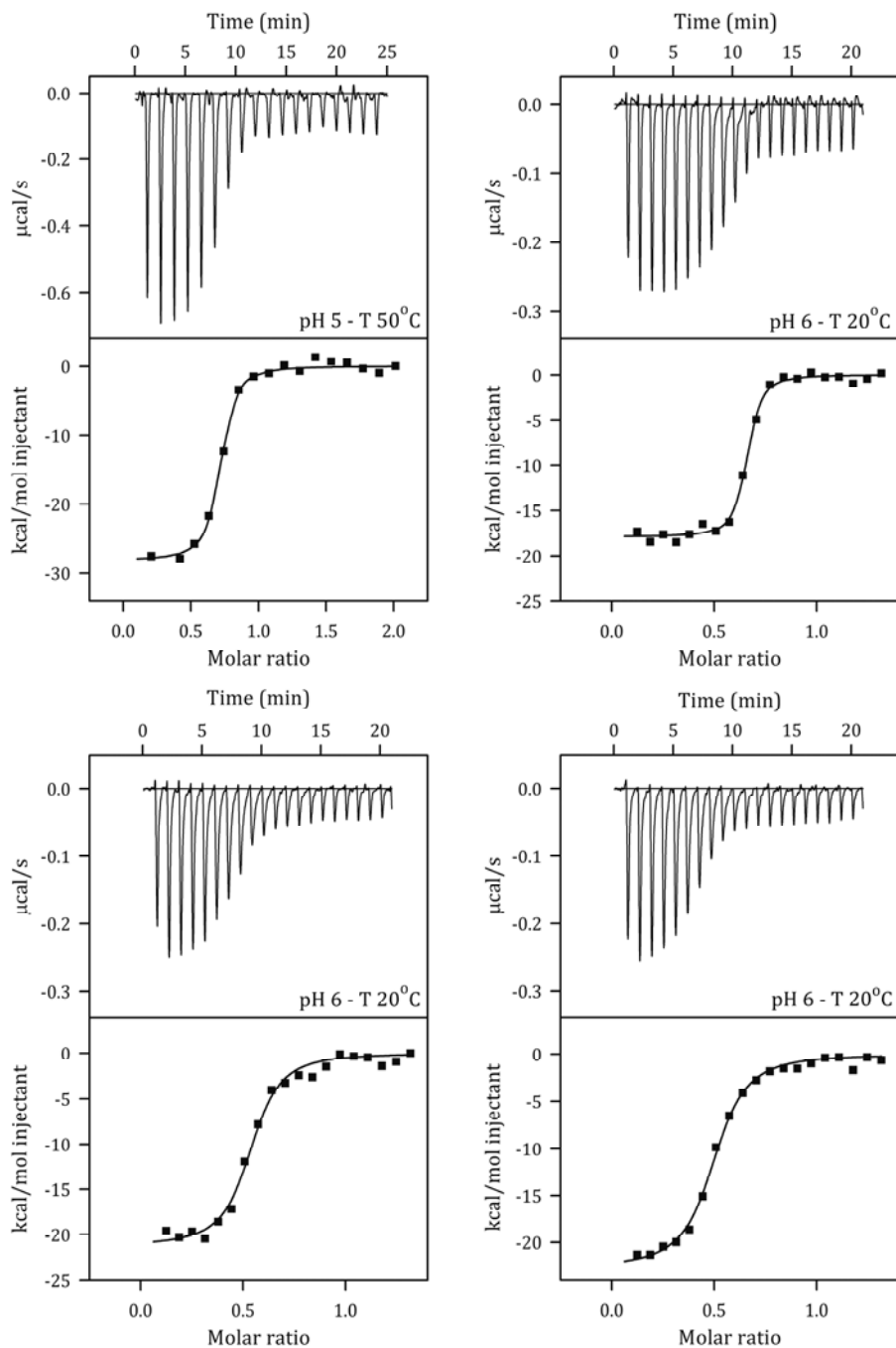
1. Hamers-Casterman, C., et al. 1993. *Naturally occurring antibodies devoid of light chains*. *Nature*, 363: p. 446-448.
2. Frenken, L.G.J., et al. 2000. *Isolation of antigen specific Llama VHH antibody fragments and their high level secretion by Saccharomyces cerevisiae*. *Journal of Biotechnology*, 78(1): p. 11-21.
3. Muyldermans, S. 2001. *Single domain camel antibodies: current status*. *Reviews in Molecular Biotechnology*, 74(4): p. 277-302.
4. Dumoulin, M., et al. 2002. *Single-domain antibody fragments with high conformational stability*. *Protein Science*, 11(3): p. 500-515.
5. Harmsen, M. and H. De Haard. 2007. *Properties, production, and applications of camelid single-domain antibody fragments*. *Applied Microbiology and Biotechnology*, 77(1): p. 13-22.
6. Klooster, R., et al. 2007. *Improved anti-IgG and HSA affinity ligands: Clinical application of VHH antibody technology*. *Journal of Immunological Methods*, 324(1-2): p. 1-12.
7. Zandian, M. and A. Jungbauer. 2009. *Engineering properties of a camelid antibody affinity sorbent for Immunoglobulin G purification*. *Journal of Chromatography A*, 1216(29): p. 5548-5556.
8. Pérez, J.M.J., et al. 2001. *Thermal unfolding of a llama antibody fragment: a two-state reversible process*. *Biochemistry*, 40(1): p. 74-83.
9. Dolk, E., et al. 2005. *Induced refolding of a temperature denatured llama heavy-chain antibody fragment by its antigen*. *Proteins: Structure, Function, and Bioinformatics*, 59(3): p. 555-564.
10. Doyle, M.L. 1997. *Characterization of binding interactions by isothermal titration calorimetry*. *Current Opinion in Biotechnology*, 8(1): p. 31-35.
11. Pierce, M.M., C.S. Raman, and B.T. Nall. 1999. *Isothermal titration calorimetry of protein-protein interactions*. *Methods*, 19(2): p. 213-221.
12. Perozzo, R., G. Folkers, and L. Scapozza. 2004. *Thermodynamics of protein-ligand interactions: history, presence, and future aspects*. *Journal of Receptors and Signal Transduction*, 24(1-2): p. 1-52.
13. Freyer, M.W. and E.A. Lewis. 2008. *Isothermal titration calorimetry: experimental design, data analysis, and probing macromolecule/ligand binding and kinetic interactions*, in *Methods in Cell Biology*, J.J. Correia and H.W. Detrich, Editors. Academic Press. p. 79-113.
14. Peters Jr, T. 1995. 2 - *The albumin molecule: its structure and chemical properties*, in *All About Albumin*. Academic Press: San Diego. p. 9-II.
15. Lumry, R. and S. Rajender. 1970. *Enthalpy-entropy compensation phenomena in water solutions of proteins and small molecules: a ubiquitous property of water*. *Biopolymers*, 9(10): p. 1125-1227.
16. Sharp, K. 2001. *Entropy-enthalpy compensation: fact or artifact?* *Protein Science*, 10(3): p. 661-667.
17. Olsson, T.S.G., et al. 2011. *Extent of enthalpy-entropy compensation in protein-ligand interactions*. *Protein Science*, 20(9): p. 1607-1618.

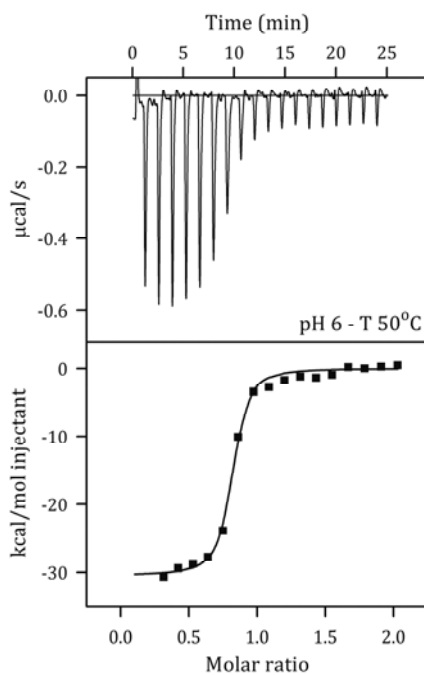
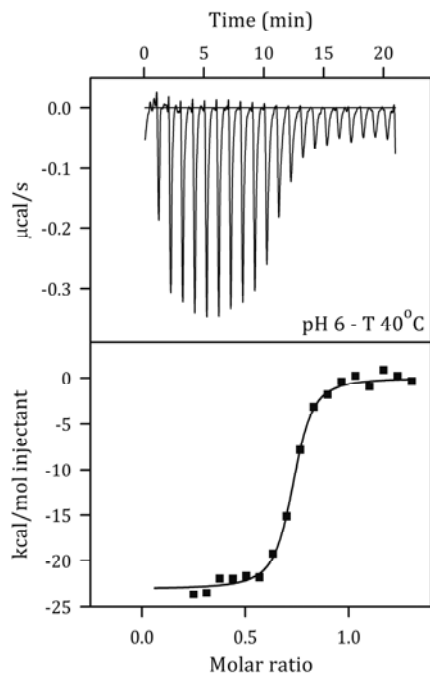
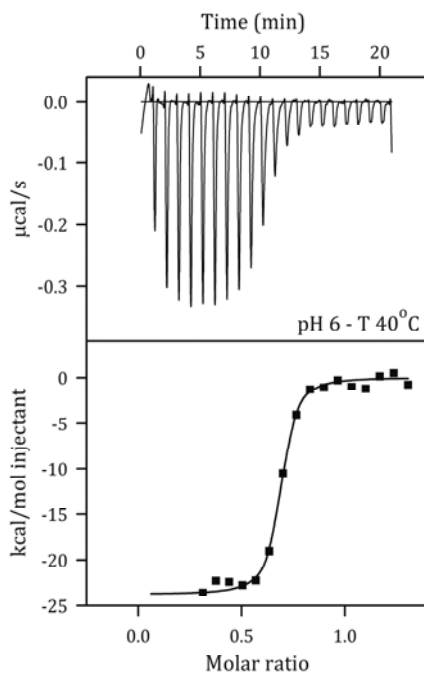
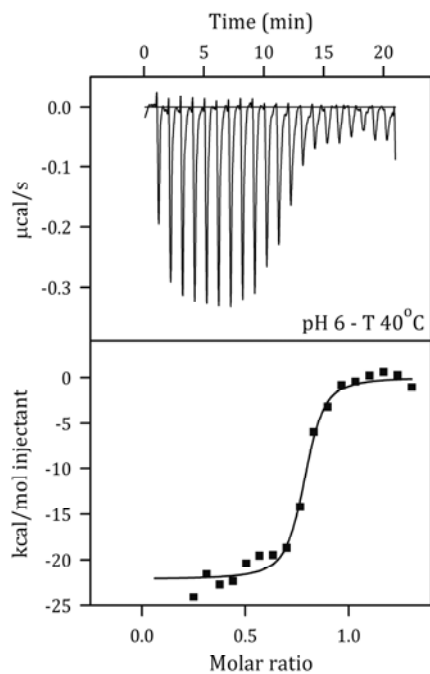
Appendix

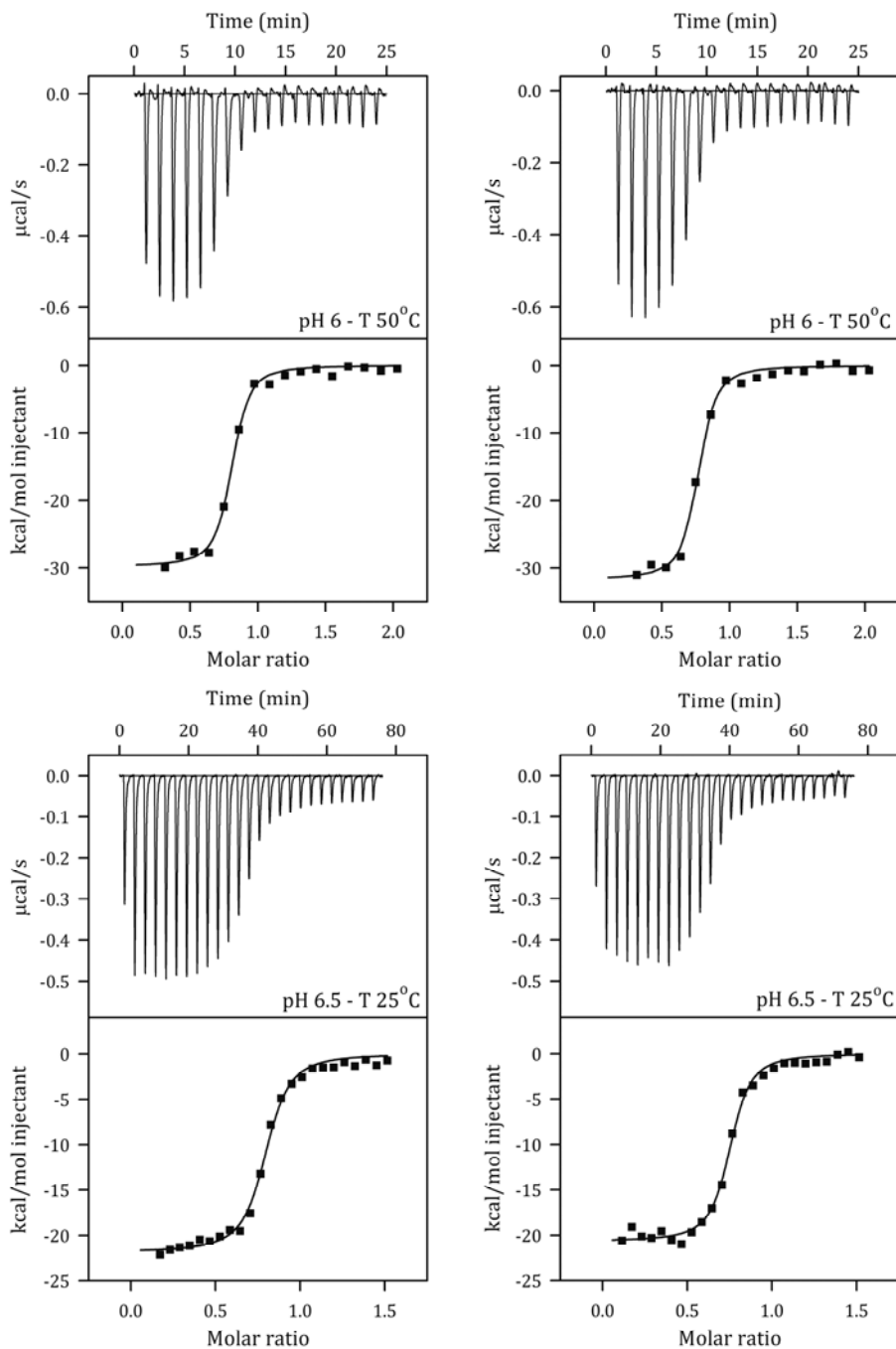
On the following pages the raw ITC heat plots (top sections) and integrated heat plots (lower sections) are shown for each measurement (see Section 3.2.1 and Figure 3.1).

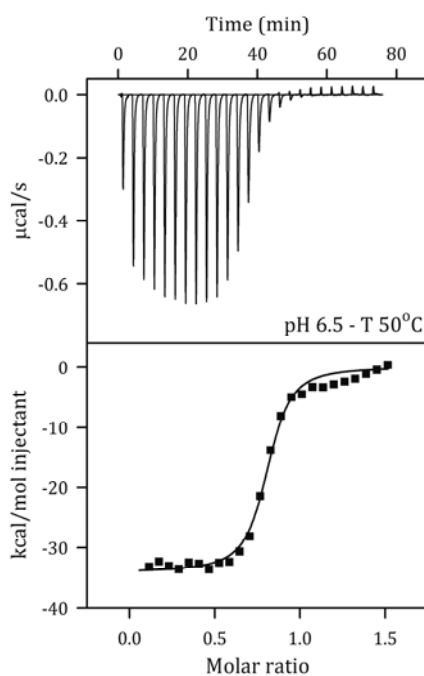
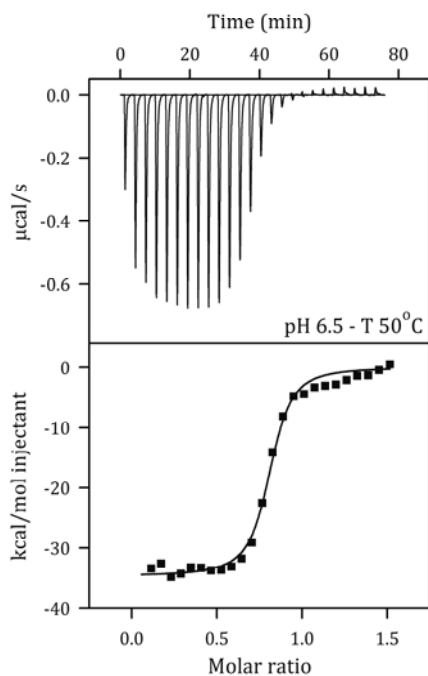
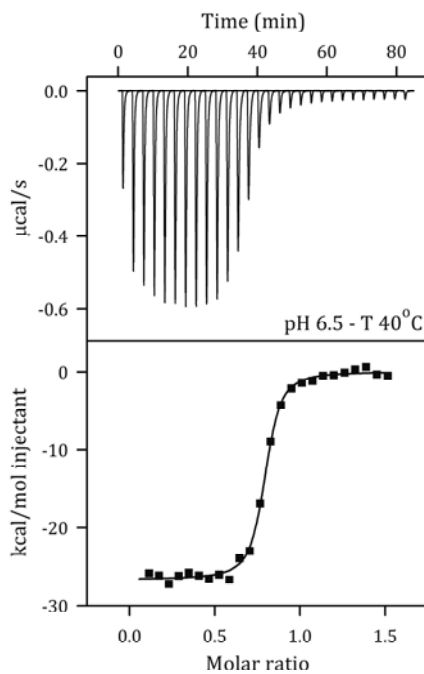
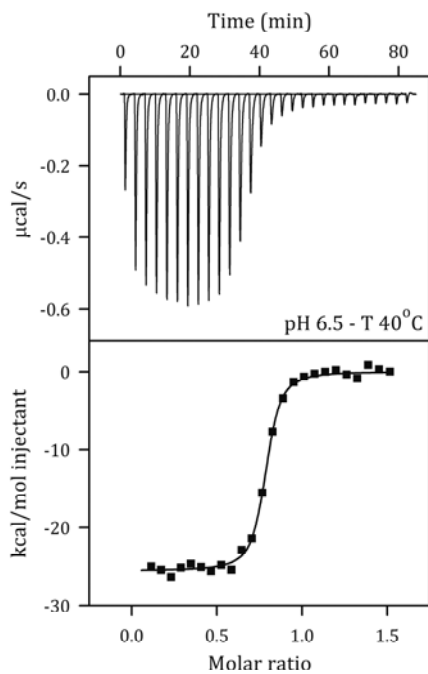


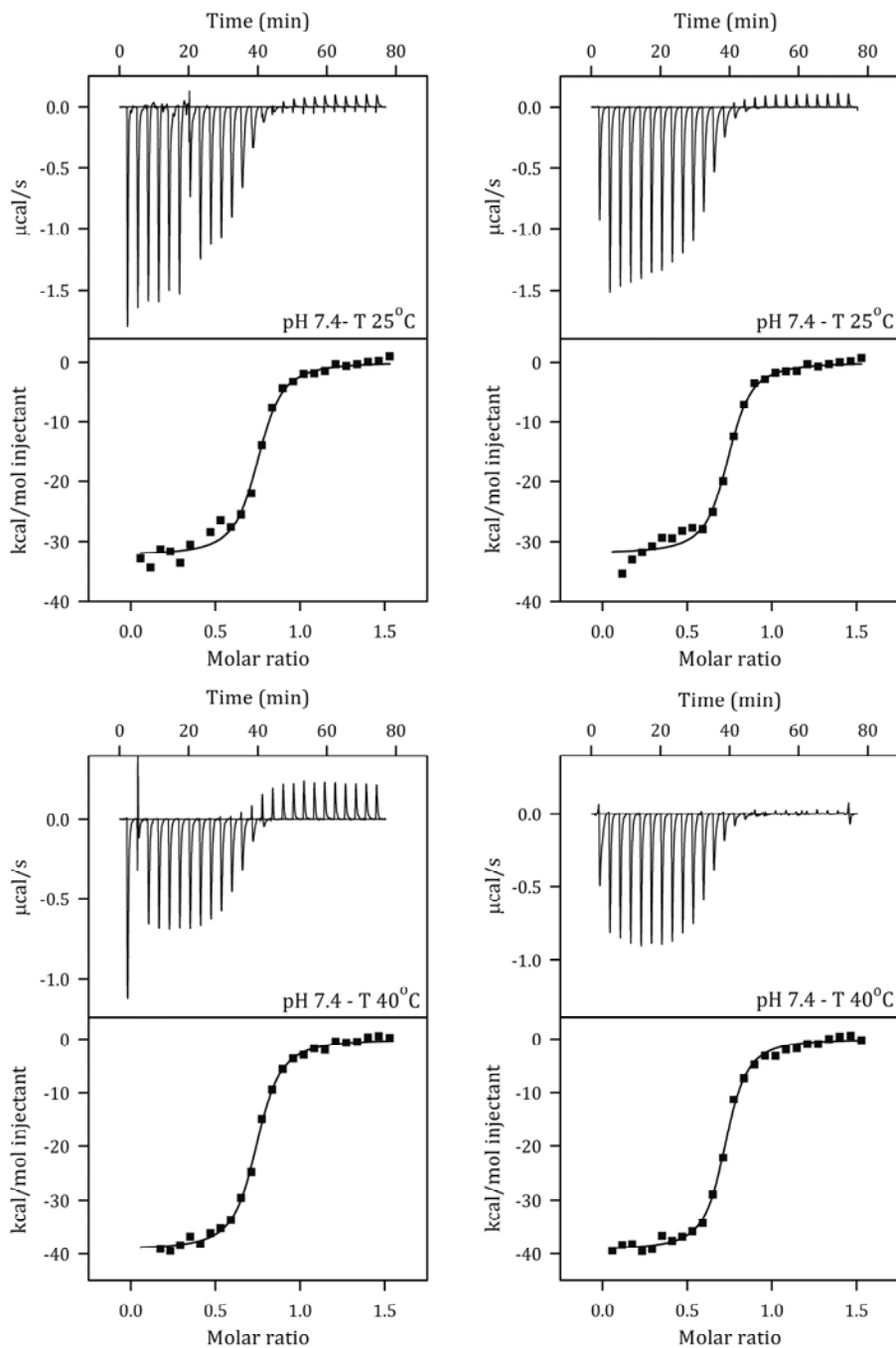


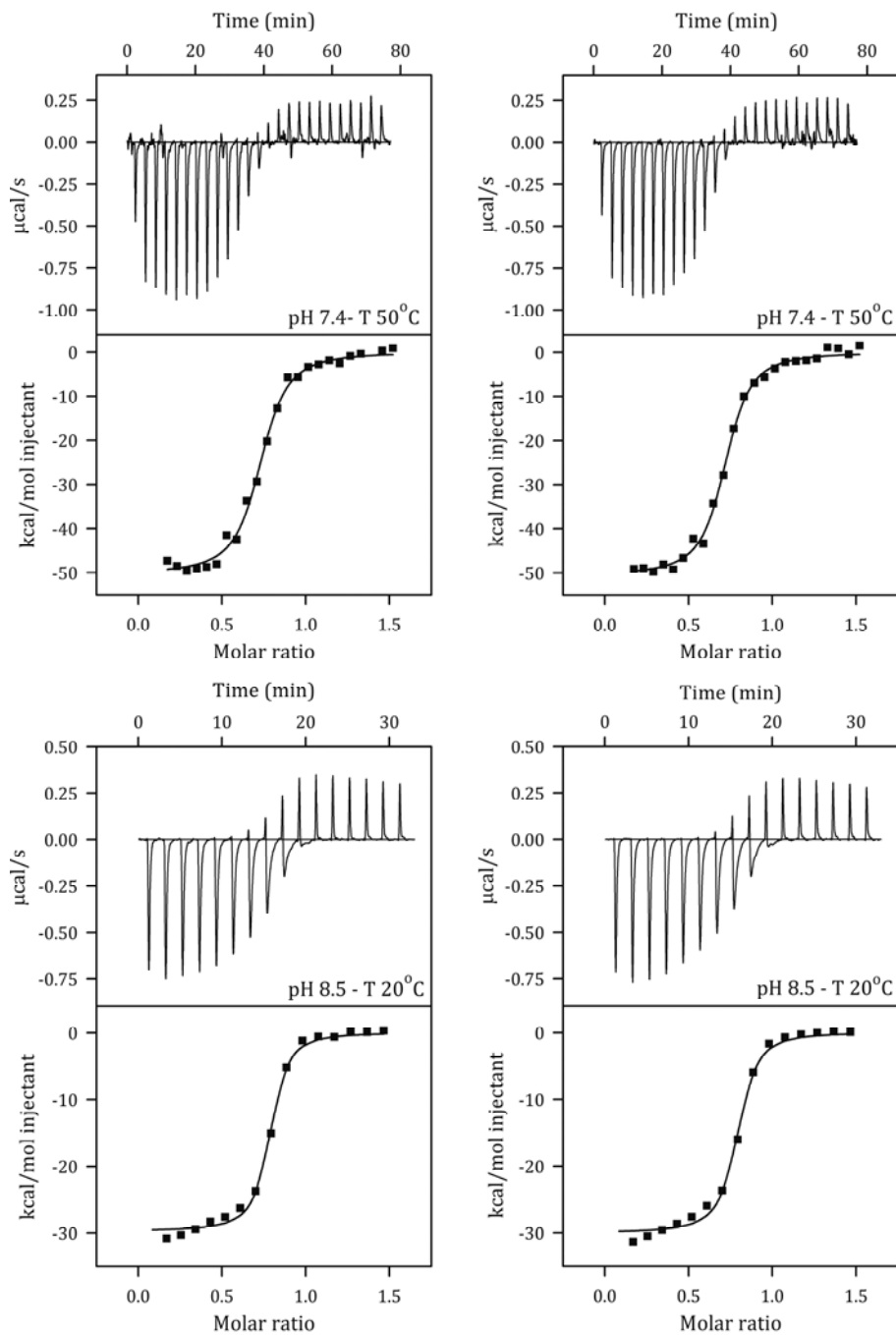


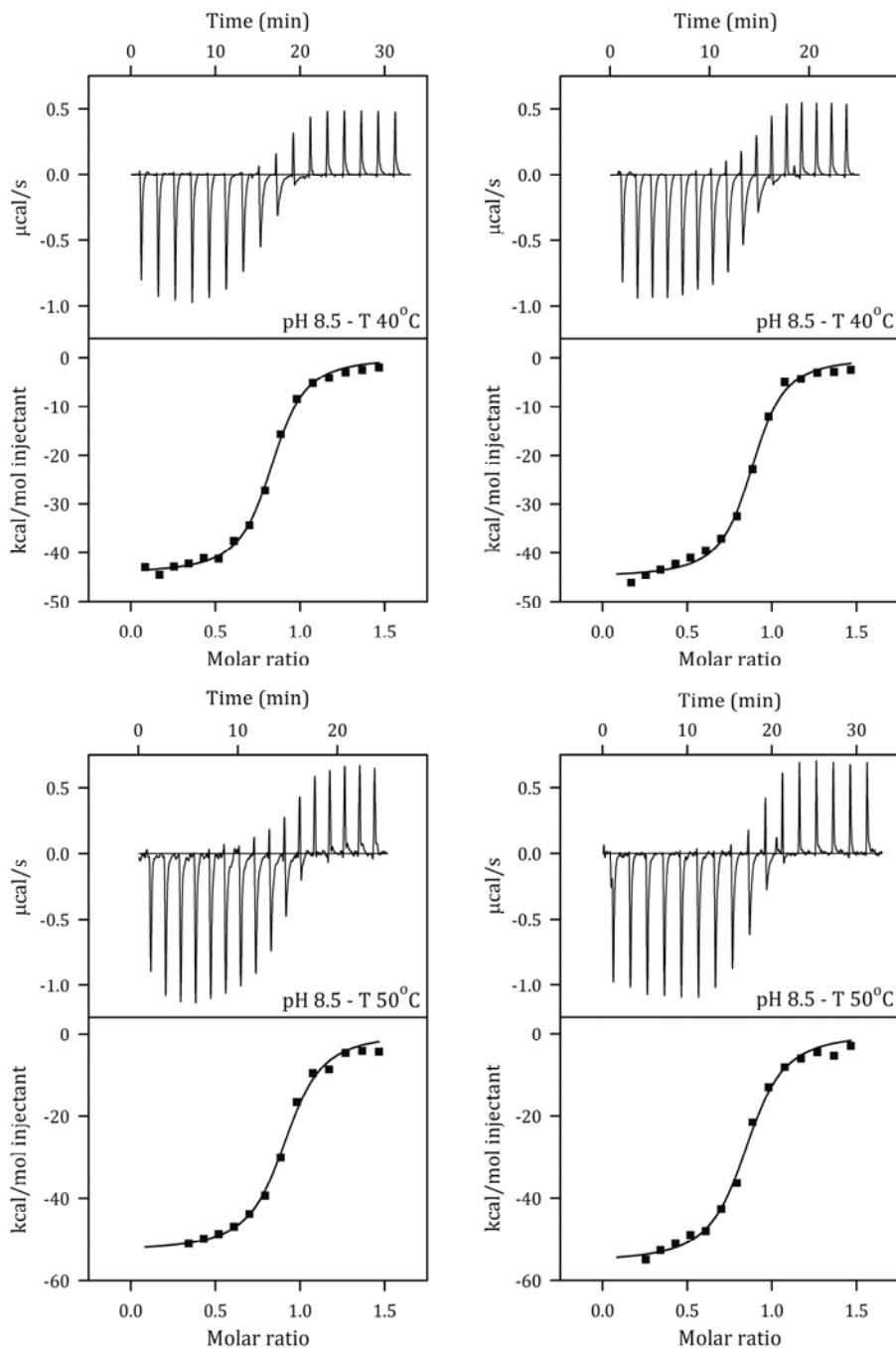












Comparison of activated chromatography resins for protein immobilization

Abstract

The adsorption of bovine serum albumin (BSA) to an immobilized camelid-derived antibody fragment against BSA was investigated using six different activated resins, of which two prototypes. The resins differed in base material (cellulose, agarose and polymethacrylate), coupling chemistry and particle size. The adsorption, washing and desorption stage of the affinity chromatography process were taken into account. Dynamic binding capacities at 10% breakthrough ranged between 0.76 and 4.8 mg BSA per ml resin. The number of column volumes required for washing ranged between 2.9 and 10 column volumes. One of the resins did not yield a higher BSA concentration in the desorption step, while the highest concentration was 13-fold. Two resins were unsuitable for this specific process because of their low dynamic binding capacity, high wash volume and hardly any product concentration. We present a method to rank and weigh the properties of the resins to find the optimal resin to meet specific requirements.

For three of the activated resins the effect of adsorption flow rate was varied, while the washing and desorption flow rate was kept the same. The dynamic binding capacity decreased with increasing flow rate, as expected. For one resin, the washing volume remained constant, but for the others it decreased with increasing adsorption flow rate. This could give an indication of the influence of intraparticle diffusion. The number of column volumes required to purify a given amount of BSA increases with increasing flow rate, which indicates that higher flow rates do not necessarily speed up the process.

This chapter is submitted as: Besselink, Tamara; Liu, Meng; Ottens, Marcel; van Beckhoven, Ruud; Janssen, Anja E.M.; and Boom, Remko M. Comparison of activated chromatography resins for protein immobilization.

4.1 Introduction

Affinity chromatography is a unique separation process because of its high selectivity for the desired target protein compared to other separation processes, such as ion exchange chromatography, salt precipitation and extraction. Affinity chromatography can often replace several unit operations in downstream processing with only one.

Affinity chromatography can be used to purify a large variety of compounds. Well-known non-protein ligands are dyes such as Cibacron Blue which is used to bind albumins and several enzymes [1, 2]. Protein-based ligands can be naturally occurring ligands such as lectins for oligosaccharide purification [3] or Protein A and G for immunoglobulin purification. It is also possible to design an affinity ligand, which is done in for example immunoaffinity chromatography. Specific antibodies are here produced against the compound of interest [4, 5]. Immunoaffinity chromatography is however mainly used for analytical and small-scale purposes because production of the antibodies is a costly process yielding only small amounts of antibody. Antibodies are also relatively large (MW > 150 kDa) which inherently limits the capacity of the system, while these large proteins are rather sensitive to denaturation. Therefore, efforts have been made to design specific ligands that are more stable and economical.

One promising type of ligand is derived from llama antibodies. In 1993 a unique type of antibodies lacking light chains was discovered in serum from *Camelidae* species [6]. From these heavy-chain antibodies the even smaller binding domain fragment called the VHH (variable heavy-chain region of the heavy-chain antibody) can be isolated. These VHH antibody fragments have high thermal and physical stability, which are important qualities for ligands in bioprocessing. The VHH can be expressed in microorganisms, such as *Saccharomyces cerevisiae* [7, 8], which is important for industrial-scale processes. More details about these affinity ligands can be found in a review by Muyldermans [9]. An affinity resin with VHH ligand against IgG has been commercialized by GE Healthcare (Uppsala, Sweden) and was recently evaluated by Zandian and Jungbauer [10].

Once the ligand is chosen, it is important to immobilize the ligand onto a solid support material, in this case a chromatography resin. Resins can be made from a variety of materials, such as agarose, cellulose, silica, polyacrylamide and polymethacrylate [11, 12]. The ligand should be covalently attached to minimize leaching into the product and loss of efficiency. It should further retain its functionality after being attached to the resin. Harsh desorption, regeneration and cleaning-in-place methods should not

harm the resin nor the ligand and its immobilization to the resin. Manufacturers of chromatography resins often provide activated resins that are already functionalized to use a specific coupling chemistry [13]. Common coupling chemistries in commercially available resins are N-hydroxysuccinimide (NHS), epoxy and aldehyde coupling.

To our knowledge, a comparison between activated resins of different materials and immobilization chemistries has not yet been performed. A comparison between commercially available Protein A resins has been made by for example Hahn et al. [14] and Fahrner et al. [15]. Many ion exchange materials have been investigated by for example Levison et al. [16] and Staby and co-workers [17-22]. Three immobilization methods for agarose resins have been compared by Van Sommeren et al. [23].

In this chapter we report on a method to choose an optimal resin in the example purification of bovine serum albumin (BSA) using immobilized VHH against BSA. Six different resins were evaluated. Four resins are commercially available, the other two are prototypes provided by the manufacturer. We immobilized a VHH against BSA onto these resins and investigated the differences in dynamic binding capacity, process volume and physical properties between the resins.

4.2 *Materials and methods*

4.2.1 *Materials*

Bovine Serum Albumin (minimum 98%, A7096) was purchased from Sigma-Aldrich (Zwijndrecht, The Netherlands). All other reagents were purchased from Merck (Darmstadt, Germany) and were of analytical grade. Multi-species albumin ligand was kindly provided by BAC BV (Naarden, The Netherlands).

A 10 times concentrated phosphate buffered saline (PBS) buffer pH 7.4 was prepared by dissolving 80 g NaCl, 2 g KCl, 17.8 g of $\text{Na}_2\text{HPO}_4 \cdot 2\text{H}_2\text{O}$ and 2.5 g KH_2PO_4 in 1 litre of Milli-Q water (Millipore, Billerica, USA). The diluted buffer was used as PBS pH 7.4. PBS pH 2 was made by acidifying this buffer with 3.5 M phosphoric acid.

4.2.2 Ligand immobilization

The properties of each resin are presented in Table 4.1. For each immobilization approximately 20 mg of ligand was added to 1 g of resin. The concentration of the ligand solution was approximately 10 mg/ml. After blocking the resins were washed alternating with 3 times PBS pH 2 and 3 times PBS pH 7.4. When the resin with immobilized ligand was not in use, it was stored in 20% ethanol at 4°C.

Table 4.1. Properties of activated resins used in this study.

	NHS Sepharose FF	Big Beads ¹	Sepabeads FP-EP400	Glyoxal Agarose	Cellufine Formyl	Pall ¹
Manufacturer	GE Healthcare	GE Healthcare	Resindion	ABT	Chisso	Pall
Backbone	4% agarose	6% agarose	poly- methacrylate	6% agarose	cellulose	cellulose
Particle size (µm)	45-165	100-300	50-100	35	125-210	80-100
Coupling chemistry	NHS	NHS	epoxy	aldehyde	aldehyde	aldehyde
Spacer arm (# -C-)	14	10	3	12	8	0
Bed height (mm)	48	105	59	48	104	104

¹ The Big Beads and Pall resins were in a development stage at the time of the experiments and are therefore not representative for existing or new commercial products.

4.2.2.1 NHS coupling

With NHS coupling the ligand is covalently attached to the resin via an amine group, creating a stable amide bond [24]. The NHS coupling protocol was followed for NHS Sepharose 4 Fast Flow and the prototype Big Beads, both obtained from GE Healthcare (Uppsala, Sweden). The ligand was first dialysed against a 10 times larger volume of coupling buffer (0.1 M HEPES, 0.5 M NaCl, pH 8). The resin was washed with 3 times 10 column volumes (CV) of cold 1 mM HCl over a sintered glass filter. After the ligand was added the mixture was incubated overnight at 4°C while rotating. The coupled resin was then filtered on a sintered glass filter. The non-reacted groups of the resin

were blocked by incubating with 0.1 M Tris, 0.5 M NaCl, pH 8 for one hour while rotating.

4.2.2.2 *Epoxy coupling*

An epoxy-activated resin can form a stable bond with amine, sulfhydryl and hydroxyl groups [25]. The Sepabeads FP-EP 400 (Resindion S.R.L., Binasco, Italy) were supplied as a powder which had to be swollen in a PBS buffer at pH 7.4. The Sepabeads were filtered on a sintered glass filter, rinsed with PBS and a few times with at least 10 CV of coupling buffer (0.1 M NaHCO₃, 0.5 M Na₂HSO₄, pH 9). The ligand was dialysed while stirring against a 20 times larger volume of coupling buffer for at least 4 hours at room temperature.

The resin and ligand solution were mixed and incubated for 64 hours at 37°C while rotating. The resin was filtered over a sintered glass filter and incubated with 5 CV of blocking buffer (0.1 M Tris, 0.5 M NaCl, pH 8) while rotating for at least one hour at room temperature.

4.2.2.3 *Aldehyde coupling*

Amine groups of the ligand can also be coupled to an aldehyde group on the resin through reductive amination [13]. Aldehyde coupling was done for the Glyoxal Agarose beads from ABT Beads (Madrid, Spain), Cellufine Formyl from Chisso (Tokyo, Japan) and an early stage prototype aldehyde resin (referred to in this chapter as Pall) provided by Pall (Portsmouth, United Kingdom). The resin was filtered over a sintered glass filter and rinsed with coupling buffer, PBS pH 7.4 with 0.5 M NaCl. The ligand solution and 30 µl of 5M cyanoborohydride per ml of resin were added and the mixture was incubated overnight at room temperature while rotating. The coupled resin was then filtered over a sintered glass filter and blocked with 0.1 M Tris, 0.5M NaCl, pH 8 for 1 hour at room temperature.

4.2.3 *BSA breakthrough experiments*

Breakthrough experiments were performed by packing the beads in Tricorn 5 columns with an inner diameter of 5 mm (GE Healthcare, Uppsala, Sweden) of varying bed height. The bed height was measured using a ruler. The bed heights of the NHS Sepharose, Sepabeads and Glyoxal Agarose columns were approximately 5 cm. For the

BigBeads, Cellufine Formyl and Pall resins the bed height was approximately 10 cm (exact values given in Table 4.1). An Äkta Explorer 100 (GE Healthcare, Uppsala, Sweden) was used to pump buffer and BSA solutions over the resin and monitor the UV absorbance at 280 nm. The system volume was determined by injecting a small amount of 3% v/v acetone solution without attaching a column and was found to be 1.14 ml.

BSA solutions with a concentration of 1 mg/ml were prepared in equilibration buffer (PBS pH 7.4). A flow rate of 0.5 ml/min (~150 cm/h) was used for equilibration (5 CV), sample application and washing. For desorption PBS pH 2 was used at a flow rate of 2 ml/min (~600 cm/h). The Big Beads, Cellufine Formyl and the Pall aldehyde resin were also evaluated at adsorption flow rates ranging between 0.17 (~50 cm/h) and 2 ml/min (~600 cm/h). Washing and desorption flow rates were kept constant at 0.5 ml/min and 2 ml/min respectively.

4.2.4 *Calculation of process properties*

To compare the resins we derived several properties from the experimental results obtained with the packed beds. To further clarify the measured properties a typical chromatogram is shown in Figure 4.1. Three stages of the purification process are visible, the equilibration and regeneration stage are left out. The first stage is the adsorption stage, which runs from the start until the first maximum in the graph. This stage is also often referred to as the breakthrough curve. The second stage is the washing stage in which the outlet concentration drops to zero or almost zero. The peak at the end of the curve indicates the third stage, the elution or desorption. The shape of the curve in each stage is determined by the resin properties and experimental conditions.

The maximum breakthrough was calculated as the maximum BSA concentration at the column outlet during adsorption divided by the BSA concentration at the inlet (in this case 1 mg/ml). This value shows to which extent the column was saturated with BSA. The dynamic binding capacity at 10% (DBC_{10%}) breakthrough was calculated as the amount of BSA bound to the column when the outlet concentration reaches 10% of the inlet concentration, divided by the column volume. In Figure 4.1 the area in the chromatogram that represents DBC_{10%} is indicated. It should be noted that the DBC_{10%} is dependent on feed concentration, a higher feed concentration will lead to a higher DBC_{10%} (up to a certain maximum). The wash volume was determined as the number

of column volumes (CV) of buffer required to wash the column after adsorption until the BSA concentration at the outlet dropped to 10% of the inlet concentration.

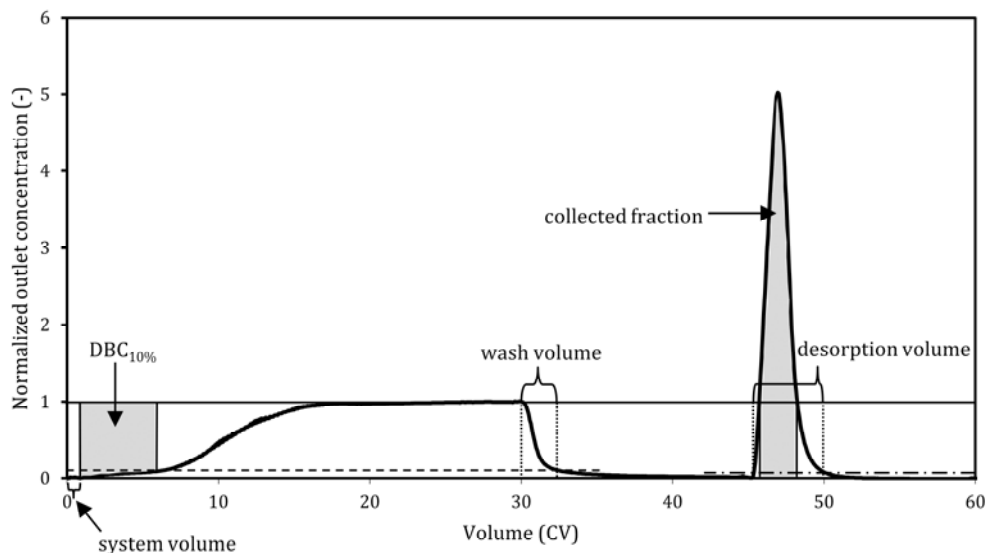


Figure 4.1. Typical chromatogram (thick solid line) as measured in this study (data from Cellufine Formyl, flow rate 0.17 ml/min). The horizontal lines indicate the 5% (dash-dotted), 10% (dashed) and 100% (solid) of the inlet concentration.

In a purification process collecting the entire desorption peak will result in a relatively dilute sample, which may then require further concentration. Therefore, we decided to specify a collected fraction, which is the fraction that has a higher concentration than the inlet concentration. This means that the left and right parts of the desorption peak were ‘discarded’. The volume of the collected fraction is expressed in column volumes (CV; see Figure 4.1). The yield was calculated as the percentage of the desorbed BSA in the collected fraction compared to the total amount of BSA desorbed. A high yield indicates a sharp and therefore more desirable desorption peak. We defined the concentration factor as the average concentration in the collected fraction divided by the inlet (feed) concentration. The process volume is determined as the number of column volumes (CV) required to purify 1 mg of BSA per ml resin. It is calculated by first determining the sum of the volume of BSA solution applied until 10% breakthrough, the wash volume and the volume of the total desorption peak (see Figure 4.1). This volume is then divided by $DBC_{10\%}$ to obtain the process volume. The right-hand tail of the desorption peak lower than 5% of the inlet concentration is not taken into account in this calculation.

4.3 Results and discussion

4.3.1 BSA breakthrough experiments

All resins could be successfully used to immobilize the VHH ligand, and bind BSA in a packed bed configuration. The chromatograms of the resins are shown in Figure 4.2, in which the outlet concentration is divided by the inlet concentration for adsorption. The steeper the breakthrough curve, the better the adsorption kinetics and mass transfer. Good mass transfer is also indicated by a short washing stage and a tall and narrow desorption peak. For all resins, the breakthrough curves are quite shallow. The prototype Big Beads and Glyoxal Agarose resins show the shallowest breakthrough curves. This could be due to the adsorption kinetics, but since the same type of ligand is used for every bead, a large difference in adsorption kinetics between the beads is not expected. Therefore, the shallow shape of the breakthrough curve is most likely due to slow diffusion into the beads. The volume required for washing is also longer for the Big Beads and Glyoxal Agarose resins, which supports the observation of slow diffusion.

The data extracted from the chromatograms are summarized in Table 4.2. Except for the Big Beads and Sepabeads, BSA was applied to the columns until at least 90% breakthrough. The Big Beads were saturated until 73% breakthrough, and the Sepabeads were saturated until 88% breakthrough. The maximum binding capacity of the different resins cannot be determined accurately from the measured breakthrough curves. In a large-scale process, adsorption is usually terminated at a specific level of breakthrough. This level of breakthrough depends on the commercial value of the target in case of preparative chromatography, or on the maximal allowed concentration in a scavenging process. Therefore, the dynamic binding capacity is more relevant to practice, and more often used than the maximum binding capacity. In case the chromatography process is aimed at purifying a target present in a low-value feed stream, it might be economically interesting to saturate the chromatography column, but even then a resin with good mass transfer properties might be more economical to use than a resin with a high binding capacity, as it will allow larger throughput.

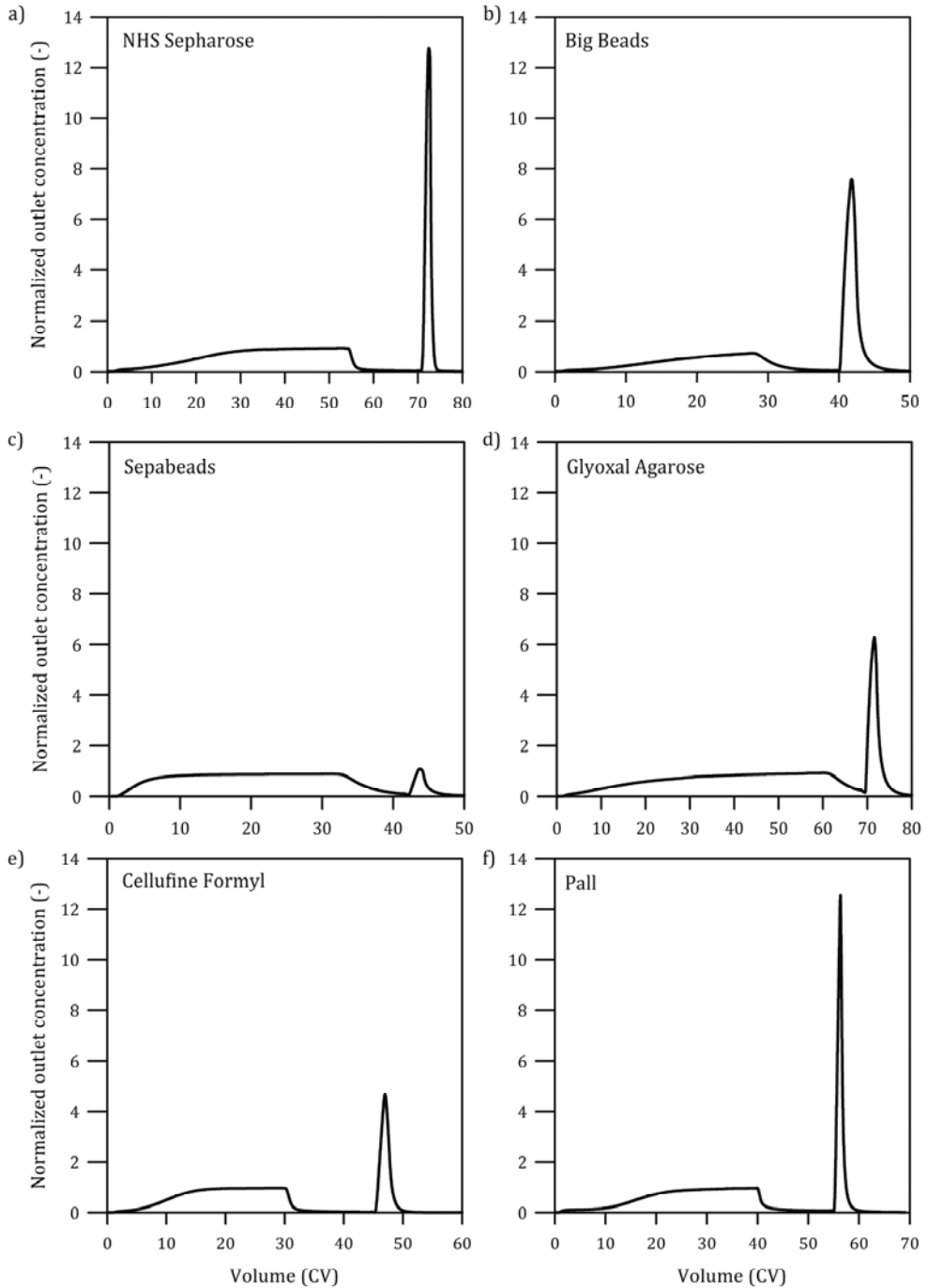


Figure 4.2. Normalized outlet concentration (outlet BSA concentration divided by the concentration of the sample) against outlet volume for the resins NHS Sepharose (a, bed height 48 mm), Big Beads (b, 105 mm), Sepabeads (c, 59 mm), Glyoxal Agarose (d, 48 mm), Cellufine Formyl (e, 104 mm) and Pall (f, 104 mm). The adsorption and wash flow rates were 0.5 ml/min and desorption flow rate was 2 ml/min.

The DBC_{10%} of the resins investigated ranged between 0.76 and 4.8 mg BSA / ml resin (Table 4.2), with the Sepabeads having the lowest and Big Beads the highest DBC_{10%}. A low DBC_{10%} can have several reasons. First, the amount of ligand immobilized to the resin can be low. The immobilized ligand may also be partly dysfunctional, which depends on the immobilization method and active group density. According to the manufacturer of the Sepabeads, the pore size is in the range of 30 to 40 nm. It is therefore likely that the BSA molecule, having a hydrodynamic diameter of approximately 8 nm, but usually at partly present in the form of dimers or even multimers, is not able to enter the bead efficiently, especially after immobilization of the VHH. Even though a difference in bed height exists between the beads, the influence on DBC_{10%}, should not be that large because the liquid velocity in the columns was the same. Besides, the DBC_{10%} was calculated per volume resin, not per column. DBC_{10%} is however not necessarily the best indicator for resin performance because it is solely based on the adsorption phase of the purification process.

Table 4.2. Measured properties of activated resins used in this study. An explanation of the properties can be found in Section 4.2.4.

	NHS Sepharose FF	Big Beads ¹	Sepabeads FP-EP400	Glyoxal Agarose	Cellufine Formyl	Pall ¹
Max breakthrough	0.94	0.73	0.88	0.92	0.98	0.97
DBC _{10%} (mg BSA /ml resin)	4.0	4.8	0.76	2.4	3.8	2.1
Wash volume (CV)	3.7	6.3	10	9.1 ²	2.9	6.1
Max desorption concentration / inlet concentration	13	7.6	1.1	6.3	4.7	12.5
Volume collected fraction (CV)	2.1	3.0	0.81	3.6	2.3	2.2
Yield	0.96	0.91	0.29	0.88	0.88	0.93
Concentration factor	7.9	4.4	0.90	3.9	3.0	5.7
Process volume (CV/mg BSA/ml resin)	3.20	3.93	22.97	9.13	3.21	6.62

¹ The Big Beads and Pall resins were in a development stage at the time of the experiments and are therefore not representative for existing or new commercial products.

² The wash step was too short to reach 10% of the inlet BSA concentration.

An often overlooked, but essential part of the purification process is the desorption step. The best desorption peaks are clearly those of NHS Sepharose and the prototype Pall resins, because they are very narrow and tall (see Figure 4.2). For each of the six resins the maximum desorption concentration compared to the inlet concentration is given in Table 4.2. In this particular case the Sepabeads do not perform well, because the BSA solution obtained after desorption is of an almost equal concentration as the feed solution. This is due to the low binding capacity, the $DBC_{10\%}$ is only 0.76 mg BSA / ml resin, and mass transfer limitation, which results in the high wash volume and a wide desorption peak. The residence time was short for the Sepabeads and the results may be improved by increasing the residence time. However, the NHS Sepharose also had an equal residence time but showed a much shorter wash volume. This indicates that mass transfer limitation for the Sepabeads is not only due to the short residence time.

The NHS Sepharose and prototype Pall resins yield the highest desorption concentration; the highest concentration in the desorption peak is 13 times higher than the initial BSA concentration (see Table 4.2). The prototype Pall resin has a wider desorption peak than NHS Sepharose, so the concentration factor of the collected fraction is highest for NHS Sepharose (see Figure 4.2). The prototype Big Beads would probably have reached a higher concentration factor if the column was further saturated, but this would require longer residence times, for example by a lower flow rate of the mobile phase.

The concentration factor alone also does not completely cover resin performance. Therefore the number of column volumes required to purify 1 mg of BSA per ml of resin, the process volume, is calculated. Table 4.2 shows that NHS Sepharose has the lowest process volume, closely followed by Cellufine and Big Beads.

4.3.2 Resin selection

Selection of resin depends on multiple criteria. Therefore it is interesting to rank the resins for important properties. In Table 4.3 an example is given for the $DBC_{10\%}$, wash volume, concentration factor and process volume. Each resin is ranked such that the resin with the best value for that property ranks as 1, the second best as number 2, etc. In case of $DBC_{10\%}$, the value should be as high as possible; therefore the resin with the highest $DBC_{10\%}$, in this case the Big Beads, is ranked number 1. For the wash volume the value should be as low as possible to be the best, and this is true for the Cellufine Formyl resin. Depending on the process, each property can be given a certain

weight according to its importance. An example may be that DBC_{10%} is considered more important than the wash volume, so the rank for DBC_{10%} could be given a weight of 3 compared to the wash volume. When all the properties of interest are ranked, the ranks are added up to a score. The lowest score should then indicate the most suitable resin. In Table 4.3 no weights have been assigned to the properties, so all properties are deemed equally important. From this table it is evident that NHS Sepharose followed by Big Beads, Cellufine Formyl and the prototype Pall resin perform better than the Sepabeads and Glyoxal Agarose. The results for the Sepabeads and Glyoxal Agarose resins may be improved by increasing the residence time, but the residence time for NHS Sepharose was equal. The Big Beads and Pall resins were examined at a development stage and therefore the final commercial products may have other properties than found in this study.

Table 4.3. Ranking and scoring of resin properties.

	NHS Sephareose	Big Beads ¹	Sepabeads	Glyoxal Agarose	Cellufine Formyl	Pall ¹
DBC _{10%}	2	1	6	4	3	5
Wash volume	2	4	6	5	1	3
Concentration factor	1	3	6	4	5	2
Process volume	1	3	6	5	2	4
Total score	6	11	24	18	11	14

¹ The Big Beads and Pall resins were in a development stage at the time of the experiments and are therefore not representative for existing or new commercial products.

4.4 Influence of adsorption flow rate on process performance

The influence of flow rate on the adsorption process was investigated for the prototype Big Beads, Cellufine Formyl and prototype Pall resins (see Appendix, Table A1 and Figure 4.3). For all resins the highest DBC_{10%} was obtained at the lowest flow rate (see Figure 4.3a), which is according to expectations, and supports the conclusion that slow diffusion is the reason of their non-optimal performance in the earlier experiments. A low flow rate implies a high residence time, which is beneficial for mass transfer and adsorption kinetics. In this case we expect intraparticle diffusion to be limiting. At a longer residence time, more time is available for BSA to diffuse into the bead. The DBC_{10%} of Big Beads and Pall are almost twice as high as the DBC_{10%} of

the Cellufine Formyl beads at 50 cm/h (0.17 ml/min), but both drop rapidly with increasing flow rate. At 300 cm/h and 600 cm/h there is no clear difference between the three beads in terms of $DBC_{10\%}$.

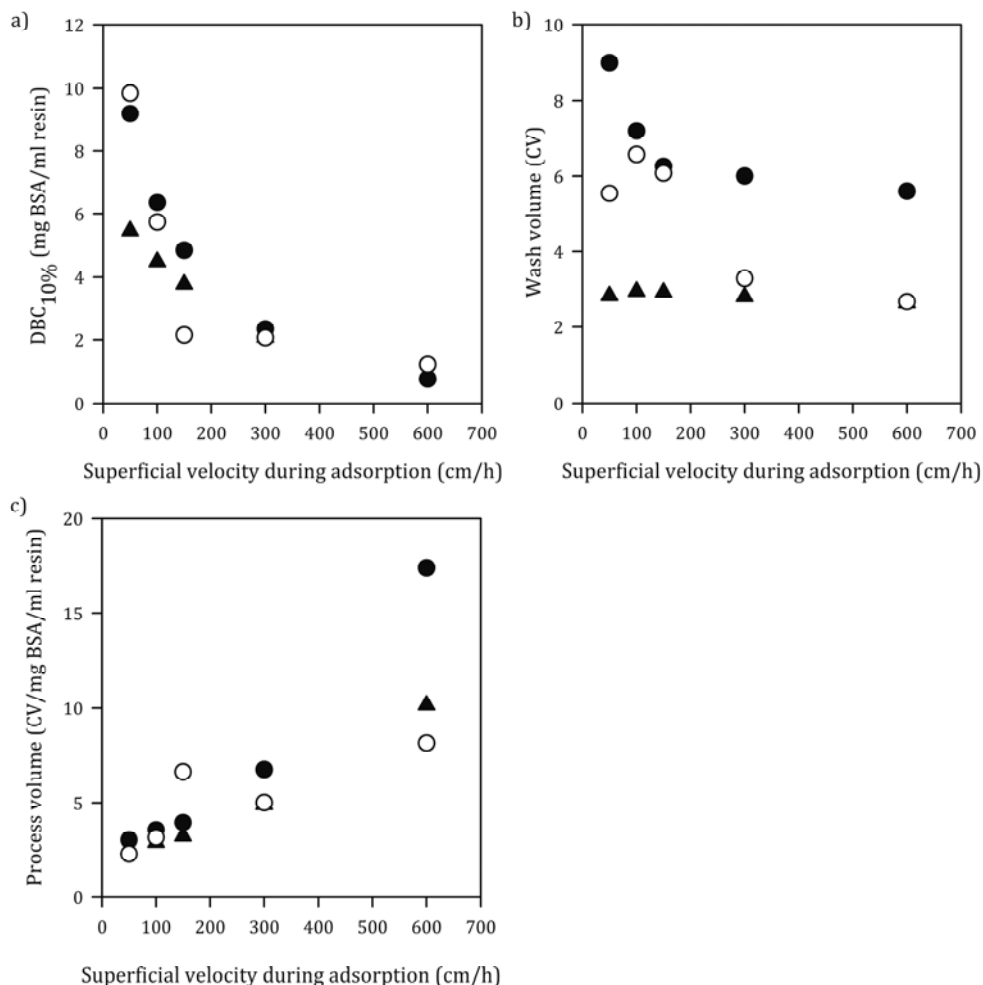


Figure 4.3. a) Dynamic binding capacity at 10% breakthrough; b) wash volume; and c) process volume as a function of superficial velocity during adsorption for Big Beads (\bullet), Cellufine Formyl (\blacktriangle) and Pall (\circ) resins.

The wash volume shown in Figure 4.3b gives insight into diffusion limitation. Only the adsorption flow rate was altered, the flow rate for washing was constant at 0.5 ml/min (150 cm/h). At a low flow rate during adsorption, the required wash volume is high, because BSA has diffused into the bead completely or almost completely. Therefore it requires more time for all the unbound BSA to leave the bead and enter the bulk liquid. In short, the wash volume should decrease with increasing adsorption

flow rate when intraparticle diffusion is limiting. Big Beads are larger than Pall and Cellufine Formyl beads (see Table 4.1) and therefore the diffusion path inside the bead is the longest of the three beads. At short residence times in the column, the BSA cannot fully saturate the Big Beads because of diffusion limitation. This effect also holds for the Pall and Cellufine Formyl beads, but to a lesser extent due to the shorter diffusion path. The Cellufine Formyl shows a constant wash volume for all flow rates, which indicates limited intraparticle diffusion limitation. This bead may well contain larger pores which help in quick transfer of BSA into and out of the beads.

The process volume increases more than linearly with increasing adsorption flow rate, which is shown in Figure 4.3c. At a low flow rate the process volume is more or less independent of the type of bead; all beads show a process volume between 2 and 3 CV per mg of BSA. As the flow rate for adsorption increases, differences between the beads become larger. The Big Beads show the highest dependence of process volume on flow rate. The Pall and Cellufine Formyl resins require half the process volume of Big Beads at an adsorption flow rate of 2 ml/min (600 cm/h). This large difference is mainly due to the much smaller amount of washing buffer required for the Pall and Cellufine Formyl resins compared to the Big Beads. All other properties measured at different adsorption flow rates for Big Beads, Cellufine Formyl and Pall resins are summarized in Table A1 in the Appendix.

The pressure drop of the resins has not been investigated, but can be an important issue for process design. Especially the smaller beads will exhibit high pressure drop. The Big Beads were specifically designed for high flow rates (the hydrodynamic resistance typically depends on the square of the bead size) and would thus be a good choice for large-scale processing. It is however important to realize that increasing adsorption flow rates will cause decreasing dynamic binding capacities and larger process volumes.

4.5 Conclusions

The activated resins investigated in this chapter could all be used to immobilize the VHH ligand and were able to bind BSA. However, large differences in performance could be observed.

Each chromatographic process has different requirements. Comparing resins based on only one property (often the $DBC_{10\%}$) will not result in finding the optimal resin available. A ranking and weighing of each property important for a particular process

enables a good decision based on experimentally determined breakthrough curves for very different resins. From the six resins investigated, the Sepabeads and Glyoxal Agarose were found to be unsuitable for the separation of BSA with the VHH ligand. The further choice of resin depends on the importance given to each of the resin properties, which may include other properties than evaluated here, such as cleaning-in-place (CIP) properties, resin life time and price.

The method of comparing resins described in this chapter is well suitable to compare resins of very different nature. It is further possible to compare results from literature by using the simple and intuitive method of ranking and weighing to find a selection of resins that can be used in the chromatography process of interest.

Acknowledgements

We would like to thank Pall (Portsmouth, United Kingdom) for providing their prototype activated cellulose resin and GE Healthcare (Uppsala, Sweden) for providing their prototype NHS-activated Big Beads. This project was supported by FrieslandCampina (Amersfoort, The Netherlands), DSM Biotechnology Center (Delft, The Netherlands), BAC BV (Naarden, The Netherlands) and SenterNovem (project IS054084).

References

1. Denizli, A. and E. Piskin. 2001. *Dye-ligand affinity systems*. Journal of Biochemical and Biophysical Methods, 49(1-3): p. 391-416.
2. Labrou, N.E., K. Mazitsos, and Y.D. Clonis. 2006. *Dye-ligand and biomimetic affinity chromatography*, in *Handbook of Affinity Chromatography*, D.S. Hage, Editor. Taylor & Francis: Boca Raton. p. 231-255.
3. Endo, T. 1996. *Fractionation of glycoprotein-derived oligosaccharides by affinity chromatography using immobilized lectin columns*. Journal of Chromatography A, 720(1-2): p. 251-261.
4. Burgess, R.R. and N.E. Thompson. 2002. *Advances in gentle immunoaffinity chromatography*. Current Opinion in Biotechnology, 13(4): p. 304-308.
5. Hage, D.S. and T.M. Phillips. 2006. *Immunoaffinity chromatography*, in *Handbook of Affinity Chromatography*, D.S. Hage, Editor. Taylor & Francis: Boca Raton. p. 127-172.
6. Hamers-Casterman, C., et al. 1993. *Naturally occurring antibodies devoid of light chains*. Nature, 363: p. 446-448.
7. Frenken, L.G.J., et al. 2000. *Isolation of antigen specific Llama VHH antibody fragments and their high level secretion by Saccharomyces cerevisiae*. Journal of Biotechnology, 78(1): p. 11-21.

8. Verheesen, P., et al. 2003. *Beneficial properties of single-domain antibody fragments for application in immunoaffinity purification and immuno-perfusion chromatography*. Biochimica et Biophysica Acta (BBA) - General Subjects, 1624(1-3): p. 21-28.
9. Muyldermans, S. 2001. *Single domain camel antibodies: current status*. Reviews in Molecular Biotechnology, 74(4): p. 277-302.
10. Zandian, M. and A. Jungbauer. 2009. *Engineering properties of a camelid antibody affinity sorbent for Immunoglobulin G purification*. Journal of Chromatography A, 1216(29): p. 5548-5556.
11. Gustavsson, P.-E. and P.-O. Larsson. 2006. *Support materials for affinity chromatography*, in *Handbook of Affinity Chromatography*, D.S. Hage, Editor. Taylor & Francis: Boca Raton p. 15-34.
12. Boschetti, E. 1994. *Advanced sorbents for preparative protein separation purposes*. Journal of Chromatography A, 658(2): p. 207-236.
13. Kim, H.S. and D.S. Hage. 2006. *Immobilization methods for affinity chromatography*, in *Handbook of Affinity Chromatography*, D.S. Hage, Editor. Taylor & Francis: Boca Raton p. 35-78.
14. Hahn, R., R. Schlegel, and A. Jungbauer. 2003. *Comparison of protein A affinity sorbents*. Journal of Chromatography B, 790(1-2): p. 35-51.
15. Fahrner, R.L., et al. 1999. *Performance comparison of protein A affinity-chromatography sorbents for purifying recombinant monoclonal antibodies*. Biotechnology and Applied Biochemistry, 30 (Pt 2): p. 121-128.
16. Levison, P.R., et al. 1997. *Performance comparison of low-pressure ion-exchange chromatography media for protein separation*. Journal of Chromatography A, 760(1): p. 151-158.
17. Staby, A., I.H. Jensen, and I. Mollerup. 2000. *Comparison of chromatographic ion-exchange resins: I. Strong anion-exchange resins*. Journal of Chromatography A, 897(1-2): p. 99-111.
18. Staby, A. and I.H. Jensen. 2001. *Comparison of chromatographic ion-exchange resins - II. More strong anion-exchange resins*. Journal of Chromatography A, 908(1-2): p. 149-161.
19. Staby, A., et al. 2004. *Comparison of chromatographic ion-exchange resins: III. Strong cation-exchange resins*. Journal of Chromatography A, 1034(1-2): p. 85-97.
20. Staby, A., et al. 2005. *Comparison of chromatographic ion-exchange resins: IV. Strong and weak cation-exchange resins and heparin resins*. Journal of Chromatography A, 1069(1): p. 65-77.
21. Staby, A., et al. 2006. *Comparison of chromatographic ion-exchange resins. V. Strong and weak cation-exchange resins*. Journal of Chromatography A, 1118(2): p. 168-179.
22. Staby, A., et al. 2007. *Comparison of chromatographic ion-exchange resins. VI. Weak anion-exchange resins*. Journal of Chromatography A, 1164(1-2): p. 82-94.
23. van Sommeren, A.P.G., P.A.G.M. Machielsen, and T.C.J. Gribnau. 1993. *Comparison of three activated agaroses for use in affinity chromatography: effects on coupling performance and ligand leakage*. Journal of Chromatography A, 639(1): p. 23-31.

24. Cuatrecasas, P. and I. Parikh. 1972. *Adsorbents for affinity chromatography. use of N-hydroxysuccinimide esters of agarose*. Biochemistry, 11(12): p. 2291-2299.
25. Mateo, C., et al. 2002. *Epoxy Sepabeads: a novel epoxy support for stabilization of industrial enzymes via very intense multipoint covalent attachment*. Biotechnology Progress, 18(3): p. 629-634.

Appendix

Table A1. The effect of flow rate on the performance of Big Beads, Cellufine formyl and Pall

	50 cm/h			100 cm/h			150 cm/h			300 cm/h			600 cm/h		
	Big Beads ¹	Cellufine formyl	Pall ¹	Big Beads ¹	Cellufine formyl	Pall ¹	Big Beads ¹	Cellufine formyl	Pall ¹	Big Beads ¹	Cellufine formyl	Pall ¹	Big Beads ¹	Cellufine formyl	Pall ¹
Residence time (min)	12.13	12.01	12.01	6.25	6.19	6.19	4.12	4.08	4.08	2.06	2.04	2.04	1.03	1.02	1.02
DBC _{10%} (mg BSA/ml resin)	9.19	5.45	9.84	6.36	4.48	5.73	4.84	3.77	2.15	2.34	2.08	2.07	0.77	0.87	1.22
Wash volume (CV)	8.99	2.84	5.54	7.19	2.95	6.57	6.25	2.93	6.08	6.00	2.81	3.29	5.60	2.64	2.68
Max desorption concentration/inlet concentration	7.76	4.93	8.19	7.66	4.73	12.17	7.58	4.67	12.47	6.98	4.65	11.27	5.68	4.48	7.31
BSA in fraction / BSA desorbed	0.91	0.91	0.94	0.90	0.89	0.94	0.91	0.88	0.93	0.90	0.88	0.93	0.90	0.88	0.91
Concentration factor	4.42	3.14	4.62	4.40	3.03	5.63	4.40	3.04	5.74	4.07	3.01	5.41	3.58	2.91	4.09
Process volume (CV/mg BSA/ml resin)	3.00	2.53	2.27	3.54	2.87	3.13	3.93	3.21	6.62	6.73	4.90	5.02	17.41	10.16	8.13

¹The Big Beads and Pall resins were in a development stage at the time of the experiments and are therefore not representative for final commercial products.

Efficiency of protein-based ligand immobilization for affinity chromatography

Abstract

Affinity chromatography often relies on specific ligands that are immobilized onto a resin. The adsorption capacities of such resins are much lower than those observed for, for example, ion exchange resins. We here report on the efficiency of ligand immobilization and subsequent protein adsorption. A llama antibody fragment against bovine serum albumin (BSA) was immobilized on three commercially available activated resins (Epoxy-activated Sepharose 6B and NHS Sepharose 4 Fast Flow from GE Healthcare (Uppsala, Sweden) and aldehyde-activated Cellufine Formyl from Chisso (Tokyo, Japan)). The adsorption capacity of the affinity resins was determined using packed bed chromatography. Between 41 and 71% of the ligand could be immobilized using the manufacturer's protocol (including coupling, blocking and washing); however, only 10 to 24% of the immobilized ligand was able to bind BSA.

We also immobilized BSA directly to the activated resins by adding different concentrations of BSA per ml resin instead of the ligand. The amount of BSA that could be immobilized increased with the amount of BSA added. The efficiency of immobilization ranged between less than 50% for the highest concentration to over 70% for the lowest BSA concentration. Thus, the concentration of the protein during immobilization is an important parameter for the final density of immobilized protein (BSA or ligand) to the resin and thus for the final adsorption capacity.

This chapter will be submitted as: Besselink, Tamara; Strubel, Maurice; van der Padt, Albert; Janssen, Anja E.M.; and Boom, Remko M. Efficiency of protein-based ligand immobilization for affinity chromatography.

5.1 Introduction

Affinity chromatography is an efficient method to specifically isolate one component from a complex mixture with high purity. In case there is a specific ligand available for the compound to be purified or removed, this ligand has to be immobilized onto a stationary phase. This procedure is often applied for immunoaffinity chromatography, which for example utilises a monoclonal antibody immobilized onto a resin (see, for example, [1]). To immobilize proteins onto chromatography resins, several procedures are possible, of which covalent attachment is the most common one. Many activated resins are available on the market, with different types of immobilization chemistry. It is crucial that the ligand is immobilized in such a way that it can bind the target compound after immobilization (see Figure 5.1). The active adsorption site should therefore not be blocked. The ligand has to be covalently attached to the resin to minimize leaching [2], but should still have enough flexibility for adsorption. A spacer arm is often applied to ensure this. An overview of immobilization chemistries can be found in a book chapter by Kim and Hage [3].

Because ligands are often expensive, the ligand should be used as efficiently as possible. Besides, the resin costs are usually a very important aspect of the economic feasibility of an affinity chromatography process. The amount of resin required depends largely on the adsorption capacity of the resin. Ion exchangers may have static adsorption capacities as high as 240 mg/ml bovine serum albumin (BSA) [4], although 100 to 150 mg/ml is more common. In molar concentrations, the capacities vary between 1.5 and 3.5 $\mu\text{mol/ml}$ resin BSA (MW ~ 67 kDa). The adsorption capacities are much lower for affinity chromatography resins, which may be due to inefficient use of the affinity ligands; for example, immobilization at the wrong side of the ligand may inhibit binding of the target component.

We distinguish two types of efficiency for affinity ligand immobilization. First, the efficiency of immobilization itself: the amount of ligand immobilized relative to the amount of ligand available for immobilization. Second, the efficiency of the ligand to bind the target: the amount of target adsorbed relative to the amount of ligand immobilized (see Figure 5.1).

Some research has been done on the efficiency of immobilization and subsequent adsorption, mainly in the field of antibody immobilization. Part of that research is aimed at immobilization to biosensors (e.g., [5, 6]). We found only few papers that quantitatively determine either the immobilization efficiency or the adsorption

efficiency [7, 8], but these papers are not very recent and the authors activated the resins themselves, which makes comparison with commercially available activated resins difficult.

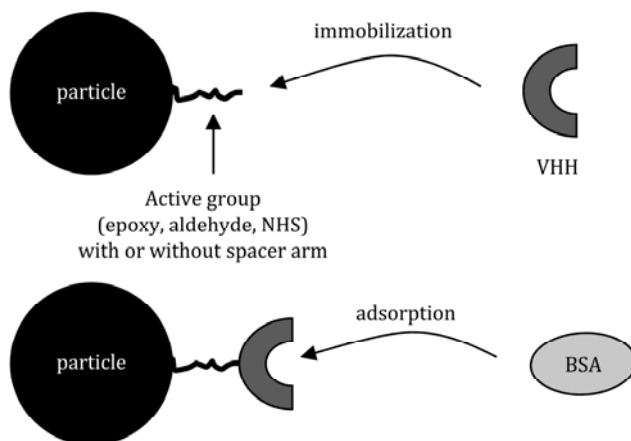


Figure 5.1. Schematic representation of immobilization and adsorption.

For commercially available affinity resins, the immobilization efficiency is unknown, but for some resins it is possible to evaluate the adsorption efficiency. As examples, one may take commercially available Cibacron Blue resins and their capacities as reported by the manufacturer. Blue Sepharose from GE Healthcare (Uppsala, Sweden) has a static adsorption capacity of more than 18 mg/ml or 0.27 $\mu\text{mol/ml}$ for human serum albumin (HSA; MW ~ 67 kDa) according to the manufacturer. A total of 7 $\mu\text{mol/ml}$ Cibacron Blue is attached to the resin, as reported by GE Healthcare, so there are 26 dye ligands available for each HSA molecule that can maximally adsorb. The adsorption efficiency with a reaction stoichiometry of 1 would then be 3.8%. Even though the stoichiometry may not be exactly 1, the dye ligands are obviously present in large excess. The Blue Trisacryl® M resin from Pall (Portsmouth, United Kingdom) has a reported adsorption capacity of up to 15 mg/ml or 0.22 $\mu\text{mol/ml}$ for HSA and up to 7 mg/ml or 0.10 $\mu\text{mol/ml}$ for BSA. The manufacturer states that 4 $\mu\text{mol/ml}$ Cibacron Blue is immobilized onto the resin, which indicates at least 18 dye ligands per HSA molecule, implying an adsorption efficiency of 5.6%. For relatively cost-effective ligands, the adsorption efficiency may not be an issue per se, but the adsorption capacity obviously is an issue, especially for larger-scale applications.

For more expensive ligands such as Protein A or monoclonal antibodies, the adsorption efficiency is even more important than a relatively inexpensive ligand as Cibacron Blue. A study by Hahn and co-workers from 2005 shows an average static

adsorption capacity of around 60 mg/ml or 0.38 $\mu\text{mol/ml}$ for several Protein A resins that bind IgG (MW ~ 160 kDa) [9]. Unfortunately, the amount of Protein A immobilized is unknown, so the adsorption efficiency is unclear. However, the adsorption capacity is relatively low, as is also mentioned by Low and co-workers [10], who stated that there is a need for higher capacity Protein A resins to keep up with antibody production.

Application of affinity chromatography in, for example, the food industry, makes improvement of adsorption capacity even more urgent, as large amounts of feedstock have to be processed, requiring high capacity purification. Even when the target concentration is low, a high capacity is important because of the high resin and equipment costs. It is therefore important to further investigate the efficiency of ligand immobilization on an activated resin.

We here report on the efficiency of immobilization of a protein-based ligand onto three commercially available activated resins. We focused on the application of fragments of antibodies produced by *Camelidae*, the so-called VHH (variable heavy-chain region of the heavy-chain antibody) [11, 12]. The VHH used was developed for adsorption of albumins, in this case bovine serum albumin (BSA). The three resins were Epoxy-activated Sepharose 6B and N-hydroxy-succinimide (NHS)-activated Sepharose 4 Fast Flow from GE Healthcare (Uppsala, Sweden), and the aldehyde-activated Cellufine Formyl from Chisso (Tokyo, Japan). We also immobilized BSA itself directly to these resins to compare the amount of immobilized BSA with the adsorption capacity of the resins for immobilized VHH ligand. We determined the influence of BSA concentration on the amount of BSA immobilized. This provides information on how to improve the immobilization of proteins for affinity chromatography.

5.2 Materials and methods

5.2.1 Materials

The VHH multi-species albumin ligand (MW 12.669 kDa) was kindly provided by BAC BV (Naarden, The Netherlands). BSA (A3059 (essentially globulin and protease free, $\geq 98\%$ pure), for the immobilization and A6003 (essentially fatty acid free, $\geq 96\%$ pure) for adsorption) was obtained from Sigma-Aldrich (Zwijndrecht, The Netherlands). Other reagents were purchased at Sigma-Aldrich or Merck (Darmstadt, Germany) and

were of analytical purity. Demineralized water was obtained using a Millipore Milli-Q system (Billerica, USA).

Epoxy-activated Sepharose 6B and NHS-activated Sepharose 4 Fast Flow were purchased at GE Healthcare (Uppsala, Sweden). Cellufine Formyl was kindly provided by Chisso (Tokyo, Japan). An overview of the activated resins is provided in Table 5.1.

Table 5.1. Overview of resins investigated

Resin	Material	Particle size (μm)	Spacer length (# -C-)	Active group	Active group density ($\mu\text{mol/ml}$)
Epoxy Sepharose 6B	Agarose	45-165	12	Epoxy	19-40
NHS Sepharose 4FF	Agarose	45-165	14	N-hydroxy- succinimide	16-23
Cellufine Formyl	Cellulose	125-210	8	Aldehyde	15-20

5.2.2 Immobilization

For the immobilization, the procedure provided by the manufacturer was followed. The coupling buffers used were 0.1 M NaHCO_3 + 0.5 M Na_2SO_4 , pH 9 for Epoxy Sepharose 6B; 0.1 M HEPES + 0.5 M NaCl, pH 8 for NHS Sepharose 4 FF; and 10 mM PBS (phosphate buffer with 137 mM NaCl and 2.7 mM KCl) pH 7.4 + 0.5 M NaCl with 30 μl 5 M cyanoborohydride per ml resin for Cellufine Formyl.

For each resin 0.1 M Tris + 0.5 M NaCl, pH 8 was used as a blocking buffer. For Epoxy Sepharose 6B and NHS Sepharose 4 Fast Flow blocking took place at room temperature for 1 hour, for Cellufine Formyl for 2 hours.

The resins were washed with 10 mM PBS pH 7.4 and pH 2, alternating the pH between steps.

Prior to VHH ligand immobilization, the ligand was dialyzed against the coupling buffer. Approximately 10 ml (exact amount measured per experiment) of ligand solution with a concentration of about 1 mM was added to 4.5 ml of each resin. Coupling took place overnight at room temperature. The resin was then filtered over a sintered glass filter prior to blocking and washing. The filtrate after coupling was kept for analysis.

For the BSA immobilization, BSA was dissolved into the coupling buffer at concentrations of approximately 15, 40 and 70 mg/ml. For each concentration 4 ml BSA solution was added to 2 ml settled resin. The coupling procedure was the same as for the VHH ligand. The same blocking procedure was used as described above, with 10 ml blocking buffer per 2 ml resin. The NHS and Epoxy Sepharose resins were washed once with 10 ml 10 mM PBS pH 2 and once with the same amount of 10 mM PBS pH 7.4. The Cellufine Formyl resin was washed once with 10 ml 10 mM PBS pH 7.4. The BSA concentrations in the blocking and wash buffers were measured in addition to the concentration in the remaining coupling buffer.

5.2.3 *Protein quantification*

The ligand and BSA concentrations were determined using HPLC with a TSKgel G2000SWxl column (7.8 mm × 30 cm, Tosoh BioScience, Tokyo, Japan). Solution A consisted of Milli-Q water with 0.1% trifluoroacetic acid (TFA), solution B of acetonitrile with 0.1% TFA. Elution was performed isocratically with 70% A and 30% B at room temperature and a flow rate of 1.5 ml/min. The proteins were detected with UV spectrometry at 214 nm.

5.2.4 *Determination BSA adsorption capacity*

The resins were poured in Tricorn 5/100 columns (GE Healthcare, Uppsala, Sweden) with a diameter of 5 mm, and a height of approximately 10 cm. The columns were connected to an Äkta Purifier 100 system (GE Healthcare, Uppsala, Sweden) with UV detection at 280 nm. A 5 mg/ml BSA solution in 10 mM PBS pH 7.4 was led over the columns at a flow rate of 0.25 ml/min until a plateau was reached. The columns were then washed with 10 mM PBS pH 7.4 until the BSA concentration dropped to zero. The BSA adsorbed was desorbed using 0.1 M glycine acidified with HCl to pH 3. The amount of BSA corresponding to the desorption peak was defined as the adsorption capacity of the column.

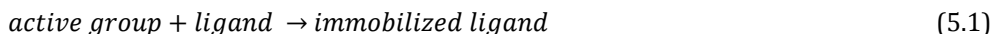
5.3 Results and discussion

5.3.1 Efficiency of VHH ligand immobilization

The three resins used all have different properties, as summarized in Table 5.1. For all the resins a spacer arm was available, which may improve immobilization and adsorption properties for small ligands. The three immobilization methods used result in random orientation because of the various positions of reactive amino acids in the ligand. The NHS and aldehyde active groups are known to react mainly with terminal amine groups or lysine residues, of which this ligand has three according to the ligand manufacturer (BAC BV, Naarden, The Netherlands). The epoxy chemistry is also capable of immobilization through hydroxyl or thiol groups. The ligand contains only two cysteine residues, which may be used for immobilization depending on their position in the protein.

The ligand concentrations and results of the experiments are shown in Table 5.2. The number of active groups available was in all cases much higher than the number of ligand molecules available.

The reaction between the active group and the ligand eventually can be summarized as follows:



Since the active groups are in excess, the amount of ligand available in the coupling buffer determines the amount of ligand that can be immobilized. The efficiency of ligand immobilization (η_{imm}) is calculated as follows:

$$\eta_{imm} = \frac{C_{VHH,0}V_c - C_{VHH,1}V_c}{C_{VHH,0}V_c} = \frac{C_{VHH,0} - C_{VHH,1}}{C_{VHH,0}} \quad (5.2)$$

In this equation, $C_{VHH,0}$ is the initial ligand concentration in the coupling buffer, V_c the volume of coupling buffer and $C_{VHH,1}$ the ligand concentration after coupling.

As shown in Table 5.2, the immobilization efficiency is between 41 and 71%. There are some other reports in which the immobilization efficiency, also referred to as the coupling efficiency, was measured (e.g., [2, 7, 8]). Van Sommeren and co-workers used a prototype of the NHS Sepharose we used in this research and found an immobilization efficiency of 100% for IgG [2]. They used several amounts of IgG: 0, 2.9, 5.4 and 11.1 mg per ml resin. Assuming a molecular weight of the IgG of 160 kDa,

the largest amount added per ml resin was 0.07 μmol which is much lower than the amount of VHH added in our experiments. This probably explains the 100% immobilization efficiency Van Sommeren *et al.* found for the IgG immobilization. If we would have applied a similar amount of VHH as they applied IgG in their experiments, the immobilization efficiency would have been higher than found here. However, the overall adsorption capacity would have been much lower because much less VHH would have been immobilized. The influence of ligand concentration on the immobilization efficiency is further investigated using BSA as a model ligand, which is discussed in Section 5.3.3.

Table 5.2. Overview of experimental conditions and results for the immobilization of VHH ligand.

	Epoxy Sephacrose	NHS Sepharose	Cellufine Formyl
Ligand concentration ($\mu\text{mol/ml}$)	0.92	1.10	0.92
Ligand added ($\mu\text{mol/ml}$ resin)	1.84	2.68	2.05
Ligand added (mol/mol active group)	0.05 - 0.10	0.12 - 0.17	0.10 - 0.14
Ligand immobilized ($\mu\text{mol/ml}$ resin) ¹	0.98	1.91	0.84
Ligand immobilized (mol/mol active group)	0.025 - 0.052	0.083 - 0.120	0.042 - 0.056
Immobilization efficiency η_{imm} (%)	53	71	41
Theoretical adsorption capacity (mg BSA/ml resin)	66	128	57
Actual adsorption capacity (mg BSA/ml resin)	6.6	20.6	13.8
Adsorption efficiency η_{ads} (%)	10	16	24

¹Based on the ligand concentration in the coupling buffer after immobilization

5.3.2 Adsorption efficiency

The adsorption efficiency of the immobilized ligand (η_{ads}) is defined as follows:

$$\eta_{ads} = \frac{Q_{BSA}}{n \cdot C_{VHH}^i} = \frac{Q_{BSA}}{Q_{BSA}^*} \quad (5.3)$$

In this equation Q_{BSA} is the amount of BSA adsorbed per volume resin, n is the number of BSA molecules that can be adsorbed by one VHH molecule and C_{VHH}^i is the immobilized ligand concentration in mass per volume resin. The theoretical adsorption capacity Q_{BSA}^* is equal to n times C_{VHH}^i . In this case n equals 1, and therefore theoretically just as many BSA molecules can be adsorbed as there are

immobilized ligands. The theoretical adsorption capacity of 128 mg/ml for NHS Sepharose lies very close to the capacity of an ion exchange resin (approximately 150 mg/ml), in contrast to the capacity that is realised in practice (see Table 5.2).

The adsorption efficiency is a measure of availability of the ligand. As summarized in Table 5.2, the values vary between 10 and 24%. There can be several reasons why the adsorption efficiency is low.

- The amount of ligand immobilized may be lower than calculated based on the ligand concentration after immobilization: some ligand may have been released after blocking and washing. Therefore, we further investigated this by using BSA as a model for the ligands, see Section 5.3.3.
- Not all ligands are necessarily functional. For example, part of the ligand may be denatured prior to the immobilization reaction. It is expected that this does not vary considerably between the resins, although there might be differences in ligand stability in different coupling buffers.
- For some immobilized ligands the adsorption site may be inaccessible because of the orientation of the ligand. The ligand can be upside-down or stretched over several active groups rendering it dysfunctional. The ligand orientation may be dependent on the immobilization method used and on the concentration of active groups. Too many active groups on the resin surface may result into many multipoint attachments which may decrease the functionality of the ligand.
- Some of the immobilized ligands may be inaccessible to BSA, because BSA cannot diffuse far enough into the pores to reach all the ligands. The VHH ligand molecule is about 5 times smaller than the BSA molecule, and the pores may have become even narrower due to the ligand immobilization. The pore sizes of the different base materials are expected to be similar.
- Finally, the adsorption efficiency depends on the BSA concentration. Based on experience (see Chapter 2), the BSA concentration used should result in saturation of the affinity resin. It is worth noting that in an actual process the product concentration is often lower than the concentration at which maximum saturation occurs.

The low adsorption efficiency is a clear indicator that more research is required to improve the activated resins further. The results show that in terms of adsorption efficiency, the immobilization of the VHH is best performed using the aldehyde chemistry, followed by NHS and epoxy. However, this may be different for another ligand, since the position of certain amino acids determines which chemistry works best.

5.3.3 BSA immobilization

The low adsorption capacities of affinity resins with immobilized ligands may be due to both the immobilization and the adsorption efficiency. The immobilization efficiency may be improved by changing the conditions for the immobilization reaction, such as the ligand concentration. Therefore, we studied the influence of the ligand concentration on the immobilization efficiency using BSA instead of VHH for the immobilization, with the same coupling procedures. Immobilized BSA is denoted as BSAⁱ to distinguish it from BSA adsorbed to immobilized VHH ligand. The immobilization capacity of BSAⁱ should be similar to the theoretical adsorption capacity as presented in Table 5.2 if both capacities are only limited by the surface area available for BSA. BSA concentrations in the solutions before and after each step were measured to accurately determine the amount of BSAⁱ immobilized. The results are summarized in Figure 5.2 and Figure 5.3.

In Figure 5.2a the amount of BSAⁱ immobilized per volume resin is plotted against the amount of BSA available for immobilization per volume resin. The amount of BSAⁱ immobilized increases upon increasing the amount of BSA added. At low concentrations (lower than 20 mg/ml resin or 0.02 mol/mol active groups), all protein is immobilised and the immobilization efficiency is 100%. This agrees with the results by van Sommeren and co-workers [2]. At higher concentrations however, the immobilisation efficiency is clearly much lower, and continues to decrease with higher concentrations of ligand offered. The line may well reach a maximum value at some point, but this value will be much higher than the values considered here.

Figure 5.2b shows that only a small number of BSAⁱ molecules is immobilized compared to the number of active groups available initially, which means that the number of active groups as such is not limiting. It is, however, possible that side reactions occur with the active groups, which do not result in BSAⁱ immobilization. NHS groups are known to rapidly hydrolyse in aqueous solutions, which competes

with the immobilization reaction [3]. This does, however, not hold for the epoxy and aldehyde groups.

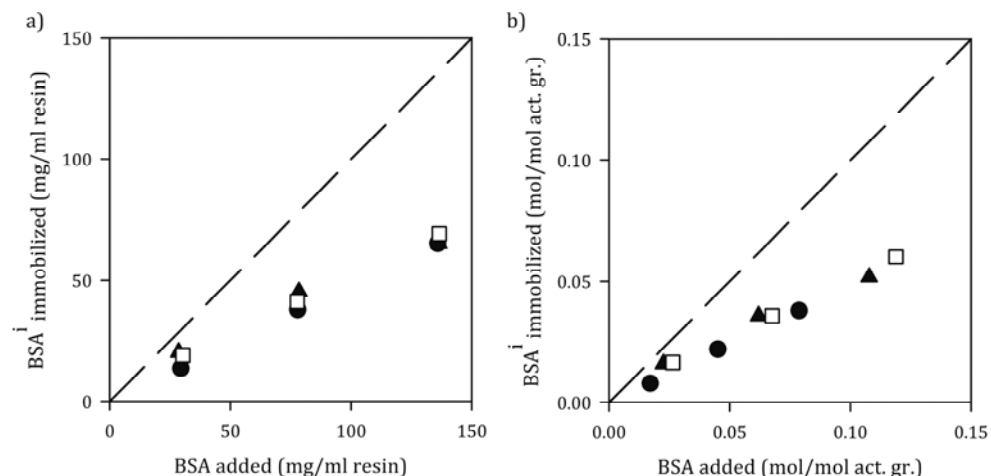


Figure 5.2. a) Amount of BSAⁱ immobilized per volume resin as a function of amount of BSA added per volume resin; b) amount of BSAⁱ immobilized per active group as a function of amount of BSA added per active group for Epoxy Sepharose (●), NHS Sepharose (▲), Cellufine Formyl (□). The dashed line indicates the theoretical maximum amount of BSA immobilized.

In Figure 5.3 the mass balance for BSA is shown for each immobilization experiment. Each section of the bar represents the amount of BSA recovered in that step of the immobilization process, divided by the total amount of BSA added initially. The lowest (black) section represents the immobilization efficiency: the amount of BSAⁱ immobilized divided by the amount of BSA added, similar to Equation 5.2 for VHH immobilization.

For Epoxy Sepharose, the immobilization efficiency is more or less constant over the range of BSA concentrations applied. The epoxy reaction is known to be rather slow and may therefore be approximated with 0th order kinetics, which may be the reason for the constant immobilization efficiency. For the NHS Sepharose and Cellufine Formyl, however, the efficiency decreases with increasing amount of BSA added. Increasing the amount of BSA results in more BSA in the residual coupling buffer and blocking and washing steps. Even though the efficiency decreases with increasing BSA concentration, the absolute number of molecules immobilized per ml resin, the immobilization capacity, increases. For affinity chromatography, the capacity should be as high as possible, partly at the expense of immobilization efficiency, especially when the non-immobilized ligands could be re-used in some way.

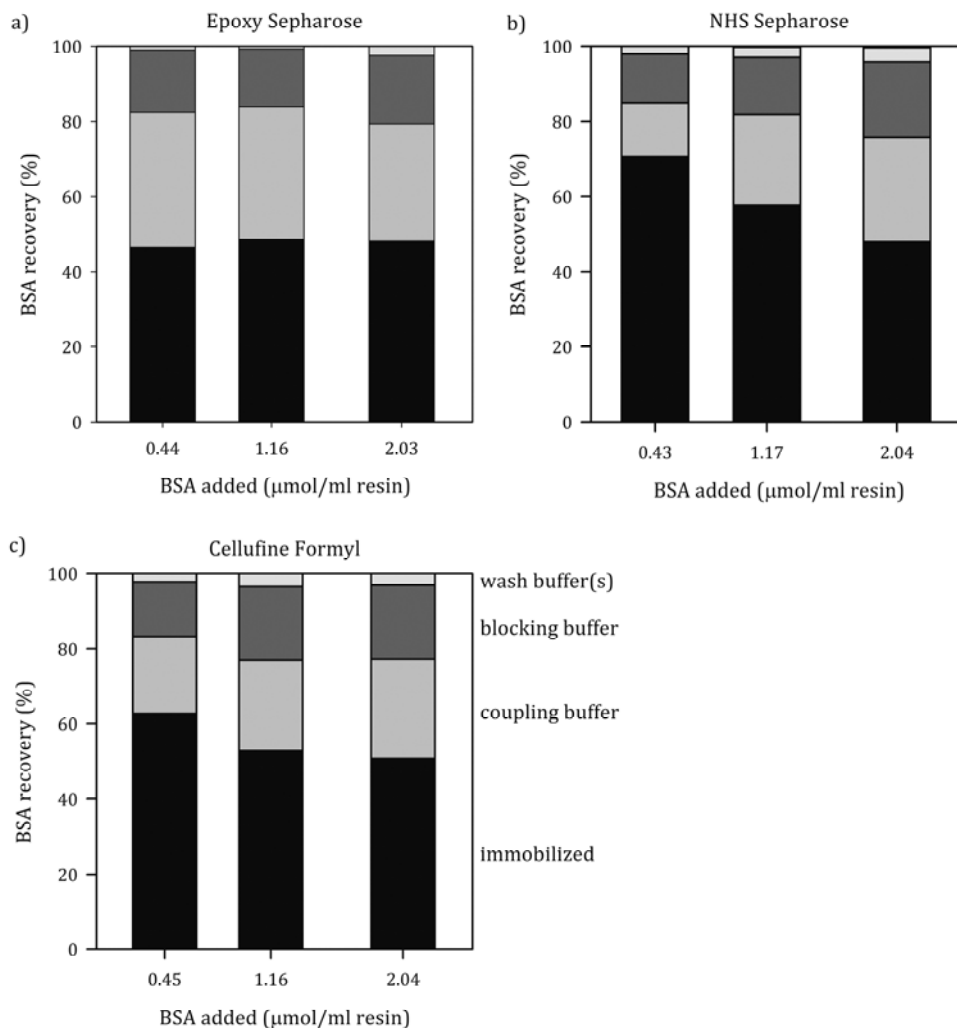


Figure 5.3. The percentage of BSA recovered in each step of the immobilization process for each BSA concentration using a) Epoxy Sepharose, b) NHS Sepharose and c) Cellufine Formyl. From bottom to top, the bar sections represent the percentage of BSAⁱ immobilized (the immobilization efficiency), the percentage of BSA in the residual coupling buffer, in the blocking buffer and in the washing steps.

After blocking of the active groups of the resins a considerable amount of BSA is retrieved in the blocking buffer. The percentage of BSA found in the blocking buffer is 15 to 20% of the amount of BSA added, and this is more than would be expected on the basis of the amount of liquid present in the pores and surrounding liquid. Some of the immobilized BSAⁱ may have been released from the resin during blocking, but it could also have been BSA that was non-specifically bound to the resin. The washing

steps account for only a small amount of BSA, probably still present in the liquid in the pores after blocking.

The results from the BSA immobilization experiments show that a lower amount of BSAⁱ can be immobilized, in our case approximately 70 mg/ml resin, compared to the amount of BSA that can be adsorbed by an ion exchanger of the same base material, at around 150 mg/ml. Steric hindrance for the activated resin is unlikely, because that would also occur during adsorption to an ion exchange resin, although the pore geometry in an ion exchange resin could be quite different compared to an activated resin. The extent of steric hindrance in an ion exchange resin may be less because the adsorption is reversible, but it would still be significant.

The immobilization capacity of BSAⁱ is higher than the actual BSA adsorption capacity of the affinity resin with immobilized VHH. BSA is a much larger protein than the VHH ligand and there are therefore more residues available for immobilization, possibly resulting in more stable bonds. Besides, for the BSAⁱ immobilization, the orientation of the protein is not an issue, because we do not require an adsorption site to be exposed such as for the VHH. The theoretical BSA adsorption capacities of the affinity resins are similar to the BSAⁱ immobilization capacities for the Epoxy-activated Sepharose and Cellufine Formyl, and higher for the NHS-activated Sepharose. It is, therefore, not unreasonable to assume that the same trends are valid for both the VHH immobilization and the BSAⁱ immobilization.

For the VHH immobilization we did not check the VHH concentrations for the subsequent steps of blocking and washing. Some of the VHH ligand probably remained in the blocking buffer, similar to the BSA experiments. If the values for VHH immobilization are similar to those of the BSAⁱ immobilization, the VHH immobilization efficiency may be overestimated and the adsorption efficiency underestimated. Even though that could indicate a deviation from the data presented in Table 5.2, the most important issue remains that the majority of the immobilized ligand is not able to bind BSA. Improving ligand functionality is therefore a potential route to optimize affinity chromatography processes.

A possibility to improve the adsorption efficiency is to selectively immobilize the ligand to expose the adsorption site to which the BSA can adsorb: site-directed immobilization. For antibodies, it is for example possible to use specific carbohydrate groups on the antibody to react with the solid support or to covalently link the antibody to an antibody-binding protein like Protein A or Protein G [6, 13, 14]. The

first method seems more suitable for larger scale processes than the last, because in the last case an extra protein is required which also needs to be immobilized in an efficient manner. It is also possible to tailor the protein to expose specific groups away from the adsorption site that can be used for immobilization. This can be done by chemical modifications or using genetic engineering [6, 13, 14]. Whether tailor-made affinity ligands will have an improved immobilization efficiency is uncertain, but it could improve the adsorption efficiency.

5.4 Conclusions

Based on the immobilization of VHH on three different activated resins we conclude that in most practical cases the initial active group density on the resins is much higher than the final density of immobilized ligand. As observed with immobilization of BSA, the amount of protein immobilized increases by increasing the amount of protein initially applied. However, the efficiency of immobilization is lower for the NHS- and aldehyde-activated resins, which means that an increasing portion of the ligand remains unused. The trends for VHH immobilization are assumed to be similar.

A significant amount of protein applied for the immobilization ends up in the blocking buffer. This may be because of non-specific adsorption, or because the immobilization bond between the protein and the resin was broken.

To make affinity chromatography with immobilized ligands cost-effective for large-scale processes, the adsorption capacity has to be dramatically improved. The immobilization efficiency may be tuned by changing the ligand concentration and densities of the active groups. However, with less than half of the immobilized ligand functional, it should be possible to bring down the resin volumes at least two-fold by further improving the adsorption efficiency. This would already significantly reduce costs and improve the applicability of affinity chromatography on larger scales.

Acknowledgements

This project was supported by FrieslandCampina (Amersfoort, The Netherlands), DSM Biotechnology Center (Delft, The Netherlands), BAC BV (Naarden, The Netherlands) and SenterNovem (project IS054084).

References

1. Hage, D.S. and T.M. Phillips. 2006. *Immunoaffinity chromatography*, in *Handbook of Affinity Chromatography*, D.S. Hage, Editor. Taylor & Francis: Boca Raton. p. 127-172.
2. van Sommeren, A.P.G., P.A.G.M. Machielsen, and T.C.J. Gribnau. 1993. *Comparison of three activated agaroses for use in affinity chromatography: effects on coupling performance and ligand leakage*. Journal of Chromatography A, 639(1): p. 23-31.
3. Kim, H.S. and D.S. Hage. 2006. *Immobilization methods for affinity chromatography*, in *Handbook of Affinity Chromatography*, D.S. Hage, Editor. Taylor & Francis: Boca Raton p. 35-78.
4. Staby, A. and I.H. Jensen. 2001. *Comparison of chromatographic ion-exchange resins - II. More strong anion-exchange resins*. Journal of Chromatography A, 908(1-2): p. 149-161.
5. Danczyk, R., et al. 2003. *Comparison of antibody functionality using different immobilization methods*. Biotechnology and Bioengineering, 84: p. 215-223.
6. Jung, Y., J.Y. Jeong, and B.H. Chung. 2008. *Recent advances in immobilization methods of antibodies on solid supports*. Analyst, 133(6): p. 697-701.
7. Pfeiffer, N.E., D.E. Wylie, and S.M. Schuster. 1987. *Immunoaffinity chromatography utilizing monoclonal antibodies: factors which influence antigen-binding capacity*. Journal of Immunological Methods, 97(1): p. 1-9.
8. Wimalasena, R.L. and G.S. Wilson. 1991. *Factors affecting the specific activity of immobilized antibodies and their biologically active fragments*. Journal of Chromatography B: Biomedical Sciences and Applications, 572(1-2): p. 85-102.
9. Hahn, R., et al. 2005. *Comparison of protein A affinity sorbents II. Mass transfer properties*. Journal of Chromatography A, 1093(1-2): p. 98-110.
10. Low, D., R. O'Leary, and N.S. Pujar. 2007. *Future of antibody purification*. Journal of Chromatography B, 848(1): p. 48-63.
11. Hamers-Casterman, C., et al. 1993. *Naturally occurring antibodies devoid of light chains*. Nature, 363: p. 446-448.
12. Muyldermans, S. 2001. *Single domain camel antibodies: current status*. Reviews in Molecular Biotechnology, 74(4): p. 277-302.
13. Rao, S.V., K.W. Anderson, and L.G. Bachas. 1998. *Oriented immobilization of proteins*. Microchimica Acta, 128(3): p. 127-143.
14. Nisnevitch, M. and M.A. Firer. 2001. *The solid phase in affinity chromatography: strategies for antibody attachment*. Journal of Biochemical and Biophysical Methods, 49(1-3): p. 467-480.

Are axial and radial flow chromatography different?

Abstract

Radial flow chromatography can be a solution for scaling up a packed bed chromatographic process to larger processing volumes. In this study we compared axial and radial flow affinity chromatography both experimentally and theoretically. We used an axial flow column and a miniaturized radial flow column with a ratio of 1.8 between outer and inner surface area, both with a bed height of 5 cm. The columns were packed with affinity resin to adsorb BSA. The average velocity in the columns was set equal. No difference in performance between the two columns could be observed.

To gain more insight into the design of a radial flow column, the velocity profile and resin distribution in the radial flow column were calculated. Using mathematical models we found that the breakthrough performance of radial flow chromatography is very similar to axial flow when the ratio between outer and inner radius of the radial flow column is around 2. When this ratio is increased, differences become more apparent, but remain small. Therefore, the choice between axial and radial flow will be based on cost price, foot print and packing characteristics. For small scale processes, axial flow chromatography is probably the best choice, for resin volumes of at least several tens of litres, radial flow chromatography may be preferable.

6.1 Introduction

Liquid chromatography is a well-known separation procedure for both analytical and preparative purposes. The demand for highly pure, specialty compounds increases, hence the necessity for a selective purification step such as preparative affinity chromatography. With affinity chromatography, it is possible to isolate one compound from a complex mixture in a single operation.

The benchmark in liquid chromatography is axial flow chromatography, consisting of a packed bed column of particles. Axial flow chromatography is thoroughly described, both theoretically and experimentally. An overview of preparative axial flow chromatography is given by Guiochon and co-workers [1]. A recent book on protein chromatography process development and scale-up has been written by Carta and Jungbauer [2], which is also mainly focused on axial flow chromatography.

Nowadays, soft beads made of agarose are commonly used for affinity chromatography. In scaling up axial flow columns from laboratory to industrial size, several problems may arise due to the low pressure resistance of the resin. Therefore, an industrial-size axial flow column is often a wide, and very short cylinder. This design makes the column expensive and difficult to handle. The equipment costs rise exponentially with the width of the column.

Radial flow chromatography is an interesting alternative to the scale-up problem of axial flow chromatography [3]. A radial flow column consists of two concentric cylinders between which the resin bed is packed. The liquid is directed from outside inwards or vice-versa, resulting in horizontal, radial flow. Small-scale radial flow columns for test purposes are usually wedge-shaped to mimic the velocity profile that exists in a full-scale radial flow column.

Radial flow chromatography has been investigated both experimentally and theoretically [3-21]. Some research has been done to compare axial flow with radial flow. Gu and co-workers [6] studied multicomponent radial flow chromatography using a theoretical approach. They showed that axial and radial flow chromatography are similar in terms of modelling and that differences between the configurations arise from a difference in mass transfer and dispersion parameters.

Tsaur and Shallcross [15] also used a theoretical approach to assess differences between axial and radial flow ion exchange. They simulated breakthrough curves of a wedge-shaped radial flow column of 254 ml with 25.6 cm bed thickness and an axial

flow column of 245 ml with 50 cm bed thickness at several flow rates and salt concentrations. The direction of flow for the radial flow column in their work was outward. They found that the radial bed was slightly more efficient, which they claimed to be due to the variation in liquid velocity in the bed and to a smaller effect of dispersion for the radial configuration.

Tharakan and Belizaire [12] found no significant difference in the antibody capture efficiency between axial and radial flow chromatography for their immunoaffinity chromatography process with similar bed thickness. They suggested that radial dispersion, mass transfer and intraparticle diffusion are probably not limiting in their case.

Kim and Lee [13] found that the flow rate in a radial flow column is 2 to 3 times higher than in an axial flow column at equal pressure drop and bed volume. In their comparison the bed thickness of the radial flow column was almost 3 times shorter than the axial flow column, which may explain the difference in flow rate. They did not find significant differences in protein purification for the two configurations.

In 2007, Cabanne and co-workers [19] compared an axial and a wedge-shaped radial flow column of equal bed thickness and volume. They separated a mixture of bovine serum albumin (BSA) and ovalbumin with radial and axial flow ion exchange chromatography. Their conclusion was that the radial flow column performed better than the axial flow column in terms of resolution, number of theoretical plates per meter, equilibration volume and peak width. However, the columns might not have been equally well-packed: the asymmetry factor of the axial flow column for an acetone pulse was 1.83, and the value for the radial flow column was 1.1. The axial flow column would usually be repacked when such an asymmetry value is measured, which then might have resulted in better performance of the axial flow column.

Even though there is literature available in which axial and radial flow chromatography are compared, we think it is necessary to perform a systematic comparison that combines practice and theory. In the available literature, the effect of the ratio between outer and inner radius of the radial flow column, i.e., the *curvature* of the radial column, is not investigated. This ratio is an important design parameter. In this paper we compare an axial flow chromatography column with a radial flow chromatography column to find out whether the two configurations are truly different in the case of single component affinity chromatography. We use small-scale columns packed with a resin with llama antibody fragment (see [22, 23] and Chapter 2) against

BSA used to purify BSA from a pure BSA solution. We also determined whether there is a difference between inward and outward flow for the radial flow column. The comparison is broadened by using the mathematical general rate model to simulate the concentration profiles inside the axial and radial flow columns with different ratios. To our knowledge, the concentration profiles along the column bed have not yet been investigated for radial flow chromatography, although these profiles give more understanding in the process. Finally, we include pressure drop and column dimensions in the comparison to determine which configuration suits best for a given chromatography process.

6.2 Definitions

In Figure 6.1 a schematic representation of both an axial and radial flow column is shown. For an axial flow column the two design parameters are r_a , the radius of the column, and L , the bed height or thickness. The variable z defines the position in the bed. For a radial flow column z also varies between 0 and bed thickness L , which is now defined as the difference between r_2 , the radius of the outer cylinder, and r_1 , the radius of the inner cylinder. Finally, H_r is the height of the radial flow column. In a radial flow column, the fluid flow is horizontal and therefore scale-up can take place by increasing H_r . The ratio between r_2 and r_1 is defined as α .

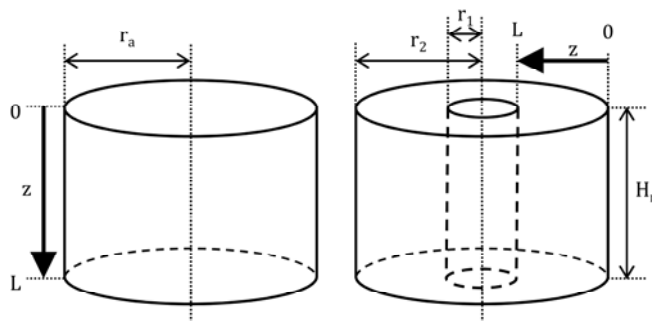


Figure 6.1. Schematic representation of an axial (left) and radial flow column (right). Variable z is indicated for downward axial flow and inward radial flow.

6.3 *Materials and methods*

6.3.1 *Materials*

Bovine serum albumin (BSA) type A3059 $\geq 98\%$ pure lyophilized powder) was purchased at Sigma-Aldrich (Zwijndrecht, The Netherlands). All other reagents used were of analytical grade and purchased at Sigma-Aldrich or Merck (Darmstadt, Germany). Demineralized water was obtained using a Millipore Milli-Q system (Billerica, USA).

Phosphate buffer (PBS) was prepared by mixing 10 mM solutions of Na_2HPO_4 and KH_2PO_4 containing 137 mM NaCl and 2.7 mM KCl until pH 7.4 was reached. The glycine buffer used for desorption was prepared by acidifying a 0.1 M glycine solution with 1 M HCl until a pH of 3 was reached.

6.3.2 *Affinity chromatography*

For the affinity chromatography experiments the columns were packed with NHS Sepharose 4 Fast Flow resin (GE Healthcare, Uppsala, Sweden) with immobilized multi-species albumin ligand derived from llama antibodies which was kindly supplied by BAC BV (Naarden, The Netherlands). An Äkta Purifier 100 (GE Healthcare, Uppsala, Sweden) was used for the column experiments with in-line UV detection at 280 nm. For both the axial and radial flow column, the packing was checked by determining the asymmetry of a 1 v/v% acetone solution as indicated by the manufacturer.

A 1 mg/ml BSA solution in 10 mM phosphate buffer pH 7.4 was used as a sample in adsorption. After adsorption, the unbound BSA was washed from the resin with adsorption buffer. Desorption took place with 0.1 M glycine/HCl pH 3 until no more BSA was detected from the column.

6.3.2.1 *Radial flow chromatography*

Radial flow affinity chromatography was performed using a micro-RFC column from Proxcys (Nieuw-Amsterdam, The Netherlands; see Figure 6.2). This column is similar to an axial flow column, but mimics a radial flow column by its conical shape. The bed thickness was 5 cm, bed volume 4.412 ml, inlet area 110 mm², outlet area 60 mm² (for inward flow, vice versa for outward flow). Adsorption and desorption were performed

with both inward (large outside surface to small inside surface, standard downflow) and outward flow (upflow) at a flow rate of 1.5 ml/min (which corresponds to an average velocity of ~ 111 cm/h).



Figure 6.2. Schematic representation of the micro-RFC column from Proxcys (Nieuw-Amsterdam, The Netherlands). Inward flow is mimicked by liquid flow from left to right, outward flow vice versa. This picture was reproduced with permission from Proxcys.

6.3.2.2 Axial flow chromatography

The radial flow column performance was also compared to an axial flow column. For the comparison a Tricorn 5/50 axial flow column (GE Healthcare, Uppsala, Sweden) of 0.5 cm diameter and 5 cm bed thickness was used. The bed thickness was equal to the bed thickness of the radial flow column. The superficial flow rate in the axial flow column was set equal to the average superficial flow rate in the radial flow column of 111 cm/h.

6.3.3 Modelling

6.3.3.1 General rate model

A mathematical model can be used to predict the outlet concentration of a radial or axial flow column at different process conditions. Many examples of the calculation and application of these models are available in literature (e.g., [1, 5, 6, 15, 17, 24-29]). The general rate model for chromatography used here consists of three parts: a mass balance over the column bed, a mass balance over the particle and a description of the adsorption kinetics.

The first part is the mass balance of BSA over the column bed. The space variable is represented by z varying from 0 to L as indicated in Figure 6.1. The concentration of BSA in the bed changes due to convection, mass transfer to the particles through the stagnant film layer surrounding the particles, and dispersion.

The mass balance is defined as:

$$\text{axial: } \frac{\partial c}{\partial t} + \frac{u}{\varepsilon_e} \frac{\partial c}{\partial z} + \frac{1-\varepsilon_e}{\varepsilon_e} k_f a (c - c_p(R_p)) = D_L \frac{\partial^2 c}{\partial z^2} \quad (6.1a)$$

$$\text{radial: } \frac{\partial c}{\partial t} + \frac{u}{\varepsilon_e} \frac{\partial c}{\partial z} + \frac{1-\varepsilon_e}{\varepsilon_e} k_f a (c - c_p(R_p)) = \frac{1}{z} \frac{\partial}{\partial z} \left(D_L z \frac{\partial c}{\partial z} \right) \quad (6.1b)$$

In Equation 6.1 c equals the concentration of BSA in the liquid, u the superficial velocity in the bed (flow rate divided by cross-sectional area of the bed), ε_e the bed porosity, k_f the mass transfer coefficient from liquid to particle, a the specific surface area of the particles ($3/R_p$ for spherical particles, with R_p the particle radius), $c_p(R_p)$ the BSA concentration at the interface between particle and liquid, and D_L the dispersion coefficient.

To complete the mass balance, two boundary conditions are defined at the inlet and outlet of the column:

$$z = 0 \quad u \cdot c_{in} = u \cdot c - \varepsilon_e D_L \frac{\partial c}{\partial z} \quad (6.2a)$$

$$z = L \quad \frac{\partial c}{\partial z} = 0 \quad (6.2b)$$

In Equation 6.2a c_{in} is the inlet concentration.

There are two differences between the axial and radial model equations. The first is that in an axial flow column, the velocity u inside the column is constant, while in a radial flow column the velocity depends on the position in the bed. Since the values for k_f and D_L also depend on the liquid velocity, these parameters are not constants for the radial flow model. Second, the dispersion term changes to cylindrical coordinates for a radial flow column.

The second part of the model is the mass balance of BSA over the particle. For porous particles a concentration profile exists inside the particle. The space variable in the particle is r which runs from 0 in the centre to R_p at the outer radius. BSA diffuses into the particle and is adsorbed on the surface of the pores. The mass balance therefore consists of an accumulation term, an adsorption term and a diffusion term.

$$\varepsilon_p \frac{\partial c_p}{\partial t} + (1 - \varepsilon_p) \frac{\partial q}{\partial t} = D_{eff} \frac{1}{r^2} \frac{\partial}{\partial r} \left(r^2 \frac{\partial c_p}{\partial r} \right) \quad (6.3)$$

In Equation 6.3, ε_p equals the particle porosity, q the amount of adsorbed BSA per particle solid volume, and D_{eff} the effective diffusion coefficient.

The boundary conditions belonging to Equation 6.3 are as follows:

$$r = R_p \quad \frac{\partial c_p}{\partial r} = k_f(c - c_p) \quad (6.4a)$$

$$r = 0 \quad \frac{\partial c_p}{\partial r} = 0 \quad (6.4b)$$

The third part of the model describes the adsorption kinetics between BSA and the VHH or any other target molecule and ligand. For this model, Langmuir kinetics were assumed:

$$\frac{\partial q}{\partial t} = k_a c_p (q_{ms} - q) - k_d q. \quad (6.5)$$

In Equation 6.5, q is defined as the amount of BSA adsorbed per particle solid volume, and q_{ms} is therefore defined as the maximum adsorption capacity per particle solid volume. Usually the maximum adsorption capacity q_m is given in amount of BSA adsorbed per column volume. From q_m , q_{ms} can be calculated as follows:

$$q_{ms} = \frac{q_m}{(1-\varepsilon_e)(1-\varepsilon_p)} \quad (6.6)$$

The initial conditions for Equations 6.1, 6.3, and 6.5 are:

$$\text{at } t = 0 \quad c = 0; c_p = 0; q = 0. \quad (6.7)$$

6.3.3.2 Parameters

For the calculation of the mass transfer coefficient k_f the Wilson-Geankoplis relation was used [30]:

$$k_f = \frac{Sh D_m}{2R_p} \quad (6.8)$$

$$Sh = \frac{1.09}{\varepsilon_e} Re^{1/3} Sc^{1/3}, \quad (6.9)$$

$$\text{with } Re = 2R_p \rho u / \eta \text{ and } Sc = \eta / (\rho D_m) \quad (6.10a-b)$$

In Equations 6.8 through 6.10, Sh equals the Sherwood number, D_m the molecular diffusivity of BSA, Re the Reynolds number, Sc the Schmidt number, ρ the density and η the viscosity of the solution. The BSA solution is assumed to have the same properties as pure water.

For the calculation of the axial dispersion coefficient D_L the following relation proposed by Chung and Wen [31] was used:

$$D_L = \frac{uL}{Pe}, \text{ with} \quad (6.11)$$

$$Pe = \frac{L}{\varepsilon_p 2R_p} (0.2 + 0.011Re^{0.48}). \quad (6.12)$$

where Pe equals the Peclet number. The effective diffusion coefficient D_{eff} inside the porous particle is estimated as follows [28, 29]:

$$D_{eff} = \frac{\varepsilon_p D_m}{\gamma} \quad (6.13)$$

where γ equals the particle tortuosity. The values for the input parameters are summarized in Table 6.1. The molecular diffusion coefficient and the molecular weight of BSA were taken from [32]. The values for the rate constants for the adsorption kinetics k_a and k_d were estimated based on data provided by BAC BV (Naarden, The Netherlands). The value for the particle tortuosity γ was taken from the paper by Barrande and co-workers [33] for SP Sepharose Fast Flow. The particle porosity ε_p for BSA was estimated to be 0.8. The bed thickness was chosen 6 cm and volume 2 l, because these dimensions represent a commercially available lab-scale radial flow column. With the parameters stated in Table 6.1, the axial flow column is 20.6 cm wide and 6 cm high. The width and height of the radial flow column depend on the ratio α between the outer and inner radius of the column. For α equal to 2, the width is 24 cm and the height 5.9 cm; for α equal to 5 the column is 15 cm wide and 11.8 cm high.

Table 6.1. Values of model input parameters.

Name	Value	Unit	Name	Value	Unit
c_{in}	1	kg/m ³	q_m	20	kg/m ³
D_m	5.9×10^{-11}	m ² /s	R_p	45×10^{-6}	m
k_a	0.3	m ³ /(kg s)	V	2×10^{-3}	m ³
k_d	5×10^{-4}	1/s	ε_e	0.4	-
L	6×10^{-2}	m	ε_p	0.8	-
MW_{BSA}	67	kg/mol	γ	1.32	-

6.3.3.3 Model simulation

The equations given in Sections 6.3.3.1 and 6.3.3.2 were implemented in the mathematical modeling software gPROMS (Process Systems Enterprise Limited, London). To solve the equations the backward finite difference method was applied with 100 discretization points over the column bed. To solve the equations for the particle, the centered finite difference method was used with 20 discretization points.

6.4 Results and discussion

6.4.1 Volume and velocity in a radial bed

The design of a radial flow column implies a velocity and resin volume distribution over the bed thickness. The cumulative resin volume for a radial bed as a function of axial or radial position z in the bed is shown in Figure 6.3a. Of course, for an axial bed the cumulative resin volume is directly proportional to the bed thickness.

The superficial velocity u at each position z and the average velocity \bar{u} at a known volumetric flow rate Φ in the radial bed can be calculated with:

$$u = \frac{\Phi}{2\pi(r_2 - z)H_r}; \quad (6.14)$$

$$\bar{u} = \frac{\Phi}{2\pi H_r} \frac{\ln(\alpha)}{L}. \quad (6.15)$$

To evaluate the influence of α , the ratio between the outer and inner radius of the column (r_2/r_1), on the velocity profile along the radial bed, we defined a dimensionless superficial velocity. This is the actual superficial velocity at each point on the radial bed, u , divided by the superficial velocity in an axial bed with equal flow rate, bed thickness and volume, u_{ax} (equal to $\Phi/(\pi r_a^2)$). The average dimensionless superficial velocity of a radial flow column can be calculated with:

$$\frac{\bar{u}}{u_{ax}} = \frac{1}{2} \frac{\alpha+1}{\alpha-1} \ln(\alpha) \quad (6.16)$$

This average dimensionless velocity of a radial flow column as a function of α is given in Figure 6.3b. A radial column with $\alpha = 1$ (both r_2 and r_1 are very large compared to their difference) is basically an axial system; therefore, the dimensionless superficial velocity at $\alpha = 1$ is necessarily 1. The average velocity increases significantly when α is increased. The dimensionless velocity profile as a function of the position in the bed (z/L) is shown in Figure 6.3c. From the dimensionless superficial velocity profile

against the relative cumulative resin volume, the cumulative volume at each point along the radial bed divided by the total volume, it is clear that for the largest portion of the resin in the radial bed the velocity is lower than the average velocity (see Figure 6.3d). The larger the ratio between the outer and inner radius, the smaller the amount of resin at which the velocity is higher than the average velocity in the bed. However, when the ratio increases, the average velocity also increases at equal flow rate and the high velocity at the outlet may be detrimental to the resin.

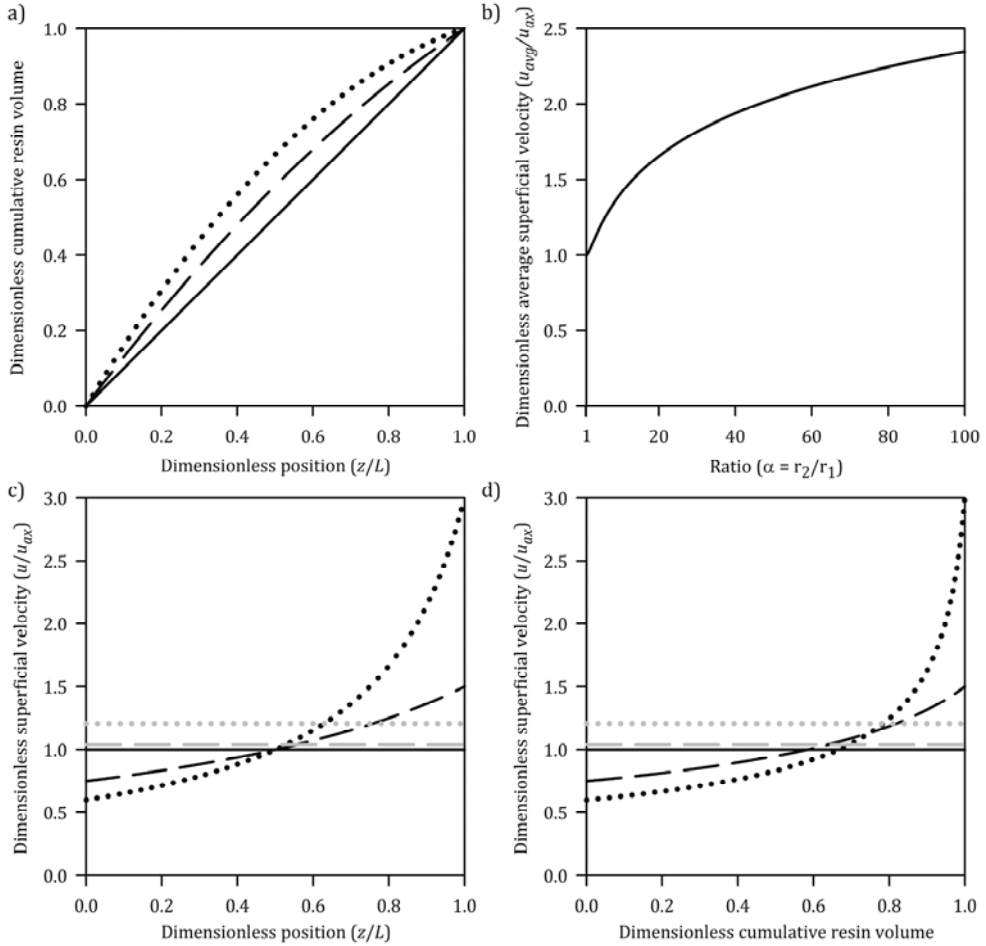


Figure 6.3. Volume distribution and superficial velocity in axial (solid) and radial flow columns (dashed for $\alpha = 2$ and dotted for $\alpha = 5$). a) Dimensionless cumulative volume of resin as a function of the axial/radial position in the bed (z/L); b) average dimensionless superficial velocity (\bar{u}/u_{ax}) as a function of the ratio α between outer and inner radius of a radial flow column; c) dimensionless superficial velocity (u/u_{ax}) as a function of the dimensionless position in the bed (z/L), grey lines indicate average velocity; d) dimensionless superficial velocity (u/u_{ax}) as a function of cumulative resin volume, grey lines indicate average velocity. The radial position variable runs from the outer cylinder to the inner cylinder as in Figure 6.1.

6.4.2 Experimental comparison axial and radial flow chromatography

A small-scale axial flow column of 5 cm bed thickness was compared to the micro-RFC column with equal bed thickness. For the micro-RFC column, the ratio α can be calculated by dividing the inlet surface area by the outlet surface area, which is equal to r_2 divided by r_1 when translated to a full-scale radial flow column. For the micro-RFC column, the value for α equals 1.83. The adsorption, washing and desorption stage of the chromatography process are shown in Figure 6.4. To compensate for differences in tubing and adapter volumes between the two experiments, the point at which the BSA concentration drops due to washing is taken as a reference to overlay the chromatograms. For both columns, the average superficial velocity was equal. The results shown in Figure 6.4 indicate that the velocity profile inside the radial flow column does not have an influence on the BSA concentration at the outlet of the column.

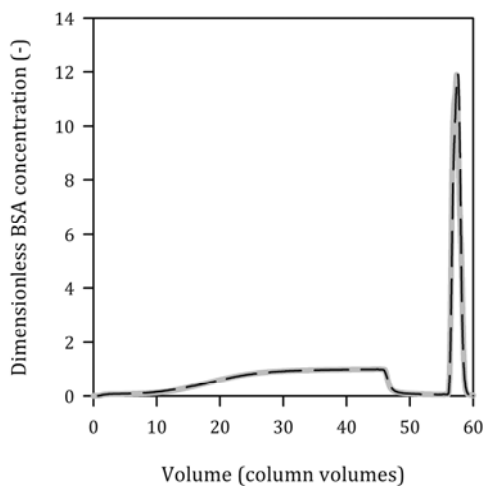


Figure 6.4. BSA concentration as a function of outlet volume for a micro-RFC column with liquid flow from large to small surface area (inward flow; solid grey) and for an axial flow column (dashed black) of 5 cm bed thickness. Superficial velocity was set at 111 cm/h (1.5 ml/min for the radial flow column), BSA inlet concentration 1 mg/ml. Adsorption and wash with 10 mM PBS pH 7.4, desorption with 0.1 M glycine/HCl pH 3.

6.4.3 Rate-limiting steps in affinity chromatography

Theoretically, the difference in mass transfer coefficient between inlet and outlet of the micro-RFC column is in the order of only 10% based on Equations 6.8 and 6.14. In the case of porous particles, the mass transfer to the particle is most likely not the limiting factor. For the model simulations this can be verified by calculating the Biot number Bi , which is the ratio between external and internal mass transfer:

$$Bi = \frac{k_f R_p}{D_{eff}} \quad (6.17)$$

For the parameter set in Table 6.1 Bi is 22 for the axial flow column and between 18 and 39 for the radial flow column at a ratio of 2. These numbers confirm that external mass transfer is not the rate-limiting step.

Diffusion inside the particles is usually very slow with effective diffusion coefficients up to 100 times lower than the free diffusion coefficient of the solute [28]. Equation 6.13 implies that D_{eff} is estimated to be $\varepsilon_p/\gamma = 0.61$ times D_m , the free diffusivity. Kaczmarski and co-workers have fitted their model to find a value for D_{eff} and found a value that was 30 times smaller than D_m [28]. Also other authors they referred to found lower values for D_{eff} . It is therefore more likely that the value for D_{eff} was overestimated with Equation 6.13 than it was underestimated. This would result in an even higher value of Bi , and a strengthening of our conclusion.

One can use the Damköhler number to estimate whether the adsorption step is rate-limiting. The Damköhler number for the adsorption step Da^a is the ratio between the adsorption rate and intraparticle diffusion:

$$Da^a = \frac{k_a c_p R_p^2}{D_{eff}} \quad (6.18)$$

With the parameters from Table 6.1, Da^a equals 9.7 at c_p equal to $0.5 c_{in}$ and 19.4 at c_p equal to c_{in} . This indicates that the process is mostly not limited by the adsorption kinetics, but is limited by intraparticle diffusion. This is even more so when indeed the value for D_{eff} is underestimated. Only in the case of very low solute concentrations in the order of 0.05 kg/m^3 , adsorption kinetics may become limiting.

A difference in adsorption behaviour between the radial and axial flow column is thus not expected, since the rate-limiting steps take place inside the particles which do not differ between the two systems.

6.4.4 *Theoretical comparison axial and radial flow chromatography*

6.4.4.1 *Breakthrough curves and concentration profiles for porous particles*

The simulation results for the adsorption of a solute in an axial and radial flow column with porous adsorbent particles are shown in Figure 6.5. In the model the effect of the ratio between the outer and inner radius of the radial flow column can be estimated by varying it over a wide range. Similar to the experiments and expectations, the simulation shows that there is only a small difference between the axial and radial flow column in terms of solute breakthrough, as shown in Figure 6.5a and b. Even when the ratio is as high as 10, only a small difference is observed, albeit always in favour of the radial flow column. However, inside the column the concentration profile is different for each ratio (see Figure 6.5c). This is mainly due to the resin volume distribution and thus the adsorption capacity distribution in the radial bed (see Figure 6.3). At the inlet of the radial flow column more solute can be bound than at the outlet. This effect is even more apparent at higher ratios between the outer and inner radii. To further illustrate that the differences in profiles are due to the distribution of resin over the column, the concentration profile is also plotted against the cumulative resin volume in Figure 6.5d. Related to the resin volume all concentration profiles more or less coincide.

Based on Figure 6.5c it may seem beneficial to use a radial flow column and use a shorter bed thickness. The comparison is, however, based on equal bed thickness. With different bed thickness, the curve for the axial flow column would also change, again resulting in a coinciding breakthrough curve.

6.4.4.2 *Non-porous particles or membranes*

Because the rate of the chromatography process is controlled by intraparticle diffusion, it is interesting to compare the systems with a process that is controlled by external mass transfer, like a stack of membranes or a bed of non-porous particles. Because of the velocity profile over the radial bed, the mass transfer coefficient k_f is not constant over the bed. For the parameter set of Table 6.1, the axial flow column has a k_f value of 1.5×10^{-5} m/s. For a radial flow column with ratio 2, the value varies from 1.4×10^{-5} m/s to 1.8×10^{-5} m/s and for a column with ratio 5 from 1.3×10^{-5} m/s to 2.7×10^{-5} m/s. The lowest value for k_f is found at the outer radius of the radial flow

column where the velocity is lowest, the highest value is found at the inner radius at the highest velocity.

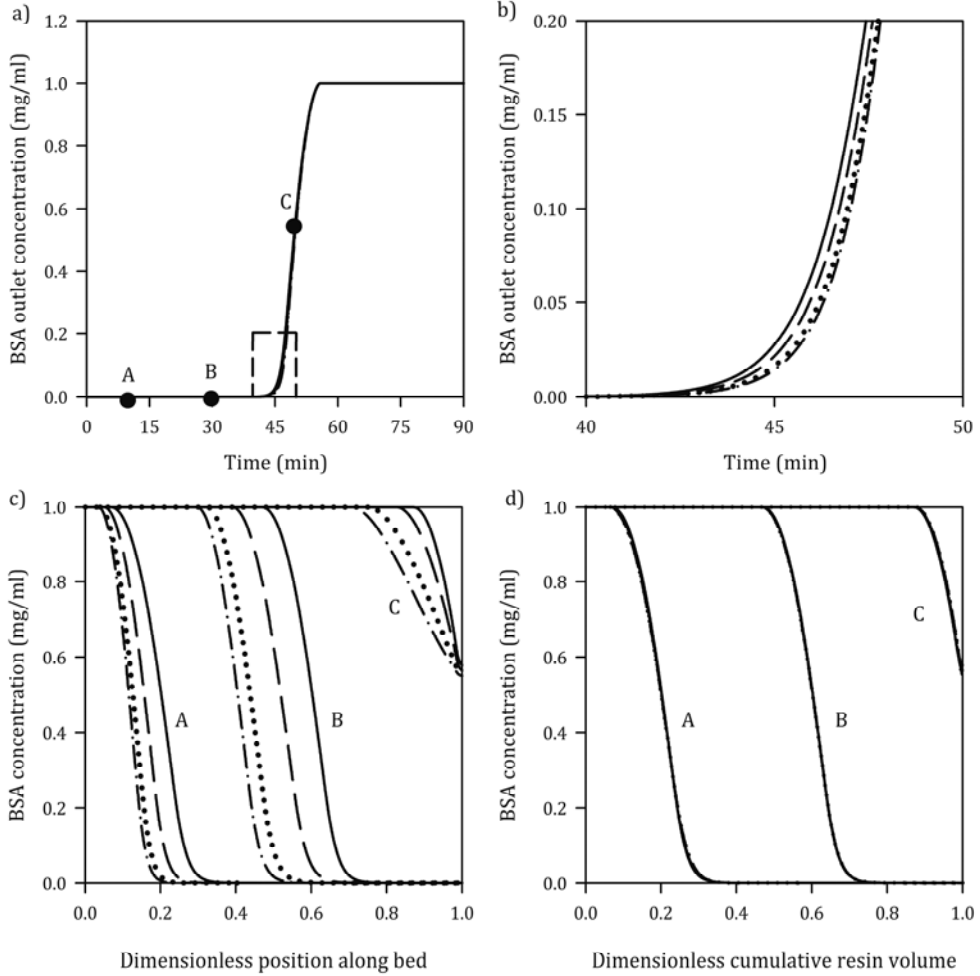


Figure 6.5. a) Breakthrough curve for axial and radial flow columns; b) zoomed-in breakthrough curve indicated with the dashed rectangle in a); c) concentration profile along the axial and radial flow column bed as a function of position along the bed (z/L); d) concentration profile along the axial and radial flow column bed as a function of dimensionless cumulative resin volume. Column volume (2 l), bed thickness (6 cm) and flow rate (superficial velocity in axial flow column is 150 cm h^{-1} , $\sim 833 \text{ ml/min}$) were equal for axial and radial flow and radial flow was directed inward. Legend: axial (solid), radial flow $\alpha = 2$ (dashed), $\alpha = 5$ (dotted) and $\alpha = 10$ (dash-dotted) and times 10 minutes (A), 30 minutes (B) and 50 minutes (C).

For non-porous particles or a membrane the adsorption capacity of BSA is much lower than for porous particles because of the lower surface area per unit resin or membrane volume. In addition, in contrast to our system, the adsorption kinetics may be limiting. This can be estimated with a modified Damköhler number:

$$Da^{a'} = \frac{k_a c^* R_p}{k_f} \quad (6.19)$$

When c^* equals c_{in} , $Da^{a'}$ would be 0.9 for an axial flow column with the parameters from Table 6.1. For a radial flow column with ratio 2, $Da^{a'}$ would lie between 0.8 and 1.0 for c^* equal to c_{in} . At lower concentrations of c^* , the value for $Da^{a'}$ is even lower. These low values indicate that not mass transfer, but adsorption is limiting here. This is the same situation as found in membrane chromatography [34]. Lowering the value for R_p does not improve the system, because this would increase the value for k_f (see Equation 6.8) cancelling out any change in R_p . The value for c^* can be increased by increasing the value for c_{in} , but this would only increase the Damköhler number for the last part of the chromatography process since at the start c^* is lower than c_{in} . The value for k_a should then be increased with at least one order of magnitude, which would no longer resemble a realistic process. Therefore, we can conclude that for practical cases an axial and radial flow chromatography column operated at equal column volume and flow rate yield almost identical breakthrough curves, regardless of the specific packing used inside the columns.

6.4.4.3 Pressure drop

An aspect that is often mentioned as an advantage of the radial flow configuration is a lower pressure drop compared to axial flow. The pressure drop over a chromatography column has two contributions: the pressure drop over the resin bed and the pressure drop over the hardware such as tubing and frits. The latter can only be determined when the complete design of the hardware is known, but is expected to be similar in both axial and radial systems.

The pressure drop over the resin bed can be estimated. For a bed of porous media the Kozeny-Carman equation is used to calculate the pressure drop over the axial flow column:

$$\Delta P_{axial} = \frac{150\eta}{D_p^2} \frac{(1-\epsilon_e)^2}{\epsilon_e^3} \frac{\Phi_{axial}}{\pi r_a^2} L ; \quad (6.20a)$$

When Equation 6.20a is converted to a derivative of pressure P over z and integrated from 0 to L , the following equation can be derived for the radial flow column:

$$\Delta P_{radial} = \frac{150\eta}{D_p^2} \frac{(1-\varepsilon_e)^2}{\varepsilon_e^3} \frac{\Phi_{radial}}{2\pi H_r} \ln(\alpha). \quad (6.20b)$$

In these equations, ΔP equals the pressure drop over the axial or radial flow column and D_p the particle diameter of the resin. The flow rate of an axial flow column compared to a radial flow column when the pressure drop, bed thickness and bed volume are kept the same is defined as:

$$\frac{\Phi_{axial}}{\Phi_{radial}} = \frac{1}{2} \frac{\alpha+1}{\alpha-1} \ln(\alpha). \quad (6.21)$$

From Equation 6.21 it is clear that at equal pressure drop, bed thickness and bed volume, the flow rate for an axial flow column is higher than for a radial flow column. The ratio between axial and radial flow rate at equal pressure drop is exactly equal to the dimensionless average velocity in a radial flow column (see Equation 6.16). In other words, the higher average superficial velocity in the radial flow column, as also indicated in Figure 6.3b, increases the pressure drop. Therefore, the potential advantage of using a radial flow column mainly lies in the possibility to use lower bed thickness without obtaining an impractical ‘pancake’ shape.

6.4.5 Inward or outward flow

6.4.5.1 Experimental comparison inward and outward flow

Inward flow is the convention for radial flow chromatography, but outward flow is also possible. The micro-RFC column was used to evaluate whether the flow direction has an influence on the breakthrough curve for BSA on the affinity resin. In Figure 6.6 the outlet concentration of the radial flow column is plotted against the outlet volume for both inward (down) and outward (up) flow. The adsorption, washing and desorption stage of the chromatography process are shown in the graph. There is a slight difference at the washing and desorption stages where outward flow seems to be advantageous. However, by changing the flow direction, the tubing volumes before and after the column were also changed. The inlet and outlet port of the radial flow column differ in volume, so the differences observed are probably not significant. Therefore, there does not seem to be a significant difference between inward and outward flow for a radial flow system with this experimental setup.

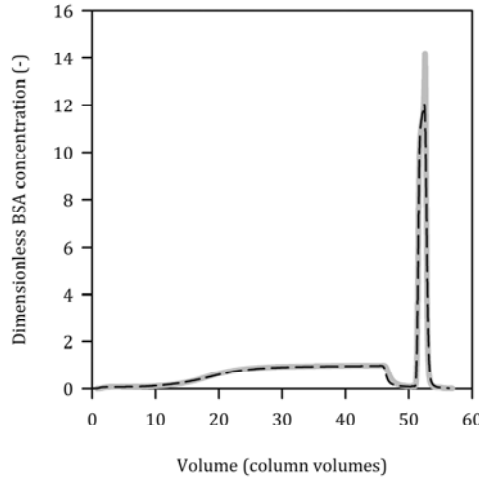


Figure 6.6. BSA concentration as a function of outlet volume for a micro-RFC column with liquid flow from large to small surface area (solid grey) and from small to large surface area (dashed black). Flow velocity was set at 111 cm/h (1.5 ml/min), BSA inlet concentration 1 mg/ml. Adsorption and wash with 10 mM PBS pH 7.4, desorption with 0.1 M glycine/HCl pH 3.

6.4.5.2 Theoretical comparison inward and outward flow

Inward flow would theoretically be beneficial compared to outward flow, because there is a large surface area and low velocity at the inlet and a small surface area and high velocity at the outlet. This effect could aid in the adsorption efficiency. In Section 6.4.5.1 we could not observe any significant differences in the experiments, but it is expected that if there is a difference, the ratio between outer and inner radius would be a parameter in this.

The only difference between inward and outward flow in the mathematical model is the expression for u , the velocity inside the column, because it runs from r_1 to r_2 for outward flow. Equation 6.14 then becomes:

$$u = \frac{\Phi}{2\pi(r_1+z)H} \quad (6.22)$$

The breakthrough curves for ratios 2 and 10 with inward and outward flow are plotted in Figure 6.7a and Figure 6.7b. From these curves it is evident that there is only a slight difference between inward and outward flow for ratio 2, but that this difference becomes significantly larger for ratio 10. Especially at the early stage of breakthrough this effect is clearly visible. Inward flow yields a sharper breakthrough front than outward flow, which corresponds to the expected benefits of using this flow

direction. The small difference between flow directions for a ratio of 2 explains why no significant difference was observed in the experimentally determined breakthrough curves shown in Figure 6.6.

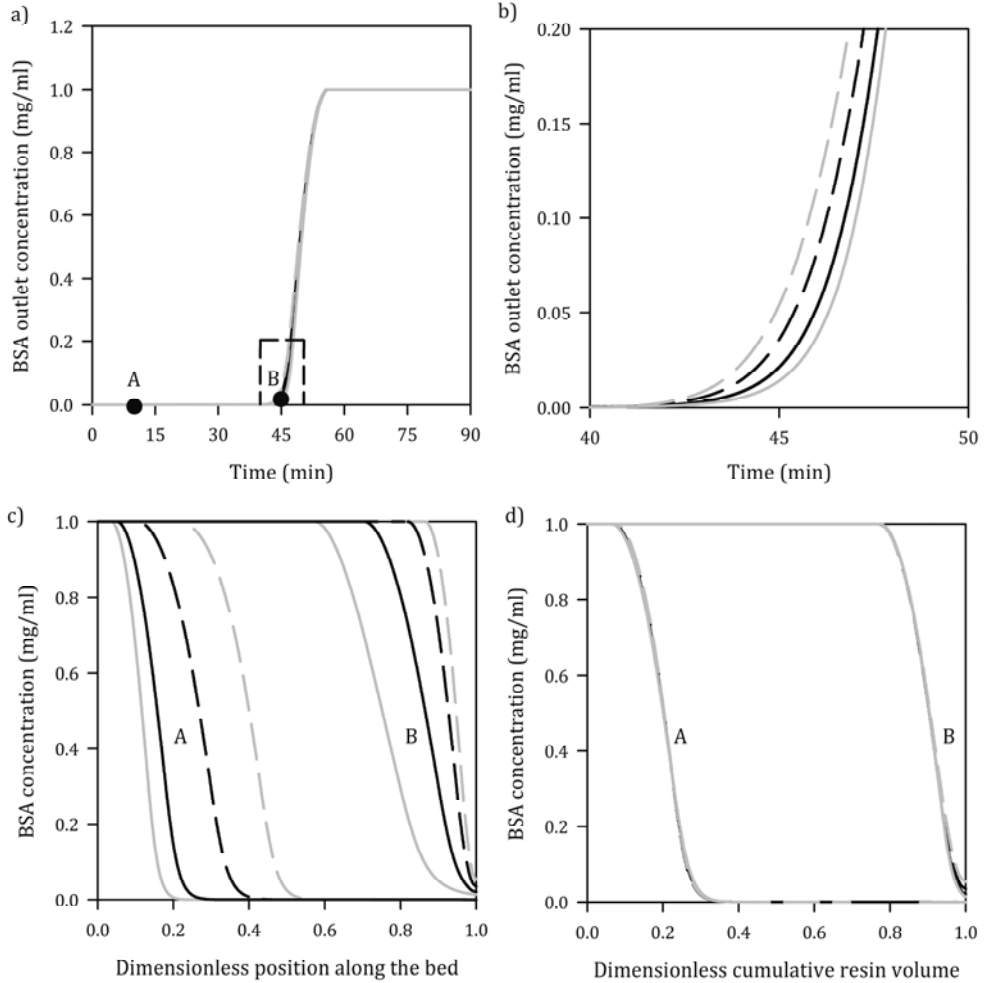


Figure 6.7. a) Breakthrough curve for radial flow columns with inward flow (solid) and outward flow (dashed); b) zoomed-in breakthrough curve indicated with the dashed rectangle in a); c) concentration profile along the radial flow column bed as a function of position along the bed (z/L); d) concentration profile along radial flow column bed as a function of dimensionless resin volume. Column volume 2 l, bed thickness 6 cm and flow rate ~ 833 ml/min (superficial velocity in similar axial flow column is 150 cm/h). Legend: inward flow (solid), outward flow (dashed), $\alpha = 2$ (black) and $\alpha = 10$ (grey), and times 10 minutes (A) and 45 minutes (B).

When the concentration profile is plotted as a function of the position along the bed (Figure 6.7c), there are large differences between ratio 2 and 10 and inward or outward flow. This is, similar to the results shown in Figure 6.5, mainly as a result of the resin volume distribution as shown in Figure 6.7d. The main differences are observed in the last 10% of the resin bed volume, where in the case of inward flow the liquid velocity is high and remaining bed thickness long and for outward flow the liquid velocity is low, but remaining bed thickness short.

From the results obtained with the simulations as shown in Figure 6.7 we conclude that inward flow is slightly advantageous compared to outward flow for radial flow chromatography. With inward flow, the solute entering the column has a longer time to diffuse and adsorb than when the flow direction is reversed, resulting in a slightly improved breakthrough curve and hence adsorption capacity. The effect of flow direction increases as the ratio between outer and inner radius of the column is increased.

6.4.6 *Column dimensions*

Neither the experimental results in Section 6.4.2, nor the model calculations in Sections 6.4.3 and 6.4.4 indicate any significant difference in adsorption efficiency between an axial and radial flow column for the adsorption process investigated. However, the main advantage of radial flow chromatography is the possibility to scale up in column height instead of diameter. For an axial flow column bed thickness is equal to column height, excluding the hardware. The bed thickness is usually restricted to approximately 20 cm for soft resins such as the Sepharose 4 FF used in this research.

In Figure 6.8 the column width and height (not to be confused with bed thickness) is plotted as a function of column volume for an axial flow column and radial flow columns with ratios 2, 5 and 10. The bed thickness is 20 cm for all columns. For a radial flow column setting the bed thickness sets the width of the column, regardless of the resin volume. A higher ratio between outer and inner radius results in a narrower and taller column. The plots indicate that for small-scale chromatography an axial flow column is less wide than a radial flow column. This results from the 'empty' space of the inner cylinder of the radial flow column. However, as the volume of the resin bed increases, so does the width of the axial flow column and at a certain column volume it becomes wider than a radial flow column. Compared to a radial flow column with ratio 2, an axial flow column is wider when its resin bed volume exceeds 100 l.

For ratios 5 and 10, the points of intersection are 39 and 31 litre respectively. The radial flow columns are obviously taller than the axial flow columns, but it is easier to transport a tall and narrow column to a clean room than a wide and short column. Assuming that column seals and flanges are cost-driving, a narrow column should also be less expensive. If the bed thickness is decreased for the radial flow column, the resin volume at which the radial flow column is less wide than an axial flow column, is of course even lower. However, at a certain point problems with the resin packing may arise due to the height of the radial flow column, and the system is better split up into two columns.

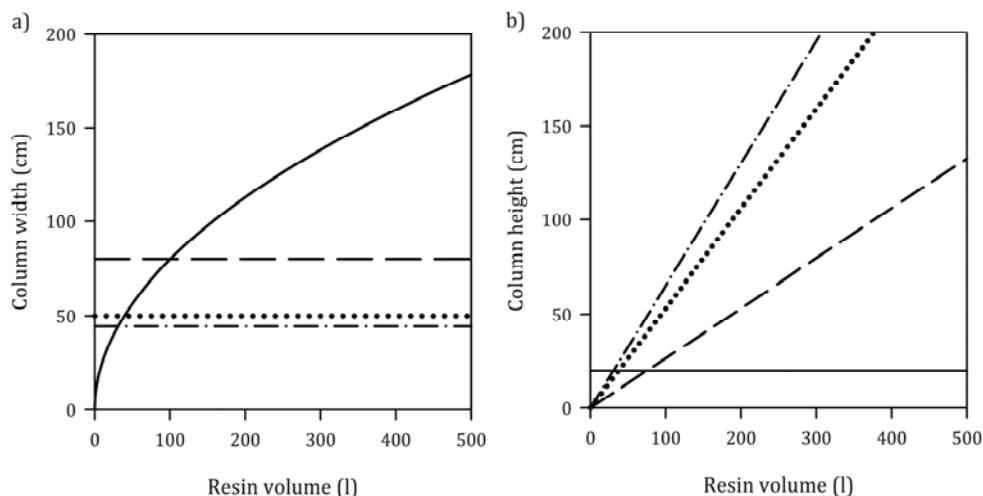


Figure 6.8. Column dimensions for an axial flow column (solid) and radial flow columns with ratio 2 (dashed), 5 (dotted) and 10 (dash-dotted) at 20 cm bed thickness; a) column width as a function of column volume; b) column height as a function of column volume.

6.4.7 Case study

As a case study we take a 15-l axial flow column of 20 cm bed thickness (to avoid large pressure drops) and a radial flow column of equal volume, but 6 cm bed thickness. These columns represent commercially available columns. A scaled representation of the two columns is shown in Figure 6.9. The flow rate is set at 10 l/min for both columns and the other parameters are set equal to those mentioned in Table 6.1. The resulting breakthrough curves are shown in Figure 6.10.

Even though the bed thickness is much shorter for the radial flow column compared to the axial flow column, the breakthrough curves cannot be distinguished from each

other. A narrow, tall radial flow column can therefore replace a wide, short axial flow column without a significant change in adsorption performance.

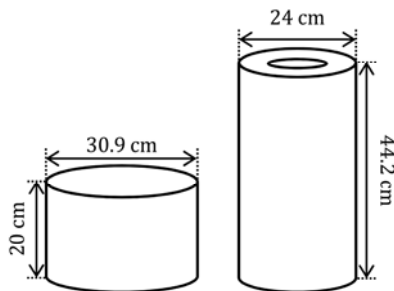


Figure 6.9. Scaled representation of an axial flow column with 20 cm bed height (left) and a radial flow column with 6 cm bed height, ratio 2 (right); both columns have a volume of 15 l.

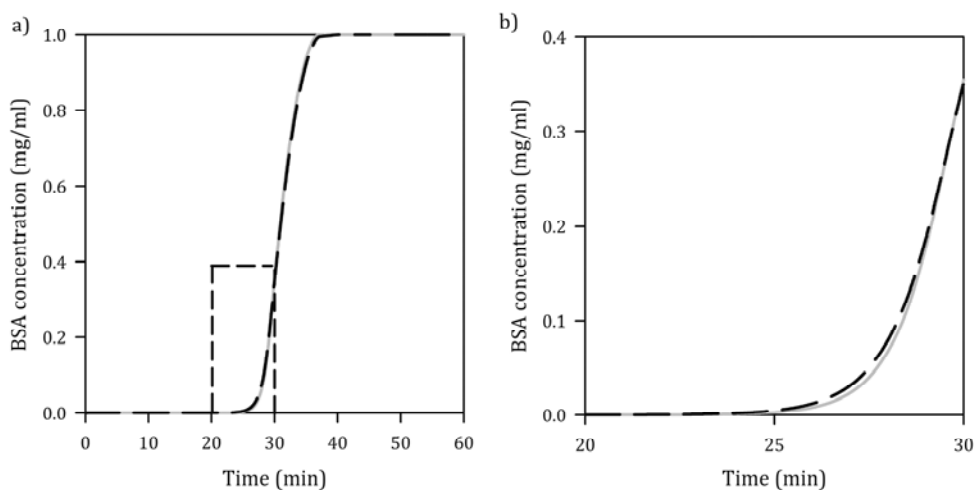


Figure 6.10. a) Breakthrough curves for an axial flow column of 20 cm bed thickness (solid grey line) and radial flow column of 6 cm bed thickness ($\alpha = 2$; dashed black line); b) zoomed-in breakthrough curve indicated with the dashed triangle in a). The bed volume is 15 l and flow rate 10 l/min in both configurations.

6.5 Conclusions

Both a practical and theoretical comparison between axial and radial flow chromatography were made based on the affinity adsorption of BSA. When the bed volume, bed thickness and flow rate are kept equal, the breakthrough curves of the two configurations coincide. Usually lab-scale experiments are performed using axial flow chromatography. The results obtained in this research suggest that these lab-

scale results can also be used to scale up to a radial flow column. However, some differences may become apparent when a high ratio between outer and inner radius of the radial flow column (>10) is used.

In theory, the radial flow column has a lower flow rate at a pre-defined pressure drop than the equivalent axial flow column at equal bed thickness and volume. However, the theory only takes into account the particle bed, other components of the column such as frits may give a different result.

The radial flow column has potential at large-scale applications, where a short bed thickness can be combined with a large inlet surface area. For pressure-sensitive resins, an axial flow column is scaled up in diameter, while the radial flow column can be scaled up vertically. This allows for the large-scale radial flow column to be easier to handle than the equivalent axial flow column, although the resin packing may limit the height of the radial flow column. On a smaller scale, the axial flow column is probably the best option.

Acknowledgements

The authors wish to thank Jan-Willem Ellen and Marcel Raedts from Proxcys BV (Nieuw-Amsterdam, The Netherlands) for their technical assistance with the micro-RFC and insight in radial flow chromatography in general. This project was supported by FrieslandCampina (Amersfoort, The Netherlands), DSM Biotechnology Center (Delft, The Netherlands), BAC BV (Naarden, The Netherlands) and SenterNovem (project IS054084).

References

1. Guiochon, G., et al. 2006. *Fundamentals of preparative and nonlinear chromatography*. 2nd ed. Elsevier: Amsterdam. 975p.
2. Carta, G. and A. Jungbauer. 2010. *Protein chromatography: process development and scale-up*. Wiley-VCH Verlag: Weinheim. 346p.
3. Saxena, V. and M. Dunn. 1989. *Solving scale-up: radial flow chromatography*. Bio/Technology, 7(3): p. 250-255.
4. Rachinskii, V.V. 1968. *Basic principles of radial chromatography*. Journal of Chromatography A, 33: p. 234-241.
5. Huang, S.H., W.-C. Lee, and G.T. Tsao. 1988. *Mathematical models of radial chromatography*. The Chemical Engineering Journal, 38(3): p. 179-186.
6. Gu, T., G.-J. Tsai, and G.T. Tsao. 1991. *A theoretical study of multicomponent radial flow chromatography*. Chemical Engineering Science, 46(5-6): p. 1279-1288.

7. McCartney, J.E. 1991. *Rapid purification of a recombinant protein using tandem radial flow ion-exchange column chromatography* BioTechniques, 11(5): p. 648-649.
8. Planques, Y., H. Pora, and F.D. Menozzi. 1991. *Affinity purification of plasminogen by radial-flow affinity-chromatography*. Journal of Chromatography, 539(2): p. 531-533.
9. Rice, R.G. and B.K. Heft. 1991. *Separations via radial flow chromatography in compacted particle beds*. AIChE Journal, 37(4): p. 629-632.
10. Gu, T., G.-J. Tsai, and G.T. Tsao. 1992. *Multicomponent affinity radial flow chromatography*. Separations Technology, 2(4): p. 176-182.
11. Gu, T., G.-J. Tsai, and G.T. Tsao. 1993. *Multicomponent radial flow chromatography*, in *Advances in Biochemical Engineering*, A. Fiechter, Editor. Springer-Verlag: Berlin Heidelberg. p. 73-95.
12. Tharakan, J. and M. Belizaire. 1995. *Ligand efficiency in axial and radial flow immunoaffinity chromatography of factor IX*. Journal of Chromatography A, 702(1-2): p. 191-196.
13. Kim, Y.-H. and E. Lee. 1996. *Comparison of axial and radial flow chromatography on protein separation speed and resolution*. Korean Journal of Chemical Engineering, 13(5): p. 466-472.
14. Tsauro, Y. and D.C. Shallcross. 1997. *Modeling of ion exchange performance in a fixed radial flow annular bed*. Industrial & Engineering Chemistry Research, 36(6): p. 2359-2367.
15. Tsauro, Y. and D.C. Shallcross. 1997. *Comparison of simulated performance of fixed ion exchange beds in linear and radial flow*. Solvent Extraction and Ion Exchange, 15(4): p. 689 - 708.
16. Wallworth, D.M. 2000. *Practical aspects and applications of radial flow chromatography*, in *Downstream Processing of Proteins*, M.A. Desai, Editor. Humana Press. p. 173-184.
17. Duong, H.M. and D.C. Shallcross. 2005. *Modeling radial-flow ion-exchange bed performance*. Industrial & Engineering Chemistry Research, 44(10): p. 3681-3691.
18. Lay, M.C., C.J. Fee, and J.E. Swan. 2006. *Continuous radial flow chromatography of proteins*. Food and Bioproducts Processing, 84(C1): p. 78-83.
19. Cabanne, C., et al. 2007. *Evaluation of radial chromatography versus axial chromatography, practical approach*. Journal of Chromatography B, 845(2): p. 191-199.
20. Dai, Y.-J., et al. 2009. *Study on the purification of polysaccharides from Nostoc flagelliforme with radial flow chromatography*. Biotechnology and Bioprocess Engineering, 14(3): p. 377-382.
21. Singh, S.M., A. Sharma, and A.K. Panda. 2009. *High throughput purification of recombinant human growth hormone using radial flow chromatography*. Protein Expression and Purification, 68(1): p. 54-59.
22. Hamers-Casterman, C., et al. 1993. *Naturally occurring antibodies devoid of light chains*. Nature, 363: p. 446-448.
23. Muyldermans, S. 2001. *Single domain camel antibodies: current status*. Reviews in Molecular Biotechnology, 74(4): p. 277-302.

24. Arve, B.H. and A.I. Liapis. 1987. *The modeling and analysis of the elution stage of biospecific adsorption in fixed beds*. Biotechnology and Bioengineering, 30(5): p. 638-649.
25. Liapis, A.I. 1989. *Theoretical aspects of affinity chromatography*. Journal of Biotechnology, 11(2-3): p. 143-160.
26. Liapis, A.I. 1990. *Modelling affinity chromatography*. Separation and Purification Methods, 19(2): p. 133-210.
27. Sridhar, P., et al. 1994. *Mathematical simulation of bioseparation in an affinity packed column*. Chemical Engineering and Technology, 17(6): p. 422-429.
28. Kaczmarski, K., et al. 2001. *Comparative modeling of breakthrough curves of bovine serum albumin in anion-exchange chromatography*. Journal of Chromatography A, 925(1-2): p. 1-17.
29. Guiochon, G. 2002. *Preparative liquid chromatography*. Journal of Chromatography A, 965(1-2): p. 129-161.
30. Wilson, E.J. and C.J. Geankoplis. 1966. *Liquid mass transfer at very low reynolds numbers in packed beds*. Industrial & Engineering Chemistry Fundamentals, 5(1): p. 9-14.
31. Chung, S.F. and C.Y. Wen. 1968. *Longitudinal dispersion of liquid flowing through fixed and fluidized beds*. AIChE Journal, 14(6): p. 857-866.
32. Peters Jr, T. 1995. 2 - *The albumin molecule: its structure and chemical properties*, in *All About Albumin*. Academic Press: San Diego. p. 9-II.
33. Barrande, M., R. Bouchet, and R. Denoyel. 2007. *Tortuosity of porous particles*. Analytical Chemistry, 79(23): p. 9115-9121.
34. Nachman, M. 1992. *Kinetic aspects of membrane-based immunoaffinity chromatography*. Journal of Chromatography A, 597(1-2): p. 167-172.

General Discussion

7.1 *Introduction*

This thesis provides an overview of different aspects involved in the isolation of proteins present at low concentrations in larger feed streams, using affinity chromatography with immobilised ligands. In Chapter 2, the technique was tested on whey as a representative feedstock. The results indicate that the ligands are selective and that a significant increase in target protein concentration can be achieved during desorption. However, traces of other components may end up in the final product. This is not necessarily a problem for many applications; but for others it may require some additional purification.

Good characterization of the affinity ligand is important because it provides insight in the process design as illustrated in Chapter 3. The thermodynamics of the binding between affinity ligand and target are complex. The information obtained from thermodynamic measurements at varying temperature and pH can be used to identify whether adsorption is favourable at the pH and temperature of the feedstock, and also how desorption can best be carried out.

Many different stationary phases exist for immobilization of the affinity ligand. Several commercially available porous particles have been investigated in Chapters 4 and 5. In Chapter 6 radial flow chromatography was presented and discussed as a possibility for scaling up affinity chromatography.

In this chapter, we will further elaborate on other types of stationary phases. Non-porous particles and membranes may provide solutions to some issues related to porous particles, but why are these not widely used? And can magnetic particles provide fast isolation of minor proteins, by avoiding diffusion limitation? We will try to identify the pros and cons of different stationary phases compared to the conventional bed of porous particles. In the final part of this discussion we give an overview of the future prospects of affinity chromatography for minor protein separation and isolation in the food industry.

7.2 Stationary phases

7.2.1 Porous versus non-porous particles in packed bed chromatography

In this thesis we focused on the use of a column packed with porous particles onto which the VHH ligand is immobilized. Porous particles exhibit a large area to volume ratio, because they have a large inner surface area. As a result of the large specific surface area, these particles can generally be quite large (in the order of 100 μm) and still exhibit high adsorption capacity. However, when the pores of the particles are too narrow for the target protein to enter, this advantage is lost. The pores might also become clogged with other components in the process liquid, such as large or aggregated proteins, or fat globules. In many cases, the diffusion of the target protein into the particle is the rate-limiting step in the adsorption process (and out of the particle in case of the desorption process). Several authors have investigated and visualized the diffusion of proteins into porous particles (e.g., [1, 2]).

To circumvent the problems of diffusion and clogging, why not use non-porous alternatives? A possibility could be to use a non-porous particle in a packed bed. The theoretical maximum adsorption capacity of a non-porous particle can be estimated with the following equation:

$$q_m = (1 - \varepsilon_e) \frac{6}{D_p} \frac{MW_t}{A_t N_{Av}} \quad (7.1)$$

In this equation, q_m equals the maximum adsorption capacity per unit packed bed volume, ε_e the porosity of the packed bed, D_p the diameter of the particle, MW_t the molecular weight of the target molecule, A_t the area occupied by the target molecule and N_{Av} equals Avogadro's number. With this equation complete surface coverage is assumed. BSA measures approximately 4 by 14 nm [3], which means it would occupy at least 44 nm². Its molecular weight is approximately 67 kDa. With porous particles a q_m of 20 mg/ml can be reached for BSA affinity chromatography (see Chapters 2 and 5). Assuming a bed porosity of 0.35, a non-porous particle should be smaller than 485 nm in diameter to have the same capacity.

The pressure drop over an axial packed bed can be calculated with the Kozeny-Carman equation:

$$\Delta P = \frac{150\eta}{D_p^2} \frac{(1-\varepsilon_e)^2}{\varepsilon_e^3} uL \quad (7.2)$$

In this equation, ΔP equals the pressure drop over the packed bed, η the liquid viscosity, u the superficial velocity in the bed (flow rate divided by cross-sectional area) and L the length of the bed. For a bed length of 20 cm and a superficial velocity of 150 cm/h a bed of 485 nm particles will yield a pressure drop exceeding 6500 bar. As a comparison, a bed of 100 μm particles would yield a pressure drop of only 0.1 bar. Packing non-porous particles into a conventional column is therefore not an option for large-scale applications. Other ways of contacting the particles and the process liquid should therefore be found, for example with magnetic particles.

7.2.2 *Magnetic particles*

7.2.2.1 *High gradient magnetic separation*

Small, non-porous particles may be used in batch adsorption in a stirred vessel to circumvent the high pressure drop. Since the adsorption is limited by either adsorption or mass transfer, and the particles are mixed intimately with the feed, equilibrium can be reached quickly. Even though only one equilibrium stage exists per stirred vessel, it could be feasible with strong and selective adsorption. It is however important to recover the particles used for the adsorption, which can be difficult with small particles. To solve this issue, several groups have investigated high gradient magnetic fishing (HGMF) or high gradient magnetic separation (HGMS) for affinity purification (e.g., [4-9]). HGMS makes use of a magnetic field to capture magnetic or magnetizable particles. This method is for example used in waste water treatment and steel production [10].

Recently, the application of HGMS has found interest for the separation of proteins in biotechnology. Adsorption here usually takes place in a stirred vessel (or a series of vessels) filled with the process liquid and magnetic (or magnetizable) particles that have an affinity for the component of interest. These particles can be several nanometres in diameter, or even porous, so adsorption capacity does not have to be limiting. Many reports on the production of magnetic particles for affinity separation can be found in literature (e.g., [5-7, 9, 11-23]).

After adsorption, the magnetic particles are filtered out of the process liquid using an external magnetic field or with a magnetized filter made of steel mesh. Washing and desorption can take place in the magnetic filter after which the particles may be returned to the stirred vessel yielding a semi-continuous system as shown in Figure

7.1. However, it is not possible to filter out and recover all magnetic particles in one step [9, 24]. Recovery of all particles is especially important for regeneration, but also for cleaning purposes and especially if the process liquid has further use, for example as a food.

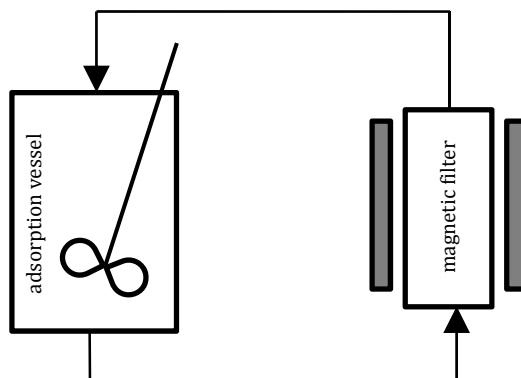


Figure 7.1. Diagram of semi-continuous HGMS.

The desorption is again important since the void space between the particles in the magnetic filter is high. Batch desorption in a stirred vessel is unfavourable because it will not yield significant concentration of the target component. Several stages of desorption would be required to fully regenerate the adsorbent particle making the process inefficient. HGMF or HGMS may be a useful separation process for the laboratory, but it is not yet feasible for larger scale affinity purification processes in the food or biotechnology industry.

7.2.2.2 *Magnetically stabilized fluidized bed*

Magnetically stabilized fluidized beds (MSFB) are columns containing magnetic/magnetizable particles which are kept in place by a magnetic field [25-40]. These columns can be viewed as an alternative for expanded bed adsorption (EBA) where the particles are hydrodynamically stabilized due to their size and density and have a more or less fixed position in the bed [41-45]. When the particles can move freely through the bed, it is called a fluidized bed. In Figure 7.2 the different configurations are shown schematically. Stabilization is necessary to prevent early and shallow breakthrough. In EBA restrictions apply to the flow velocity, which may not exceed the terminal settling velocity of the lightest particles. In an MSFB this flow

velocity may be higher due to the magnetic field applied. For MSFB it is also possible to force the particles to flow counter-current to the feed flow allowing a continuous system when multiple MSFBs for adsorption, washing and desorption are placed in series [27]. Finally, one can stabilize a packed bed of non-magnetic particles with magnetic particles [32]. In that case, the magnetic particles do not play a role in the actual separation process.

In MSFBs the magnetic field strength applied is crucial. If the field is too strong, the magnetic particles will start to form chains in the bed. This greatly reduces the efficiency of the bed [46]. If the field is not strong enough, particles break through. Because of the large magnetic fields required and the difficulty to maintain a stable bed, an MSFB is not a feasible large-scale process for the near future.

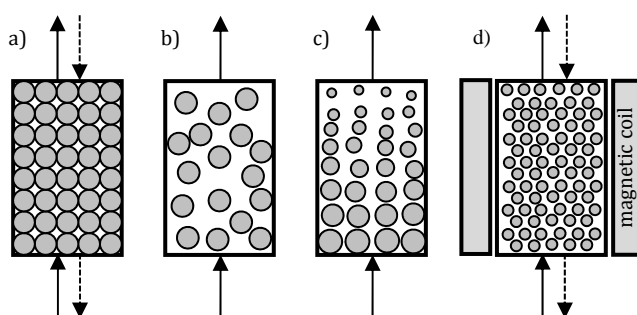


Figure 7.2. Schematic representation of an axial packed bed (a), a fluidized bed (b), an expanded bed stabilized by size (c), and a magnetically stabilized fluidized bed (d). For the axial and magnetically stabilized bed both upward and downward flow are possible.

7.2.3 Membranes

In membrane affinity adsorption, the feed stream is led through a membrane or along it (cross-flow). The affinity ligands are located in the pores of the membrane. When the feed stream flows through the membrane pores, the target protein comes into close contact with the ligand, which reduces diffusion limitation. These pores are much larger than the pores in porous particles, which enables convective flow through the membrane. This convection is seen as a main advantage of membrane adsorption, since mass transfer is not limited by pore diffusion as in porous particles. Because of the fast mass transfer, the kinetics of adsorption can become limiting.

The best known configurations are sheet membranes and hollow fibres [47-58]. A major problem with single sheet membranes is the variation in thickness and

porosity. Even small variations may lead to less performance caused by uneven permeation rates. It is therefore better to use thicker membranes, or stacks of them [48]. Thicker membranes or stacked membranes will increase the pressure drop, but it generally remains lower than for porous particles at equal superficial velocity and bed height. Since the feed usually has to pass through the membrane pores, the system can become easily plugged or fouled by, for example, fat globules or protein aggregates. This would, however, also be true for packed beds of particles.

7.2.3.1 Adsorption capacity of membranes

Membranes seem to compare quite well to the conventionally used packed bed of porous particles. However, a membrane has a low surface area to volume ratio compared to porous particles. When very large molecules or particles have to be purified, the surface area available for adsorption may be low for a porous particle as well: the component simply cannot enter the pore as it is too big. This can for example be the case for DNA purification or viral clearance.

There are not many affinity membranes commercially available as opposed to the widely used porous particles. A few ion exchange membranes are available, such as the Mustang Q and S membranes from Pall with a dynamic adsorption capacity of 60 mg/ml membrane volume at 10% breakthrough for BSA [59]. This should be compared to the porous cellulose particles from Pall, Q and S Hypercel resin, which exhibit a dynamic adsorption capacity at 10% breakthrough of up to 198 mg/ml resin volume [60]. A Sartobind Q ion exchange unit (Sartorius Stedim Biotech, Aubagne France, [61]) can adsorb approximately 29 mg BSA/ml membrane volume in total. The adsorption capacity may be further improved by increasing the specific surface area of the membrane for example by grafting polymers to the membrane surface (e.g., [62]). However, these surface modifications may result in diffusion limitation once more.

7.2.3.2 Potential for membrane chromatography

The main advantage of membrane chromatography is the low pressure drop at high flow velocities. When the target molecule is very large, the adsorption capacity of membranes can be higher than for porous particles. Membranes are said to be cheaper to produce than porous particles and may therefore be suitable for disposable systems which avoid the need of extensive washing, regeneration and validation of the

chromatography bed. However, disposable systems are probably not suitable for affinity chromatography, since the affinity ligands would be discarded as well, leading to higher costs. In addition, for large-scale processes, disposable systems are not feasible due to sustainability considerations.

For large-size components, such as DNA and viruses, membranes are probably a better choice than porous beads. For single proteins and smaller components, the choice between membranes and beads has to be determined for each specific process. Larger flow rates can be used for membrane adsorption, but too high flow rates can result in poor adsorption due to adsorption limitation.

7.2.3.3 *Mixed-matrix membrane adsorbers*

Mixed-matrix membrane adsorbers consist of grinded or otherwise small porous particles which are immobilized in a membrane-like porous structure, developed by Avramescu and co-workers [63-65] (see Figure 7.3). The particles (usually ion exchangers) are used to adsorb the target component; the membrane does not contribute to the separation itself but serves as a matrix. This type of membrane can be used in both sheet and hollow fibre configurations. The porous particles may improve the adsorption capacity of the system when it is compared to a regular membrane. The length of diffusion is shorter than for full-sized porous particles. However, the void space per unit of membrane volume is considerable, approximately 75%, and thus the capacity per unit volume is again lower than for a packed bed of porous particles.

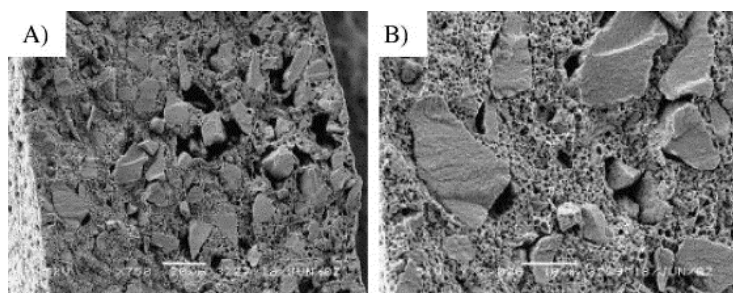


Figure 7.3. Cross-section SEM photographs of ion-exchange mixed-matrix membranes. A) magnification 750x, size bar indicates 20 µm; B) magnification 2000x, size bar indicates 10 µm. Picture reproduced from [63] with permission from Elsevier.

7.2.4 *Monoliths*

Monolithic columns are also referred to as continuous beds. Monolithic columns are comparable to packed beds, but they consist of only one 'particle'. There are many ways to produce monolithic columns (see e.g., [66] and [67]). It is also possible to produce so-called structured monoliths with uniform channels. Monoliths composed from cryogels (the gel is formed at a very low temperature, in which ice crystals act as porogens) can be dried and reused [67]. Monoliths can be formed into fibres, which can be placed in parallel. Monolithic disks [68] resemble membranes, but are thicker. By forming tubes, a radial flow monolith can be produced, by which scale-up can take place by increasing the length of the tube.

Monoliths can have a large surface area when they have micropores as well as macropores allowing for liquid convection. They may therefore have a larger adsorption capacity than membranes, but lower than porous beads when proteins and small-sized molecules are concerned. The target component moves to the affinity ligand mainly through convection, which makes this process faster than processes with porous beads.

Due to the larger pores, the pressure drop along a monolithic column is lower than in a conventional column. However, when the height or thickness increases, the pressure drop naturally increases as well. The process can be scaled up by increasing the diameter for axial flow, or height for radial flow. As in all chromatography processes with a large diameter, care must be taken to accomplish uniform flow through the column [56, 66, 69-71].

As with any type of affinity adsorbent, the monolith has a limited life time. For porous particles this is usually between 100 and 200 cycles. The packed bed of particles is then emptied and filled with fresh particles. However, the monolith has to be tightly attached to the walls of its casing, because otherwise liquid would preferably flow along the walls instead of through the monolith (i.e., channelling). Therefore, once a column is filled with monolith, it cannot be easily replaced without replacing the entire module. It may be advantageous to use a radial flow module, where attachment of the monolith is required to the top and bottom of the module instead of the outer wall.

At this moment it is not possible to produce large scale monoliths; the largest monolith available from BIA Separations (Villach, Austria) is 8 l [72]. The question is whether effort should be put in trying to make larger monolithic adsorption devices. It

is probably more interesting to use smaller scale monolithic devices in parallel to obtain the required capacity. However, for large scale systems this is probably not an efficient method of operation.

7.2.5 Summary stationary phases

In Table 7.1 an overview of the most important advantages and disadvantages of the stationary phases for affinity chromatography are summarized. To make a decision on the stationary phase suitable for a small or large-scale affinity chromatography process, Table 7.2 can be used. For each stationary phase a small sub-table indicates its general applicability for affinity chromatography depending on target molecular weight and process scale.

Table 7.1. Overview of important advantages and disadvantages of stationary phases for affinity chromatography

Stationary phase	Advantages	Disadvantages
Porous particles (packed bed)	<ul style="list-style-type: none"> + highest capacity up to medium-MW targets + concentrated product + easily available and flexible 	<ul style="list-style-type: none"> - intraparticle diffusion limitation - bed height limitation → scale-up - filtration required for particulate matter
Non-porous particles (batch or small bed)	<ul style="list-style-type: none"> + suitable for high-MW targets + suitable for particulate matter + no diffusion limitation 	<ul style="list-style-type: none"> - limited adsorption capacity - low final product concentration - high pressure drop when packed
Membranes	<ul style="list-style-type: none"> + mass transfer through convection + low pressure drop at high flow rates + possibility for disposable systems 	<ul style="list-style-type: none"> - adsorption kinetics may become limiting - limited adsorption capacity - limited availability
Monoliths	<ul style="list-style-type: none"> + mass transfer through convection and possibly (limited) diffusion + low pressure drop at high flow rates + potentially higher capacity than membranes 	<ul style="list-style-type: none"> - adsorption kinetics may become limiting - tight attachment to casing required - currently only small volumes (< 8 l) available

Table 7.2. Applicability of stationary phases based on process scale (lab, pilot or industrial) and target molecular weight (low for sugars and peptides; medium for proteins; high for DNA or viruses). Dark grey indicates that the stationary phase is first choice, lighter grey second choice.

porous particles			
MW _{target}	lab	pilot	industry
low	dark grey	light grey	light grey
medium	dark grey	dark grey	dark grey
high	light grey	light grey	light grey

membrane			
MW _{target}	lab	pilot	industry
low	light grey	dark grey	dark grey
medium	light grey	dark grey	light grey
high	light grey	dark grey	dark grey

non-porous particles			
MW _{target}	lab	pilot	industry
low	light grey	light grey	light grey
medium	light grey	light grey	light grey
high	light grey	light grey	light grey

monolith			
MW _{target}	lab	pilot	industry
low	light grey	dark grey	light grey
medium	light grey	light grey	light grey
high	light grey	light grey	light grey

7.3 Future of minor protein separation in the food industry

Affinity separation has a reputation of being expensive. As shown in Chapters 2 and 5, the adsorption capacity of BSA to the VHH affinity resin is around 20 mg/ml. With this capacity, a column of at least 50 l is required to produce 1 kg of product.

7.3.1 Adsorption capacity

It is common to describe the adsorption capacity of an adsorbent in terms of the dynamic or static adsorption capacity at a relatively high target concentration. In the case of dedicated product streams, such as fermentation broths for the production of monoclonal antibodies, the target concentration is indeed high. However, for minor component separation, the adsorption capacity at that concentration in the fluid may be much lower than the adsorption capacity mentioned by the manufacturer. Of course the number of ligands available plays a role, but the equilibrium constant is at least as important. When the adsorption is very strong, almost horizontal adsorption isotherms are measured and even for low concentrations a considerable capacity may be reached. This is illustrated in Figure 7.4 where a Langmuir adsorption isotherm is assumed:

$$q = \frac{q_m K_a c}{1 + K_a c} = \frac{q_m c}{K_d + c} \quad (7.3)$$

In Equation 7.3, q equals the equilibrium adsorption capacity, q_m the maximum adsorption capacity, K_a the adsorption equilibrium constant (adsorption rate constant divided by desorption rate constant) and c the target's equilibrium concentration, K_d is the desorption equilibrium constant ($1/K_a$).

The dependence of the adsorption isotherm on K_a is illustrated in Figure 7.4a. A value of 10^9 M^{-1} for the equilibrium constant is very high but possible for antibody-antigen adsorption. For the immobilized affinity ligand we investigated in this thesis we found a value of $1.37 \times 10^6 \text{ M}^{-1}$ (see Chapter 2), which is close to the dash-dotted line in Figure 7.4. A lower value of K_a results in a lower adsorption capacity for components present at low concentrations. In Figure 7.4b the influence of the K_a value on the relative adsorption capacity is indicated for target concentrations ranging between 0.1 and $10 \text{ }\mu\text{M}$. This graph again shows that having a ligand with a high value of K_a is crucial for optimal adsorption from a feed with a low concentration of the target component.

After adsorption, the product needs to be released from the affinity resin. High K_a values usually result in harsh conditions for desorption, for example by using low pH buffers or high salt concentrations. This may eventually lead to product degradation, depending on the stability of the product in the desorption buffer and the use of large amounts of buffer resulting in large waste streams. Besides, the harsh conditions may decrease the life time of the affinity resin and the ligands.

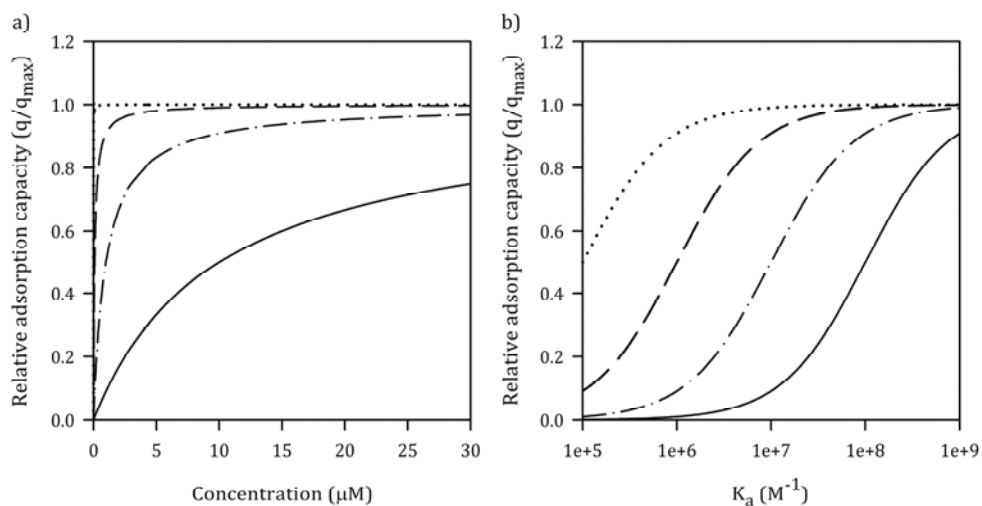


Figure 7.4. a) Relative adsorption capacity as a function of the concentration of the target component at equilibrium constant (K_a) values of 10^5 M^{-1} (solid), 10^6 M^{-1} (dash-dotted), 10^7 M^{-1} (dashed) and 10^9 M^{-1} (dotted); b) relative adsorption capacity as a function of equilibrium constant K_a at equilibrium target concentrations of 10 nM (solid), $0.1 \text{ }\mu\text{M}$ (dash-dotted), $1 \text{ }\mu\text{M}$ (dashed) and $10 \text{ }\mu\text{M}$ (dotted).

It may be possible to increase the target concentration before the adsorption step by for example ultrafiltration. Prior to applying the feed to a chromatography column with porous particles, the feed is usually filtered using a microfilter to remove larger impurities which reduce the performance of the adsorption process and have a negative effect on the resin life time. Subsequent ultrafiltration could then be used to concentrate the target. However, ultrafiltration of complete large streams for the isolation of just minor components is a costly operation; it also increases the concentration of other components which may interfere with the ultrafiltration and the adsorption process. For feeds that would be used for other purposes after the adsorption (e.g., milk, or in the case of scavenging processes), it would not be feasible to use ultrafiltration.

7.3.2 Buffer usage

Research on affinity chromatography in literature usually focuses on the adsorption phase and only sometimes discusses the desorption step. The washing step is often ignored, even though the amounts of buffer required can be quite large [73]. In Chapter 4 the lowest amount of wash buffer required to drop to 10% of the initial protein concentration was 3 column volumes when using pure protein solution as a feedstock. In Chapter 2 both pure protein solutions and whey were used as a feedstock. For the pure protein solutions, the wash volume was approximately 5 column volumes, for whey it was 10 column volumes. For an industrial-sized column 10 column volumes of buffer require very large storage tanks and good waste management. The large wash volumes probably rise from the slow diffusion inside the porous beads. Since disposing the resin is not an option because of the high resin costs, resins have to be improved to minimize washing. Macroporous particles, membranes and monoliths would probably require lower wash volumes, but will have less favourable adsorption capacities. Careful design of the pores, ensuring that the pores are wide and short enough to avoid diffusion limitation, is important.

7.3.3 Resin costs and life time

The affinity ligands investigated in this thesis have a current cost price that is approximately equal to the cost price of the bare activated resin onto which it has to be immobilized (personal communication with BAC BV (Naarden, The Netherlands) in 2010). That means that half of the total resin costs is due to the ligand, which is already a significant improvement compared to the price of monoclonal antibodies.

Lab-scale quantities of activated resin are approximately 3 times more expensive than a similar ion exchanger [74].

As discussed in Chapter 5, a significant portion of the ligand applied during the immobilisation does not end up on or in the resin, but approximately 50% stays in the solution. We performed the experiments in Chapter 5 using the standard protocols and optimization is still possible, for example by changing the ligand concentrations. More striking is the fraction of immobilized ligand that is functional in the adsorption process: maximum 25%. Multiplying these numbers indicate that only 12.5% of the ligand present initially is used in the final process. If we have to purify a minor component with a concentration of 1 μM and a K_a value of 10^6 M^{-1} we can see in Figure 7.4b that only 50% of the maximum adsorption capacity can be used when the resin is fully saturated. This drops the ligand usage to 6.25% of the ligand purchased. This shows large potential for the technology to be improved. It is therefore crucial that the immobilization of ligands is optimized such that the loss of functional ligand is further minimized.

Since the affinity resin is relatively expensive, it is necessary to reuse it as often as possible. Regeneration and cleaning-in-place methods have to be optimized. Unfortunately, these steps take a considerable amount of time in the total process cycle, in which the column cannot be used for purification. In addition, affinity ligand may be hydrolyzed. To maximize the productivity, it may be worthwhile to have two columns which can operate in turn, which is quite common in industrial processes. The final value of the minor component determines whether the costs are acceptable or not.

7.3.4 Process example

In this thesis we investigated important aspects in the separation of low-concentrated protein using affinity chromatography. The combination of the findings in the preceding chapters provides a basis for the design of a large-scale process, for example in the food industry. A hypothetical process provides insight into the actual feasibility of protein isolation using affinity chromatography with the current knowledge and materials available.

Whey is a good example of a food industry side stream that contains valuable components. For this example we assume that we want to isolate a protein with similar properties as BSA, present at a concentration of 0.1 g/L. A total of 10 m^3 whey

has to be processed per hour, and the adsorption stage may not take longer than 12 hours.

In Chapter 4 we found that the NHS Sepharose 4 FF resin (GE Healthcare, Uppsala, Sweden) was one of the best resins available amongst the resins tested. The maximum adsorption capacity of this resin was 21.6 mg BSA per ml packed resin (Chapter 2). Using the isotherm from Chapter 2, we can calculate that the maximum capacity at the feed concentration of 0.1 g/L is 14.5 mg/ml resin. Each hour a total of 1 kg product ($10 \text{ m}^3/\text{h}$ with a concentration of 0.1 g/l) is applied, so 12 kg for each batch of 12 hours. Full saturation of the column with this product concentration would require a resin volume of 828 l.

However, full saturation does not yield the highest productivity (see Chapter 2). The productivity will depend on the breakthrough curve, which depends on the column design. We assume a similar breakthrough curve as found for the isolation of BSA from 0.12 mg/ml pure BSA solution using a 0.93-ml column in Chapter 2. The bed height and residence time will, of course, not be the same for the large-scale process. The highest productivity with the lab-scale column was reached at 33% breakthrough, when a total of approximately 10 mg of BSA was adsorbed. At 33% breakthrough 12 mg of BSA was applied, so around 17% of product was lost in the flow-through. According to the isotherm, the maximum equilibrium capacity would have been 14.2 mg for this column, so approximately 70% of the available capacity was utilized at 33% breakthrough. In other words, we need approximately 45% extra capacity compared to full saturation, so a column of 1.2 m^3 instead of 828 l. For washing, desorption and regeneration at least 24 column volumes are required (Chapter 2), which is approximately 30 m^3 of buffer. When the same flow rate is used as for adsorption, these steps would add 3 hours to the process time. In total, we would be able to isolate 83% of the product present in the feed (17% would be lost in the flow-through), which is 10 kg product in 15 hours.

The recommended superficial velocity for the NHS Sepharose resin is 150 cm/h. For a flow rate of $10 \text{ m}^3/\text{h}$ a flow-through area of 6.7 m^2 is required, which is a diameter of 2.9 m. For a 1.2-m^3 column, the bed height would be 18 cm. Because of its soft structure the bed height or thickness is restricted to approximately 30 cm. Based on a maximum bed length of 30 cm instead of maximum superficial velocity, the axial column would be 2.26 m wide, resulting in a velocity of 250 cm/h. Columns with a width of up to 2 m are readily available, above $\sim 2.5 \text{ m}$ packing of the resin and sealing of the column may become difficult. A wide axial flow column can be replaced by a

radial flow column (Chapter 6). Using a more rigid particle could offer an increase in bed length and liquid velocity. However, the drawbacks would be an increase in pressure drop and a shallower breakthrough curve.

A 1.2-m³ radial flow column with a ratio of 2 between outer and inner cylinder and a bed thickness of 18 cm would be 72 cm wide and 3.9 m high. The average superficial velocity inside the column would be slightly higher than 150 cm/h: 156 cm/h (see Chapter 6). Radial flow columns with these dimensions are currently not available and problems may arise when packing resins to such a height. With a bed thickness of 30 cm and a ratio of 2, the radial flow column would be 1.2 m wide and 1.4 m high with an average superficial velocity of 260 cm/h. A radial flow column of these dimensions is commercially available. Increasing the ratio between outer and inner cylinder will decrease the width and increase the height and average velocity.

As observed in the resin comparison in Chapter 4, an increase of the liquid velocity leads to a decrease of the dynamic binding capacity. For the Big Beads resin (GE Healthcare, Uppsala, Sweden) the dynamic binding capacity at 10% breakthrough drops from 4.8 mg/ml resin to 2.34 mg/ml resin when increasing the superficial velocity from 150 cm/h to 300 cm/h. For sake of simplicity, we assume that this reduction decreases linearly with increasing velocity over this range and that the same reduction holds for the dynamic binding capacity at 33% breakthrough. An increase in superficial velocity from 150 cm/h to 250 cm/h would then decrease the dynamic capacity by a factor 1.6, leading to only 6.3 kg of product. Of course the column volume could be increased, but this would again lower the velocity and increase the costs.

By improving the efficiency of ligand immobilization (see Chapter 5) the overall capacity of the resin may be increased. This would, for example, limit the increase in resin volume required due to higher liquid velocities. It may also be possible to improve the adsorption capacity of membranes and monoliths, although care must be taken that adsorption kinetics do not become limiting. However, it does not seem likely that sufficient capacity can be obtained with membranes and monoliths, since the surface area available for adsorption will still be lower than for porous beads. An ideal stationary phase should have a good balance between macropores, or void space between particles, for convective mass transfer, and micropores for increased surface area taking into account the rate of adsorption. The stationary phase should be designed taking into account the size and nature of the target component and would therefore not be a “one-size-fits-all” type.

Another improvement for the process other than improving the stationary phase would be a different method for desorption. In total 10 column volumes, in this case well over 10 m³, of acidic desorption buffer is required for only a few kilograms of product. We found that temperature has a limited effect on the bond between BSA and the ligand (see Chapter 3), but careful design of the ligand may provide other options.

7.4 Conclusions

Highly selective ligands are indispensable for the separation and isolation of minor proteins. Because of the low concentration of these proteins, the specificity is crucial for adsorption and concentration of the protein. The availability of affinity ligands is highly improved by using recombinant proteins produced by for example yeast cells [75-77].

This thesis shows that there are many aspects involved in protein isolation using affinity chromatography. The concentration of the minor protein as well as the adsorption strength of the affinity ligand are of importance for the purification process. Even though many different adsorbents have been invented, none seem to be able to compete with the packed bed of porous beads just yet. Many attempts have been made to improve mass transfer, but it is important to note that adsorption kinetics can become limiting as well.

Seemingly non-interesting parts of the separation process, such as ligand immobilization, column washing and desorption, are of importance to determine the feasibility of affinity separation on a large scale. Ligand functionality after immobilization has to be improved to improve the economic feasibility of affinity separation, but we showed that there also is potential for that. A challenge lies ahead to find adsorbents with high adsorption capacity that are not significantly limited by diffusion and exhibit low pressure drops. Until now, affinity separation seems to be limited to highly valuable products, but we here proved that there are many possibilities for improvement which may eventually lead to a wide-spread use of affinity separations in the food industry.

References

1. Hubbuch, J., et al. 2002. *Dynamics of protein uptake within the adsorbent particle during packed bed chromatography*. Biotechnology and Bioengineering, 80(4): p. 359-368.
2. Stone, M.C. and G. Carta. 2007. *Patterns of protein adsorption in chromatographic particles visualized by optical microscopy*. Journal of Chromatography A, 1160(1-2): p. 206-214.
3. Peters Jr, T. 1995. 2 - *The albumin molecule: its structure and chemical properties*, in *All About Albumin*. Academic Press: San Diego. p. 9-II.
4. Hubbuch, J.J., et al. 2001. *High gradient magnetic separation versus expanded bed adsorption: a first principle comparison*. Bioseparation, 10(1): p. 99-112.
5. Hubbuch, J.J. and O.R.T. Thomas. 2002. *High-gradient magnetic affinity separation of trypsin from porcine pancreatin*. Biotechnology and Bioengineering, 79(3): p. 301-313.
6. Heebøll-Nielsen, A., et al. 2004. *Superparamagnetic adsorbents for high-gradient magnetic fishing of lectins out of legume extracts*. Biotechnology and Bioengineering, 87(3): p. 311-323.
7. Heebøll-Nielsen, A., et al. 2004. *Superparamagnetic cation-exchange adsorbents for bioproduct recovery from crude process liquors by high-gradient magnetic fishing*. Separation Science and Technology, 39(12): p. 2891-2914.
8. Meyer, A., et al. 2005. *Demonstration of a strategy for product purification by high-gradient magnetic fishing: recovery of superoxide dismutase from unconditioned whey*. Biotechnology Progress, 21(1): p. 244-254.
9. Franzreb, M., et al. 2006. *Protein purification using magnetic adsorbent particles*. Applied Microbiology and Biotechnology, 70(5): p. 505-516.
10. Yavuz, C.T., et al. 2009. *Magnetic separations: from steel plants to biotechnology*. Chemical Engineering Science, 64(10): p. 2510-2521.
11. Halling, P.J. and P. Dunnill. 1980. *Magnetic supports for immobilized enzymes and bioaffinity adsorbents*. Enzyme and Microbial Technology, 2(1): p. 2-10.
12. Goetz, V., M. Remaud, and D.J. Graves. 1991. *A novel magnetic silica support for use in chromatographic and enzymatic bioprocessing*. Biotechnology and Bioengineering, 37(7): p. 614-626.
13. Prioult, G., et al. 2000. *Rapid purification of nisin Z using specific monoclonal antibody-coated magnetic beads*. International Dairy Journal, 10(9): p. 627-633.
14. Tong, X.D., B. Xue, and Y. Sun. 2001. *A novel magnetic affinity support for protein adsorption and purification*. Biotechnology Progress, 17(1): p. 134-139.
15. Heebøll-Nielsen, A. 2002. *High Gradient Magnetic Fishing: support functionalisation and application for protein recovery from unclarified bioprocess liquors*. PhD Thesis. Technical University of Denmark: Biocentrum-DTU. 172p.
16. Bucak, S., et al. 2003. *Protein separations using colloidal magnetic nanoparticles*. Biotechnology Progress, 19(2): p. 477-484.
17. Heebøll-Nielsen, A., S.F.L. Justesen, and O.R.T. Thomas. 2004. *Fractionation of whey proteins with high-capacity superparamagnetic ion-exchangers*. Journal of Biotechnology, 113(1-3): p. 247-262.

18. Moeser, G.D., et al. 2004. *High-gradient magnetic separation of coated magnetic nanoparticles*. AIChE Journal, 50(11): p. 2835-2848.
19. Ding, Y. and Y. Sun. 2005. *Small-sized dense magnetic pellicular support for magnetically stabilized fluidized bed adsorption of protein*. Chemical Engineering Science, 60(4): p. 917-924.
20. Basar, N., et al. 2007. *Lysozyme purification with dye-affinity beads under magnetic field*. International Journal of Biological Macromolecules, 41(3): p. 234-242.
21. Chen, L., et al. 2007. *Isolation of lactoferrin from acid whey by magnetic affinity separation*. Separation and Purification Technology, 56(2): p. 168-174.
22. Hoshino, A., et al. 2007. *Separation of murine neutrophils and macrophages by thermoresponsive magnetic nanoparticles*. Biotechnology Progress, 23(6): p. 1513-1516.
23. Tuzmen, N., et al. 2010. *Development of the magnetic beads for dye ligand affinity chromatography and application to magnetically stabilized fluidized bed system*. Process Biochemistry, 45(4): p. 556-562.
24. Šafařík, I., L. Ptáčková, and M. Šafaříková. 2001. *Large-scale separation of magnetic bioaffinity adsorbents*. Biotechnology Letters, 23(23): p. 1953-1956.
25. Rosensweig, R.E., *Process for operating a magnetically stabilized fluidized bed*, 1978, Exxon Research & Engineering Co.: United States.
26. Sada, E., et al. 1981. *Performance of fluidized-bed reactors utilizing magnetic fields*. Biotechnology and Bioengineering, 23(11): p. 2561-2567.
27. Siegel, J.H., J.C. Pirkle, and G.D. Dupre. 1984. *Cross-flow magnetically stabilized bed chromatography*. Separation Science and Technology, 19(13-1): p. 977-993.
28. Burns, M.A. and D.J. Graves. 1985. *Continuous affinity chromatography using a magnetically stabilized fluidized bed*. Biotechnology Progress, 1(2): p. 95-103.
29. Burns, M.A. and D.J. Graves. 1987. *Application of magnetically stabilized fluidized beds to bioseparations*. Reactive Polymers, Ion Exchangers, Sorbents, 6(1): p. 45-50.
30. Lochmuller, C.H. and L.S. Wigman. 1987. *Affinity separation in magnetically stabilized fluidized beds: synthesis and performance of packing materials*. Separation Science and Technology: p. 2111-2125.
31. Siegel, J.H. 1987. *Liquid-fluidized magnetically stabilized beds*. Powder Technology, 52(2): p. 139-148.
32. Chetty, A.S. and M.A. Burns. 1991. *Continuous protein separations in a magnetically stabilized fluidized bed using nonmagnetic supports*. Biotechnology and Bioengineering, 38(9): p. 963-971.
33. Liu, Y.A., R.K. Hamby, and R.D. Colberg. 1991. *Fundamental and practical developments of magnetofluidized beds: a review*. Powder Technology, 64(1-2): p. 3-41.
34. Noble, R.D., et al., *Stationary magnetically stabilized fluidized bed for protein separation and purification*, 1992, The University of Colorado Foundation, Inc.: United States.
35. Goto, M., T. Imamura, and T. Hirose. 1995. *Axial dispersion in liquid magnetically stabilized fluidized beds*. Journal of Chromatography A, 690(1): p. 1-8.

36. Fee, C.J. 1996. *Stability of the liquid-fluidized magnetically stabilized fluidized bed*. AIChE Journal, 42(5): p. 1213-1219.
37. Seibert, K.D. and M.A. Burns. 1998. *Effect of hydrodynamic and magnetic stabilization on fluidized-bed adsorption*. Biotechnology Progress, 14(5): p. 749-755.
38. Böhm, D. and B. Pittermann. 2000. *Magnetically stabilized fluidized beds in biochemical engineering - investigations in hydrodynamics*. Chemical Engineering & Technology, 23(4): p. 309-312.
39. Hou, Y.Y. and R.A. Williams. 2002. *Magnetic stabilisation of a liquid fluidised bed*. Powder Technology, 124(3): p. 287-294.
40. Tong, X.D. and Y. Sun. 2003. *Application of magnetic agarose support in liquid magnetically stabilized fluidized bed for protein adsorption*. Biotechnology Progress, 19(6): p. 1721-1727.
41. Chase, H.A. and N.M. Draeger. 1992. *Affinity purification of proteins using expanded beds*. Journal of Chromatography A, 597(1-2): p. 129-145.
42. Chase, H.A. and N.M. Draeger. 1992. *Expanded-bed adsorption of proteins using ion-exchangers*. Separation Science and Technology, 27(14): p. 2021 - 2039.
43. Hjorth, R. 1997. *Expanded-bed adsorption in industrial bioprocessing: recent developments*. Trends in Biotechnology, 15(6): p. 230-235.
44. Anspach, F.B., et al. 1999. *Expanded-bed chromatography in primary protein purification*. Journal of Chromatography A, 865(1-2): p. 129-144.
45. Hubbuch, J., J. Thömmes, and M.-R. Kula. 2005. *Biochemical engineering aspects of expanded bed adsorption*. Advances in Biochemical Engineering/Biotechnology, 92: p. 101-123.
46. Franzreb, M., et al. 2001. *Liquid-phase mass transfer of magnetic ion exchangers in magnetically influenced fluidized beds: I. DC fields*. Reactive and Functional Polymers, 46(3): p. 247-257.
47. Brandt, S., et al. 1988. *Membrane-based affinity technology for commercial scale purifications*. Nature Biotechnology, 6(7): p. 779-782.
48. Suen, S.-Y. and M.R. Etzel. 1992. *A mathematical analysis of affinity membrane bioseparations*. Chemical Engineering Science, 47(6): p. 1355-1364.
49. Josic, D., et al. 1992. *High-performance membrane chromatography of serum and plasma membrane proteins*. Journal of Chromatography A, 590(1): p. 59-76.
50. Tennikova, T.B. and F. Svec. 1993. *High-performance membrane chromatography: highly efficient separation method for proteins in ion-exchange, hydrophobic interaction and reversed-phase modes*. Journal of Chromatography A, 646(2): p. 279-288.
51. Roper, D.K. and E.N. Lightfoot. 1995. *Separation of biomolecules using adsorptive membranes*. Journal of Chromatography A, 702(1-2): p. 3-26.
52. Thömmes, J. and M.R. Kula. 1995. *Membrane chromatography - an integrative concept in the downstream processing of proteins*. Biotechnology Progress, 11(4): p. 357-367.
53. Sridhar, P. 1996. *Design of affinity membrane bioseparations*. Chemical Engineering and Technology, 19(5): p. 398-404.
54. Charcosset, C. 1998. *Review: Purification of proteins by membrane chromatography*. Journal of Chemical Technology & Biotechnology, 71(2): p. 95-110.

55. Klein, E. 2000. *Affinity membranes: a 10-year review*. Journal of Membrane Science, 179(1-2): p. 1-27.
56. Zou, H., Q. Luo, and D. Zhou. 2001. *Affinity membrane chromatography for the analysis and purification of proteins*. Journal of Biochemical and Biophysical Methods, 49(1-3): p. 199-240.
57. Ghosh, R. 2002. *Protein separation using membrane chromatography: opportunities and challenges*. Journal of Chromatography A, 952(1-2): p. 13-27.
58. Charcosset, C. 2006. *Membrane processes in biotechnology: an overview*. Biotechnology Advances, 24(5): p. 482-492.
59. Pall Corporation. *Mustang® membrane chromatography starter kits*. [cited: 2012, March 5th]. Available from: <http://www.pall.com>.
60. Pall Corporation. *Q and S HyperCel™ sorbents*. [cited: 2012, March 5th]. Available from: www.pall.com.
61. Sartorius Stedim Biotech. *Sartobind® ion exchange MA units*. [cited: 2012, March 5th]. Available from: www.sartorius-stedim.com.
62. Gebauer, K.H., J. Thommes, and M.R. Kula. 1997. *Breakthrough performance of high-capacity membrane adsorbers in protein chromatography*. Chemical Engineering Science, 52(3): p. 405-419.
63. Avramescu, M.-E., Z. Borneman, and M. Wessling. 2003. *Mixed-matrix membrane adsorbers for protein separation*. Journal of Chromatography A, 1006(1-2): p. 171-183.
64. Avramescu, M.-E., Z. Borneman, and M. Wessling. 2003. *Dynamic behavior of adsorber membranes for protein recovery*. Biotechnology and Bioengineering, 84(5): p. 564-572.
65. Avramescu, M.-E., et al. 2003. *Preparation of mixed matrix adsorber membranes for protein recovery*. Journal of Membrane Science, 218(1-2): p. 219-233.
66. Zou, H., et al. 2002. *Monolithic stationary phases for liquid chromatography and capillary electrochromatography*. Journal of Chromatography A, 954(1-2): p. 5-32.
67. Jungbauer, A. and R. Hahn. 2004. *Monoliths for fast bioseparation and bioconversion and their applications in biotechnology*. Journal of Separation Science, 27(10-11): p. 767-778.
68. Tennikova, T.B. and R. Freitag. 2000. *An introduction to monolithic disks as stationary phases for high performance biochromatography*. Journal of High Resolution Chromatography, 23(1): p. 27-38.
69. Josic, D. and A. Buchacher. 2001. *Application of monoliths as supports for affinity chromatography and fast enzymatic conversion*. Journal of Biochemical and Biophysical Methods, 49(1-3): p. 153-174.
70. Frey, D.D. and X. Kang. 2005. *New concepts in the chromatography of peptides and proteins*. Current Opinion in Biotechnology, 16(5): p. 552-560.
71. Kecili, R., et al. 2007. *Purification of penicillin acylase through a monolith column containing methacryloyl antipyrine*. Separation and Purification Technology, 55(1): p. 1-7.
72. BIA Separations. 2012. *CIM® cGMP Columns*. [cited: 2012, March 22nd]. Available from: <http://www.biaseparations.com>.

-
73. Aldington, S. and J. Bonnerjea. 2007. *Scale-up of monoclonal antibody purification processes*. Journal of Chromatography B, 848(1): p. 64-78.
 74. GE Healthcare Life Sciences. 2012. *Price list IEX Sepharose FF and NHS Sepharose FF*. [cited: 2012, March 8th]. Available from: www.gelifesciences.com.
 75. Frenken, L.G.J., et al. 2000. *Isolation of antigen specific Llama VHH antibody fragments and their high level secretion by Saccharomyces cerevisiae*. Journal of Biotechnology, 78(1): p. 11-21.
 76. Muyldermans, S. 2001. *Single domain camel antibodies: current status*. Reviews in Molecular Biotechnology, 74(4): p. 277-302.
 77. Harmsen, M. and H. De Haard. 2007. *Properties, production, and applications of camelid single-domain antibody fragments*. Applied Microbiology and Biotechnology, 77(1): p. 13-22.

Summary

Many product or even waste streams in the food industry contain components that may have potential for e.g. functional foods. These streams are typically large in volume and the components of interest are only present at low concentrations. A robust and highly selective separation process should be developed for efficient isolation of the components. Affinity chromatography is such a selective method. Ligands immobilized to a stationary phase (e.g., a resin or membrane) are used to bind the component of interest. Affinity chromatography is, however, a costly process, due to the batch-wise operation, the large amount of solvents required and the high costs of the ligands and stationary phases. Therefore, its current use is mainly limited to lab-scale purifications and pharmaceutical applications.

The aim of this research was to investigate the potential of affinity chromatography for the isolation of minor protein in the food industry. The discovery of the VHH ligand, based on the binding domain of a llama antibody, has led to a new class of highly selective ligands, which can be produced on a large scale. We studied the chromatography process to measure productivity, but also to develop a rational protocol for decisions on suitable stationary phases and process configurations. The research presented in this thesis provides insights in the opportunities and challenges for large-scale affinity chromatography.

The isolation of protein using affinity chromatography requires several stages: adsorption, washing, and desorption. In Chapter 2, we studied these stages for the isolation of bovine serum albumin (BSA) from pure BSA solutions with high and low concentration and from actual feedstock, in this case cheese whey. A small-scale packed bed column was used to investigate the yield and productivity. BSA was retrieved in highly pure and concentrated form in the desorption stage. Furthermore, we found that the productivity of the system strongly depended on the point at which the adsorption stage is terminated.

Acids or salts are commonly used to disrupt the bond between ligand and target protein during desorption. This results in the use of large quantities of chemicals, whilst the potential of other methods for desorption, such as an increase in temperature, is not fully explored. In Chapter 3 we measured the thermodynamics of

the adsorption reaction between BSA and the VHH ligand with isothermal titration calorimetry (ITC). Temperature and pH were varied to find other conditions for desorption. A buffer with high pH could be used for desorption, and an increase of temperature seemed to weaken the bond between protein and ligand. However, the acidic buffer would in this case still be most effective.

Apart from the bond between ligand and target protein, the stationary phase to which the ligand is immobilised plays a key role in the chromatography process. Many supports are available, of which we investigated a selection of resins for packed bed chromatography in Chapter 4. We found that some resins were unsuitable for our process due to their low adsorption capacity. A ranking and weighing method was presented to determine the optimal resin depending on the requirements of the process.

An important issue we found for all the resins investigated, was the low adsorption capacity compared to other types of adsorptive chromatography processes, such as ion exchange chromatography. Therefore, we studied the immobilization of the ligand to three resins in more detail in Chapter 5. The efficiency of ligand immobilization depended on the ligand concentration used in the immobilization procedure. However, only approximately one out of five immobilized ligands was able to bind to the target. Improvement of ligand immobilization is therefore a potential route to increase the feasibility of affinity chromatography for large-scale processes.

Eventually the lab-scale process has to be scaled-up to industrial scale. The commonly used axial flow column, essentially a cylinder filled with resin through which the feed flows in the axial direction, can have problems at scale-up, because of increased pressure drop as the column is lengthened. Therefore, scale-up usually takes place by widening the column. Another option is to use a radial flow column, in which the resin is confined between two concentric cylinders and liquid flows from the outside inwards or from the inside outwards. The radial flow column can be scaled up in height instead of width. In Chapter 6 we compared axial and radial flow affinity chromatography both experimentally and theoretically. We found that the differences in performance were minimal, because the process was limited by diffusion inside the resin particle. At a small process scale, radial flow columns are impractical in terms of size, but at a larger process scale they may compete with axial flow columns because of their smaller foot print and possibly lower construction costs.

The research in this thesis was focused on a defined ligand-protein system and commercially available resins in packed-bed configuration. The potential of other stationary phases, such as non-porous (magnetic) particles, membranes and monoliths was therefore discussed in Chapter 7. We found that currently the packed bed of porous resin beads still seems to be the most suitable configuration. A radial flow column with porous affinity resin is in theory capable of isolating a low-concentrated protein from a large feed of 10 m³/h. However, the relatively low capacity of the resin, the limited liquid velocity, as well as large buffer usage and the current costs remain important issues to resolve to further expand the opportunities of affinity chromatography for minor protein isolation.

Samenvatting

In de levensmiddelenindustrie bevatten product- of reststromen vaak hoogwaardige componenten die bijvoorbeeld een gezondheidsbevorderend effect hebben. Deze hoogwaardige componenten zijn vaak in kleine hoeveelheden aanwezig, terwijl de product- of reststroom vaak erg groot is. Om deze componenten efficiënt te kunnen isoleren, is een robuust en zeer selectief scheidingsproces nodig, zoals affiniteitschromatografie. Voor affiniteitschromatografie worden liganden geïmmobiliseerd op een stationaire fase, bijvoorbeeld een hars of een membraan. Deze liganden binden de gewenste component. Affiniteitschromatografie is echter een kostbaar proces, omdat het batch-gewijs uitgevoerd wordt, er grote hoeveelheden oplosmiddel of buffer gebruikt worden en zowel de liganden als de harsen en membranen kostbaar zijn. Om deze redenen wordt affiniteitschromatografie vooral gebruikt op labschaal en voor farmaceutische doeleinden.

Het doel van dit onderzoek was om de mogelijkheden voor isolatie van laaggeconcentreerde eiwitten in de levensmiddelenindustrie met behulp van affiniteitschromatografie te analyseren. De ontdekking van het VHH ligand, gebaseerd op het bindingsdomein van het antilichaam van een lama, heeft geleid tot een nieuwe klasse van zeer selectieve liganden die op grote schaal kunnen worden geproduceerd. We hebben de productiviteit van het chromatografieproces geanalyseerd, en ook een methode ontwikkeld om een keuze te kunnen maken tussen verschillende stationaire fasen en procesconfiguraties. Het onderzoek in dit proefschrift geeft inzicht in de mogelijkheden en uitdagingen voor affiniteitschromatografie op grote schaal.

Het proces van eiwitisolatie met behulp van affiniteitschromatografie bestaat uit drie fasen: adsorptie, wassen en desorptie. In Hoofdstuk 2 hebben we deze fasen onderzocht voor de isolatie van runderalbumine (BSA) uit pure BSA oplossingen met hoge en lage concentratie, en uit kaaswei als voorbeeld voor een reststroom. We hebben een kleine gepakte kolom gebruikt om de opbrengst en productiviteit van het proces te bepalen. Aan het eind van het proces werd een geconcentreerde en zeer zuivere BSA oplossing verkregen. De productiviteit van het proces bleek sterk af te hangen van het moment waarop de adsorptie-fase wordt beëindigd.

In de meeste gevallen worden voor desorptie zuren of zouten gebruikt om de binding tussen het ligand en het eiwit te verbreken. Hierdoor worden grote hoeveelheden chemicaliën gebruikt. Andere opties voor desorptie, zoals bijvoorbeeld het verhogen van de temperatuur, zijn niet uitgebreid onderzocht. In Hoofdstuk 3 hebben we de thermodynamica van de bindingsreactie tussen BSA en het VHH ligand als functie van temperatuur en pH gemeten met behulp van isotherme titratie calorimetrie (ITC). Een basische buffer in combinatie met een verhoogde temperatuur zou kunnen worden gebruikt om de binding tussen BSA en het VHH ligand te verzwakken. Een zure desorptiebuffer is echter effectiever.

Naast de binding tussen ligand en BSA, speelt de stationaire fase waarop het ligand is geïmmobiliseerd een belangrijke rol in het chromatografieproces. In Hoofdstuk 4 hebben we verscheidene harsen voor gepakte bedden met elkaar vergeleken. Een aantal harsen bleek ongeschikt voor dit proces vanwege de lage bindingscapaciteit. Door een rangorde aan te brengen waarbij een gewicht kan worden toegekend aan de verschillende eigenschappen van de harsen, kan een keuze worden gemaakt tussen de harsen. De harsen die we hebben onderzocht, hadden allen een veel lagere bindingscapaciteit dan harsen voor andere typen chromatografie, zoals bijvoorbeeld ionenwisselingschromatografie.

In Hoofdstuk 5 hebben we de immobilisatie van ligand verder bestudeerd voor drie commercieel verkrijgbare harsen. De efficiëntie van de immobilisatie bleek afhankelijk van de gebruikte ligandconcentratie in de immobilisatie-oplossing. Echter, slechts één van de vijf geïmmobiliseerde liganden kon BSA binden. Het verbeteren van de bindingscapaciteit is daarom een mogelijke route om de affiniteitschromatografie op grote schaal breder toe te kunnen passen.

Een proces op labschaal zal uiteindelijk opgeschaald moeten worden tot industriële schaal. De gepakte kolom, in feite een cilinder gevuld met hars waar de vloeistof in axiale richting doorheen stroomt, kan problemen geven bij opschaling. Het grootste probleem is de verhoging van de drukval wanneer de kolom langer wordt gemaakt; daarom wordt vaak opgeschaald in de breedte. Een radiale kolom, waarbij het hars tussen twee concentrische cilinders wordt gepakt en de vloeistof van buiten naar binnen of van binnen naar buiten stroomt, kan in dit geval uitkomst bieden. Dit type kolom kan worden opgeschaald in hoogte zonder de drukval te verhogen. In Hoofdstuk 6 vergeleken we een axiale en een radiale kolom, zowel theoretisch als met behulp van experimenten op labschaal. Beide kolommen presteren vrijwel gelijk, omdat het proces gelimiteerd is door de diffusie in de harsdeeltjes. Op kleine schaal is

een radiale kolom niet praktisch, maar op grotere schaal (vanaf enkele tientallen liters hars) zou dit type kolom een goed alternatief kunnen vormen voor de axiale kolom, vanwege de kleinere footprint en mogelijk goedkopere constructie.

Het onderzoek in dit proefschrift was gericht op een specifiek ligand-eiwit systeem en commercieel verkrijgbare harsen in gepakte bedden. Andere stationaire fasen, zoals non-poreuze (magnetische) deeltjes, membranen en monolieten werden besproken in Hoofdstuk 7. Op dit moment lijkt een gepakt bed van poreuze harsdeeltjes nog steeds de meest geschikte methode voor affiniteitschromatografie. Theoretisch gezien kan een gepakt radiaal bed een laaggeconcentreerd eiwit zuiveren uit een grote reststroom van 10 m³/h. De relatief lage capaciteit van de harsen, de beperkte stroomsnelheid, de benodigde hoeveelheden buffer, en de huidige kosten blijven belangrijke kwesties die opgelost moeten worden om affiniteitschromatografie voor de isolatie van laaggeconcentreerde eiwitten breder toepasbaar te maken.

Dankwoord

Het mag dan wel alleen mijn naam zijn die op de kaft staat, in werkelijkheid hebben vele mensen bijgedragen aan de totstandkoming van dit proefschrift. Op de eerste plaats staan natuurlijk mijn begeleiders. Anja, bedankt dat je mij hebt gevraagd voor dit onderzoek. Het onderwerp was voor ons allebei nieuw en dat was af en toe even zoeken. Jouw vertrouwen en opbouwende kritiek hebben mij door heel wat lastige momenten heen geholpen. Remko, bedankt voor al je ideeën en je enthousiasme. De term ‘voortschrijdend inzicht’ zal me altijd bijblijven.

Bij deze wil ik ook iedereen die betrokken is geweest bij het SEISMIC project bedanken, in het bijzonder: Ingeborg, Pim, Frank, Ruud, Jeroen, Meng, Karin, Marc en Alfred. Bedankt voor al jullie input en de plezierige bijeenkomsten. Albert, jij hoort ook in dit rijtje, maar daarnaast heb ik veel geleerd van jouw ervaring en kritische blik op onder andere het schrijfwerk. Daarnaast wil ik ook Marcel bedanken voor de leuke discussies over radiale flow chromatografie.

Ook binnen de vakgroep heb ik veel hulp en steun gehad. Jos, bedankt voor je hulp met onder andere de radiale kolom. Maurice, zonder jouw hulp met de HPLC, de Äkta, en later ook de ITC had ik heel wat minder data gehad om mee te werken. I would also like to thank the students whom I supervised: Ghulam, Ids and Jie. I learned a lot from working with you. Naast inhoudelijke en praktische hulp was er ook meer dan voldoende ruimte voor gezelligheid, waarvoor ik iedereen van bio- en levensmiddelenproceskunde wil bedanken.

Ik wil ook mijn familie en vrienden bedanken dat ik bij hen mijn proefschrift af en toe even kon loslaten. Daphne en Kevin, bedankt dat jullie mijn paranimfen willen zijn. Hopelijk vinden we nu wat vaker de tijd om samen wat leuks te ondernemen. Pap en mam, zonder jullie steun was ik nooit zo ver gekomen. Bedankt dat jullie er altijd voor mij zijn. Mijn kleine, lieve dochter Evy, als ik in jouw pretoogjes kijk, verdwijnen al mijn zorgen als sneeuw voor de zon. En dan natuurlijk mijn lieve echtgenoot Jan-Willem: wat ben ik blij en dankbaar dat ik altijd alles bij je kwijt kan en jij me door heel wat moeilijke momenten hebt geloodst. Ik kijk uit naar onze toekomst samen.

Tamara

Curriculum Vitae

Tamara Besselink was born on November 20th, 1984 in Gendringen, The Netherlands. A few years later she moved to Ulf, where she lived until she graduated from secondary school Isala in Silvolde at the age of 17. In 2002 she started her first year of Biotechnology at Wageningen University from which she graduated with honors in 2006. After her BSc, she continued with an MSc in Biotechnology with the specialization Process Technology. At the Food and Bioprocess Engineering Group, she conducted her MSc thesis research on stochastic modeling of starch hydrolysis, for which she received the Unilever Research Prize in 2007. During her internship at Royal Friesland Foods Corporate Research (Deventer, The Netherlands) Tamara investigated the shear sensitivity of yoghurt. After her graduation (cum laude) in the summer of 2007, she started her PhD research in the SEISMIC (Separation and Isolation of Minor Components) project at the Food Process Engineering Group of Wageningen University. The results obtained during this research are described in this thesis. On October 1st 2012, Tamara started working as a process engineer at Iv-Industrie in Arnhem.

Publications

Besselink, Tamara; Janssen, Anja E.M.; and Boom, Remko M. *Isolation of bovine serum albumin from whey using affinity chromatography*. Will be submitted for publication.

Besselink, Tamara; Strubel, Maurice; Janssen, Anja E.M.; and Boom, Remko M. *The influence of pH and temperature on bovine serum albumin – VHH ligand binding*. Manuscript in preparation.

Besselink, Tamara; Liu, Meng; Ottens, Marcel; van Beckhoven, Ruud; Janssen, Anja E.M.; and Boom, Remko M. *Comparison of activated chromatography resins for protein immobilization*. Submitted for publication.

Besselink, Tamara; Strubel, Maurice; van der Padt, Albert; Janssen, Anja E.M.; and Boom, Remko M. *Efficiency of protein-based ligand immobilization for affinity chromatography*. Will be submitted for publication.

Besselink, Tamara; van der Padt, Albert; Janssen, Anja E.M.; and Boom, Remko M. *Are axial and radial flow chromatography different?* Submitted for publication.

Besselink, Tamara; Baks, Tim; Janssen, Anja E.M.; and Boom, Remko M. 2008. *A stochastic model for predicting dextrose equivalent and saccharide composition during hydrolysis of starch by alpha-amylase*. *Biotechnology and Bioengineering* 100(4): p. 684-697.

Overview of completed training activities

Discipline-specific

Numerical methods for chemical engineers (OSPT)	2007
Molecular affinity separations (OSPT)	2008
Thermodynamics in biochemical engineering (DECHEMA)	2008
A unified approach to mass transfer (VLAG/OSPT)	2008
Process economics and cost engineering (OSPT)	2009
Introduction to gPROMS (PSE)	2009
Dynamic optimization and model validation with gPROMS (PSE)	2010
Netherlands Process Technology Symposium (NPS)	2007-2010

General

PhD competence assessment (WGS)	2007
Information literacy for PhD (WGS)	2007
VLAG PhD week (VLAG)	2008
Organizing and guiding BSc/MSc students (DO)	2008
Project and time management (WGS)	2008
Effective behaviour in your professional surroundings (WGS)	2009
Gespreksvaardigheden één op één (DO)	2009
Techniques for writing and presenting a scientific paper (WGS)	2009
Career orientation (WGS)	2011

Optional

Food and Bioprocess Engineering PhD study tour to Japan	2008
Brain & Game meeting Food and Bioprocess Engineering group	2008
Presentation FrieslandFoods Chromatography day	2008
Organization gPROMS course in Wageningen, the Netherlands	2010
Food Process Engineering Symposium	2010
Food Process Engineering Group meetings	2009-2012

Cover: word cloud generated using Tagxedo (<http://www.tagxedo.com>) with important words and phrases from this thesis.

The research described in this thesis was supported by FrieslandCampina (Amersfoort, The Netherlands), DSM Biotechnology Center (Delft, The Netherlands) and BAC (Naarden, The Netherlands) and Agentschap NL (formerly SenterNovem, project SEISMIC (Separation and Isolation of Minor Components), IS054084).